

ESTIMATION OF ICE RESISTANCE OF SHIPS BASED ON
MEASUREMENTS OF ICE THICKNESS, SPEED AND POWER

MASTER THESIS

BY

ANDERS MADSEN

JUNE 14, 2010

SUPERVISOR:

PROF. BERNT J. LEIRA

NORWEGIAN UNIVERSITY OF SCIENCE AND TECHNOLOGY

FACULTY OF ENGINEERING SCIENCE AND TECHNOLOGY

DEPARTMENT OF MARINE TECHNOLOGY

MASTER THESIS 2010
for
Master Stud. Anders Madsen

Estimation of Ice Resistance of Ships based on Measurements of Ice Thickness, Speed and Power
Estimering av Motstandskrefter for Skip i Is basert på Målinger av Is Tykkelse, Hastighet og Effekt

The maritime trade and activity in Polar areas is expected to grow significantly in the near future, mainly influenced by the following factors:

- Increased exploitation and transport of oil & gas in Arctic areas (Russian and Canadian waters)
- Increased flow of tourists to Arctic and Antarctic waters
- Increased transport of dry bulk and cargo in Arctic waters

In order to transport large volumes of oil and gas from Russia to western markets (mainly the US), future ships will be larger than the current ships operating in Arctic areas. The number of ships strengthened for ice breaking operations will increase. This include ship types as ice breakers, offshore support ships, oil tankers, LNG transport, bulk carriers , and to some extent also container carriers and passenger cruise vessels.

The objective of the DnV managed project, *Ice Load and Monitoring (ILM)*, which is supported by the Norwegian Research Council, is to develop a decision support system for ship operation under severe ice conditions and in case of accidental situations.

The purpose of the present work is to consider how the measurements which are available as a result of this project also can be applied for the purpose of estimating ice resistance. This will be an important parameter e.g. in order to estimate the additional transportation cost for arctic as compared to non-arctic areas.

The following subjects are to be examined:

1 Different types of sea ice and their mechanical/physical properties are to be briefly described. Models for calculation of contact pressure acting on a structure due to ice are also to be summarized and discussed together with relevant input parameters to these models.

2 A review of ice-class rules and the corresponding procedures for calculation of ice pressure and hull scantlings is to be given. Some comparative calculations of ice pressure and the resulting hull scantlings may also be performed.

3 A description of the measurements system for KV Svalbard is to be given. Both the different types of measurements and the locations of the given sensors are to be presented.

4. A review of formulations in the literature which provide estimation of ship resistance in ice should be given. Furthermore, it should be outlined how the ice-resistance can be estimated for the particular case of KV Svalbard based on the available measurements of

e.g. ice thickness, speed and power. Formulations based on equilibrium and/or energy considerations are to be discussed.

5Based on the proposed formulation, the ice-resistance is to be estimated for selected sequences of the available measurements. Comparison should be made between different formulation for the ice resistance and the resistance which is estimated from the measurements. Error estimation should also be part of the assessment.

6Based on the results from item 5 (and in particular the error estimates), it should be discussed whether a statistical or deterministic model of the ice resistance is most well-suited. If it is found that a statistical model is most appropriate, the parameters which define the statistical properties should be estimated based on the available data.

7Conclusions and recommendation for further work

Literature studies of specific topics relevant to the thesis work may be included.

The work scope may prove to be larger than initially anticipated. Subject to approval from the supervisor, topics may be deleted from the list above or reduced in extent.

In the thesis the candidate shall present his personal contribution to the resolution of problems within the scope of the thesis work.

Theories and conclusions should be based on mathematical derivations and/or logic reasoning identifying the various steps in the deduction.

The candidate should utilize the existing possibilities for obtaining relevant literature.

The thesis should be organized in a rational manner to give a clear exposition of results, assessments, and conclusions. The text should be brief and to the point, with a clear language. Telegraphic language should be avoided.

The thesis shall contain the following elements: A text defining the scope, preface, list of contents, summary, main body of thesis, conclusions with recommendations for further work, list of symbols and acronyms, references and (optional) appendices. All figures, tables and equations shall be numerated.

The supervisor may require that the candidate, in an early stage of the work, presents a written plan for the completion of the work. The plan should include a budget for the use of computer and laboratory resources which will be charged to the department. Overruns shall be reported to the supervisor.

The original contribution of the candidate and material taken from other sources shall be clearly defined. Work from other sources shall be properly referenced using an acknowledged referencing system.

The report shall be submitted in two copies:

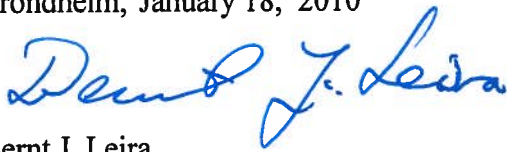
- Signed by the candidate

- The text defining the scope included
- In bound volume(s)
- Drawings and/or computer prints which cannot be bound should be organised in a separate folder.

Supervisor: Prof. Bernt J. Leira

Deadline: June 14, 2010

Trondheim, January 18, 2010



Bernt J. Leira

Preface

This report is a project thesis in marine structures carried out during the spring 2010 at the Department of Marine Technology, Norwegian University of Science and Technology in Trondheim. Professor Bernt Leira has been supervisor and responsible for preparation of the task text.

The main purpose of this thesis is to consider how the measurements which are available as a result of the *Ice Load and Monitoring* (ILM) project also can be applied for the purpose of estimating ice resistance. The thesis also deals with the challenges that may encounter when operating in Arctic environment. Introduction to physical and mechanical properties of sea ice will be briefly described together with different models for calculation of contact pressure due to ice. A review of ice-class rules with corresponding procedures for calculation of ice pressure and hull scantlings is also given.

I would like to thank my supervisor Bernt Leira for helpful guidance throughout the work of this thesis. Also I would like to thank PhD Candidate Abdillah Suyuthi for valuable guidance to question that has encountered.

Trondheim, June 14, 2010

Anders Madsen

Abstract

The activity in the polar marine areas is increasing from offshore and shipping activities supporting both commercial and tourist operations. Particular of interest is the expansion in offshore oil and gas exploration and productions activities in ice covered waters in the northern hemisphere. The presence of sea ice is the main factor for the complexity for operations in these regions.

The presence of sea ice is the main factor hindering the operations in Arctic. Sea ice is a complex material, and induces high pressures in contact with ships or structures. Different types of sea ice and their mechanical and physical properties are briefly described.

There exist different models for calculation of contact pressure acting on a vessel or a structure due to ice. This thesis will briefly present three different and popular approaches to predict ice pressure on structures and ships, namely; empirical pressure relationships, physical models and stochastic models. The best approach to predict ice pressure depends much on the problem and what kind of data that is available.

Ice class rules for vessels operating in ice infested waters are reviewed. The ice-class rules developed by IACS and DNV are summarized, and both principles behind the rules and the numerical values have been compared. The main difference is that IACS use a plastic method of approach, while DNV uses an elastic method. Despite the difference in method of analyses, the numerical comparison shows they are relative similar. The IACS rules are typically most conservative for larger vessels with large displacement, while the DNV rules are conservative for smaller vessels with small displacement.

A review of two different formulations for estimation of ice resistance for ship is given. This is inexpensive analytical models that can give an early estimation of the ice resistance and power requirement. Using main properties from KV Svalbard the two different formulations is compared, and they seem to compare quite well for thin ice ($h_i < 1m$) when the vessel speed is low. For higher vessel speeds the results differs more from each other.

The increasing activity in polar areas is the main motivation for Det Norske Veritas project *Ice Load and Monitoring* (ILM). The overall aim of the ILM-project is to increase the

knowledge about the actual ice conditions a vessel meets and its effect on the hull. As a part of the project a prototype of a monitoring system was mounted on the coast guard vessel KV Svalbard, which is described. During research work with KV Svalbard for a total of two weeks in late March 2007 operating in ice covered waters around Spitsbergen, measurement from the ILM-system was stored for later usage.

Based on conservation of energy a formulation is outlined to describe how the ice resistance can be estimated for a particular case. In this thesis KV Svalbard is used with available measurements of ice thickness, speed and power from the voyage in late March 2007. The estimated resistance is compared with the two reviewed formulations from literature, and the trend in the results seems to agree well.

In the final task, a regression analysis was used to find the "best fit" line or curve to the estimated resistance of KV Svalbard. Different Least Square curves was evaluated and discussed and it was found out that an exponential curve fitted best to the estimated data.

Contents

1	Introduction	1
1.1	Outline of the Thesis	2
2	The Arctic	3
3	Types of Sea Ice and their Physical and Mechanical Properties	5
3.1	Types of sea ice and features	5
3.1.1	Sea ice types	5
3.1.2	Sea ice features	6
3.2	Physical and mechanical properties	6
3.2.1	Growth and microstructure of sea ice	7
3.2.2	Ice thickness	7
3.2.3	Ice salinity and porosity	7
3.2.4	Ice density	8
3.2.5	Tensile strength	8
3.2.6	Flexural strength	9
3.2.7	Shear strength	9
3.2.8	Compressive strength	10
3.3	Summary	10
4	Models for Calculation of Contact Pressure	13
4.1	Empirical pressure relationships	13
4.2	Physical model	14

4.3	Stochastic model	16
4.4	Summary of contact pressure	17
5	Ice Class Rules	19
5.1	Introduction	19
5.1.1	DNV ice class rules	20
5.1.2	IACS Polar Rules	21
5.2	Introduction to Structural Requirements	23
5.3	Design loads	23
5.3.1	Rule Methodology	23
5.3.2	DNV Design loads	24
5.3.3	IACS Design loads	25
5.4	Plating requirements	27
5.4.1	DNV requirements	27
5.4.2	IACS requirements	28
5.5	Framing requirements	30
5.5.1	DNV Stiffeners and Girder requirement	30
5.5.2	IACS Stiffeners and Girder requirement	30
5.6	Comparison of DNV and IACS rules	31
6	Numerical Comparison of Rule Requirements	33
6.1	Design load	33
6.1.1	DNV design load	34
6.1.2	IACS design load	34
6.1.3	Comparison of DNV and IACS design loads	35
6.2	Plate thickness requirement	37
6.3	Summary	37
7	Estimation of Ice Resistance of Ships	39
7.1	Lindqvist	40

7.1.1	Crushing	40
7.1.2	Breaking by bending	41
7.1.3	Submersion	41
7.1.4	Speed	42
7.2	Riska	43
7.2.1	Level ice resistance	43
7.3	Comparison	45
8	Measurement System for KV Svalbard	49
8.1	Fiber Optic strain sensors	50
8.2	Electro magnetic ice thickness measuring device	50
8.2.1	Method description	51
8.2.2	Accuracy over level ice	51
8.3	Other measurements	52
9	Collected Data from KV Svalbard	53
9.1	Sequences of Interest	53
9.1.1	Screening	53
9.2	Quality of measurement	56
9.2.1	Power measurements	56
9.2.2	Speed measurements	57
9.2.3	Ice Thickness Sensor	57
9.2.4	Summery of screening and quality of measurements	58
10	Resistance Formulation	59
10.1	Conservation of energy	60
10.2	Average Force	60
10.3	Resistance Formulation	61
10.4	Summery	63

11 Processing of Collected Data	65
11.1 MATLAB System	65
11.1.1 Screening	65
11.1.2 Loading and selecting data	66
11.1.3 Processing and analysing	66
11.2 Results	67
11.2.1 March 24th	67
11.2.2 March 25th	68
11.2.3 March 26th	69
11.3 Comparison and summary	70
11.3.1 Comparison with existing formulation	70
12 Curve Fitting	75
12.1 Least Squares method	76
12.1.1 Linear curve fitting	76
12.1.2 Linearizing	77
12.1.3 Coefficient of Determination	77
12.2 Choosing a Curve Fit Model	78
12.2.1 March 24th	79
12.2.2 March 25th	82
12.2.3 March 26th	84
12.3 Comparison and summery	87
13 Conclusion	89
14 Recommendation for Further Work	91
Bibliography	93
A Ice Conditions	I

B Sequences of Interest	V
C Processed Data	XVII
D Contents on Attached CD	XXV

List of Figures

2.1	Arctic boundary, navigation routes and areas with oil/gas resources	3
3.1	Sea ice zones	5
3.2	Plot of density versus temperature for four different salinities[18]	8
3.3	Tensile strength of first-year ice as a function of total porosity[18]	9
3.4	Flexural strength versus the square root of the brine volume[18]	10
4.1	Design curve based on contact area[12]	13
4.2	Long term response analysis of ice loads[16]	15
4.3	Long term distribution of ice load on a bow frame[9]	16
4.4	The PSD function obtained form test data and model[21]	17
5.1	Ice reinforced areas from DNV and IACS rules[7]	24
5.2	Design scenarios for derivation of ice loads[5]	26
5.3	Contact area and penetration depth[5]	26
5.4	Plate strip analogy	27
5.5	Yield line analysis according to IACS Polar ships	29
5.6	Three limit states for a frame	31
6.1	DNV design loads	34
6.2	IACS design load	36
6.3	Comaprison of DNV and IACS design load	36
6.4	Comparison of plate thickness DNV and IACS	38

LIST OF FIGURES

7.1	KV Svalbard in ice	39
7.2	The forces acting in Ice breaking	40
7.3	Ferry breaking ice in the baltic sea	43
7.4	Ice resistance versus ship speed deduced from full scale tests	44
7.5	Ice resistance comparison Riska vs Lindqvist, different ice thickness	46
7.6	Ice resistance comparison Riska vs Lindqvist, different speed	47
8.1	The Ice Load Monitoring system (ILM)	49
8.2	Frames instrumented with sensors	50
8.3	Measuring of ice thickness[15]	51
8.4	Different parameters measured onboard KV Svalbard	52
9.1	Ice observations from March 26th	58
10.1	Ice resistance is an average force	59
10.2	Time variation of force during collision and average force	60
10.3	Equilibrium between resistance and thrust when speed is constant	62
10.4	Time sequence illustrated	63
11.1	March 24th - Resistance vs mean ice thickness, 10 min sequences	67
11.2	March 24th - Resistance vs mean ice thickness, 5 min sequences	68
11.3	March 25th - Resistance vs mean ice thickness, 10 min sequences	68
11.4	March 25th - Resistance vs mean ice thickness, 5 min sequences	69
11.5	March 26th - Resistance vs mean ice thickness, 10 min sequences	69
11.6	March 26th - Resistance vs mean ice thickness, 5 min sequences	70
11.7	March 24th–26th - Resistance vs mean ice thickness, 10 min sequences	71
11.8	March 24th–26th - Resistance vs mean ice thickness, 5 min sequences	71
11.9	Results compared with Riska and Lindqvist formulations	72
11.10	Results compared with Riska and Lindqvist formulations with 500kN shift	72
11.11	Results from March 26th compared with Riska and Lindqvist using equal speed and ice thickness	73

12.1 Illustration of Least Squares method	75
12.2 General shape of various curve fits	79
12.3 March 24th - Linear regression with formula and R^2	79
12.4 March 24th - $\ln(y)$ transformation with formula and R^2	80
12.5 March 24th - $\log(x)$ - $\log(y)$ transformation with formula and R^2	80
12.6 Comparison of fitted curves	82
12.7 March 25th - Linear regression with formula and R^2	82
12.8 March 25th - $\ln(y)$ transformation with formula and R^2	83
12.9 March 25th - $\log(x)$ - $\log(y)$ transformation with formula and R^2	83
12.10 Comparison of fitted curves	84
12.11 March 26th - Linear regression with formula and R^2	85
12.12 March 26th - $\ln(y)$ transformation with formula and R^2	85
12.13 March 26th - $\log(x)$ - $\log(y)$ transformation with formula and R^2	85
12.14 Comparison of fitted curves	86
12.15 Comparison of fitted curves	87
12.16 Fitted curves compared with Riska and Linqvist	88
B.1 March 24th	VI
B.2 March 24th	VII
B.3 March 24th	VIII
B.4 March 25th	IX
B.5 March 25th	X
B.6 March 25th	XI
B.7 March 26th	XII
B.8 March 26th	XIII
B.9 March 26th	XIV
B.10 March 26th	XV
B.11 March 26th	XVI

LIST OF FIGURES

List of Tables

3.1	Sea ice types	6
3.2	Sea ice features and definitions	6
5.1	Basic and Ice Strengthening and Ice Strengthening for the Northern Baltic[7]	21
5.2	Vessels for Arctic and Ice Breaking Service[7]	22
5.3	Polar Class Description[7]	22
6.1	Class factors used in IACS rules	35
7.1	Main properties of KV Svalbard used in the comparison	46
9.1	Sequences of interest for March 24th	55
9.2	Sequences of interest for March 25th	55
9.3	Sequences of interest for March 26th	56
11.1	Measurements received	66
12.1	Transformations to Linearize	77
C.1	March 24th - 10 minutes long sequences	XVIII
C.2	March 24th - 5 minutes long sequences	XIX
C.3	March 25th - 10 minutes long sequences	XX
C.4	March 25th - 5 minutes long sequences	XXI
C.5	March 26th - 10 minutes long sequences	XXII
C.6	March 26th - 5 minutes long sequences	XXIII

LIST OF TABLES

Chapter 1

Introduction

The activity in the polar marine areas is increasing from offshore and shipping activities supporting both commercial and tourist operations. Particular of interest is the expansion in offshore oil and gas exploration and productions activities in ice covered waters in the northern hemisphere. Presence of sea ice is the main factor for the complexity for operations in these regions.

In order to transport large volumes of oil and gas from Russia to western markets, the number of ships strengthened for ice breaking operation will increase. This does not only include oil and gas tankers, but also ice breakers, offshore support ships, bulk carriers and to some extent also container carriers and passenger cruise vessels.

Evaluation of the actual load on the hull is identified as one of the major uncertainties when operating ships in ice, and this is the background for the *Ice Load and Monitoring* (ILM) by Det Norsk Veritas (DNV) with partners. The overall aim of the ILM-project is to increase the knowledge about the actual ice conditions a vessel meets and its effect on the hull.

The purpose of the present work is to consider how the measurements which are available as a result of this project also can be applied for the purpose of estimating ice resistance. This will be an important parameter e.g. in order to estimate the additional transportation cost for arctic as compared to non-arctic areas.

1.1 Outline of the Thesis

This thesis is divided into chapters, covering the following topics:

- 2: The Arctic** This chapter gives an introduction to the Arctic area and why this area is interesting for companies and government.
- 3: Types of Sea Ice and their Physical and Mechanical Properties** Different types of sea ice and features is presented together with a brief review of mechanical and physical properties for ice with focus on important engineering properties.
- 4: Models for Calculation of Contact Pressure** This chapter presents three different and popular approaches to predict ice loads on structures and ships with relevant examples of methods.
- 5: Ice Class Rules** The class society's focuses on additional risks when moving ship operations from worldwide trade to cold-climate areas. A review of DNV and IACS ice class rules and corresponding procedures for calculation of ice pressure and hull scantlings are briefly described in this chapter.
- 6: Numerical Comparison of Rule Requirements** A numerical study between the two rule sets presented in last chapter.
- 7: Estimation of Ice Resistance of Ships** A review of two different formulations for estimation of ship resistance in ice.
- 8: Measurement System for KV Svalbard** This chapter gives a short description of the measuring system installed on board KV Svalbard due to the ILM project.
- 9: Collected Data from KV Svalbard** This chapter points out the sequences of interest from the measured data during the scientific voyage in March 2007 with KV Svalbard, and discusses the data quality.
- 10: Resistance Formulation** Based on conservation of energy a formulation is developed to estimate resistance in ice using available measurements from the ILM project.
- 11: Processing of Collected Data** Based on the proposed formulation the ice resistance is estimated for selected sequences of interest from the available measurements.
- 12: Curve Fitting** This chapter studies if it possible to fit a model to the estimated resistance.
- 13: Conclusion** This chapter conclude important findings from preceding chapters.
- 14: Recommendation for Further Work**

Chapter 2

The Arctic

The Arctic area has numerous of definitions, in the past the Arctic Circle ($66^{\circ} 33' N$) was frequently used. Today it is based on climate and ecology, such as the $10C^{\circ}$ isotherm in July. This corresponds roughly to the tree line in most of the Arctic [10].

The extent of sea ice in the arctic areas varies significantly throw the year and during winter time the ice covers most part of the Arctic basin. The thickness of the sea ice in the Arctic varies from sea to sea. Areas were ice is present throw the whole year (multi-year ice) ice thickness is approximately 3-4m. In areas with only ice present during the winter month (first-year ice), ice thickness of 1-2m can be expected. First-year ice is also present in sub-arctic region such as in the Bohai Sea in China, Baltic Sea, Caspian Sea in Kazakhstan, the Sea of Okhotsk in Russia, Cook Inlet in Alaska and several rivers and lakes in Scandinavia, Russia and North America. The thickness of the ice in these areas will vary between 0.4-1.0m [16].

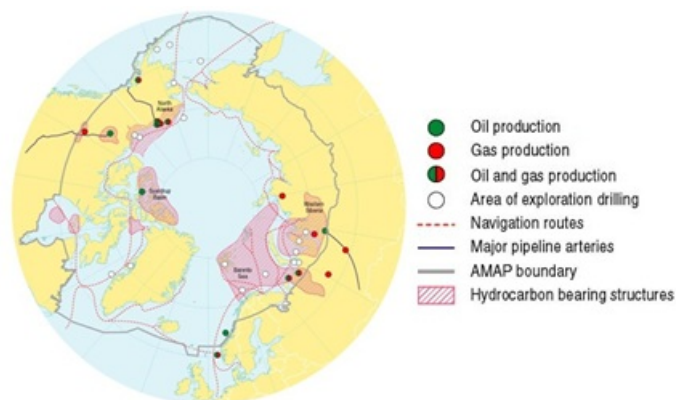


Figure 2.1: Arctic boundary, navigation routes and areas with oil/gas resources

Problems due to sea ice have been reported since the days Nansen (1897) reported his

experiences with the vessel "Fram" in the Arctic Basin. These first attempts to understand the Arctic were based on "trial and error" methods, and the researchers defied the harsh and cold climate in Arctic taking significant risks to achieve their goals [2]. Nowadays Arctic research is carried out by national and international companies and governments to achieve better knowledge of this area.

If the ice pack in the Arctic melts from global warming, it is predict that this area will have large reserves of offshore oil and gas, new shipping routes and fishing grounds. A total amount of 25% of undiscovered resources is expected to be in the Arctic region [16]. With lack of agreement for distribution of this territory, different countries try to claim for area in Arctic. With being present in the Arctic, countries hope to get a greater piece of the undiscovered resources.

In comparison with areas like the North Sea, the arctic area offers lack of infrastructure and effect of low temperatures, ice and reduced daylight. To operate in this harsh and cold environment is challenging, and arctic engineering requires knowledge about ice types, ice behavior, physics and mechanical properties.

Chapter 3

Types of Sea Ice and their Physical and Mechanical Properties

3.1 Types of sea ice and features

In literature and in everyday talk about sea ice different names of ice types, features and definitions are used. This section will shortly mention and describe some of the most frequency used. Some of the ice types and features are used later in this thesis with now further explanation.

3.1.1 Sea ice types

Looking at figure 3.1 we first have the fast ice zone with sea ice that has frozen along the coast or to the seafloor over shallower parts. Further out we have the pack ice zone with grounded ice bergs and drift ice that floats on the water surface, and packed together in large masses we call it pack ice. The general types of sea ice is described in table 3.1.

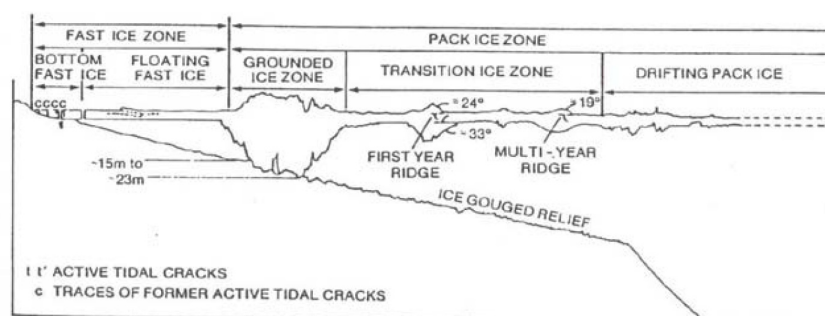


Figure 3.1: Sea ice zones

Sea ice type	Description
New ice	A general for for recently formed ice. Thickness <10cm
Young ice	Ice in transition between new ice and first-year ice. Thickness 10 - 30cm
First-year ice	1 years's growth, level when undeformed, but ridges and hummocks occur. Thickness 30cm - 2m
Multi-year ice	More that 1 year's growth, hummocks and ridges are smooth. Thickness >2m

Table 3.1: Sea ice types

Sea ice feature	Description
Polynia	Open water surrounded by sea ice
Fast ice	Sea ice that remains fast along the coast, or grounded icebergs
Pancake ice	Pieces of new ice, circular shaped 30cm - 3m across
Nilas	Continuous thin sheet of young ice, transparent
Ice floe	Flat piece of ice, >20m across and >1m thick
Level ice	Sea ice that is unaffected by deformation
Deformed ice	General term for ice that has been squeezed together
Rafted ice	A form of pressure ice in which one floe overrides another
Brash ice	Accumulations of ice made up of fragments
Hummocked ice	A form of pressure ice in which pieces of ice are piled arbitrarily
Ridge	A ridge or wall of broken ice forced up by pressure

Table 3.2: Sea ice feauteres and definitions

3.1.2 Sea ice features

Sea ice is not always flat and unaffected by deformation, different sea ice features and definitions are given in table 3.2.

3.2 Physical and mechanical properties

In Arctic regions, presence of sea ice is the main factor hindering the operations. This effect the shipping, and oil and gas exploration and development. This chapter will look at some physical properties (microstructure, thickness, salinity, porosity and density) and some mechanical properties (tensile, flexural, shear, and compressive strength) for first-year ice. This is typically engineering properties that are essential in Arctic design. The source of this information is mainly taken from *a review of the engineering properties of*

sea ice by G.W. Timco et. al[18].

3.2.1 Growth and microstructure of sea ice

Sea ice is a complex material that is composed of solid ice, brine, gas, and depending upon the temperature, various types of solid salt. The different variations in the environmental conditions results in different grain structures. The most common grain structures include granular, columnar, and discontinuous columnar. Granular ice forms in the initial stages of sea ice formations, and usually occur between the ice crystals instead of within the crystals. Columnar ice forms at the surface when the conditions are relatively calm, and they may extend through nearly the complete thickness. This columnar crystal follows the direction of the heat flow, which normally is vertical in the ice sheet. The brine and salt inclusions are located in vertically planes within the columnar crystals.

3.2.2 Ice thickness

The thickness of ice determines its volume and strength. For most engineering purpose, thickness is a key parameter to estimating the force acting on structures. This is therefore the most important property to measure and predict. For instance, the speed of a ship in ice is directly related to the thickness of sea ice.

The thickness of first-year ice is controlled by the air temperature, freezing time, covering snow type and thickness, wind speed, ocean heat flux and surface radiation balance. The first two parameters, air temperature and freezing time are governing. Ice is therefore thickest in arctic areas with cold and long winters.

The thickness of the first-year ice can be estimated with the freezing degree method, which determines the thickness based on energy balance. The maximum growth of sea ice during a winter season is about 2 meters.

3.2.3 Ice salinity and porosity

In sea ice there is normally a salinity variation with depth in the ice sheet. This is because salt within the ice migrates downward through the ice during the winter. The salinity fraction in the ice varies much, so often an average salinity profile is used as a first approximation.

The porosity is assumed to be expressed by the sum of relative brine volume and relative air volume. During the spring and early summer when the temperature increases, the

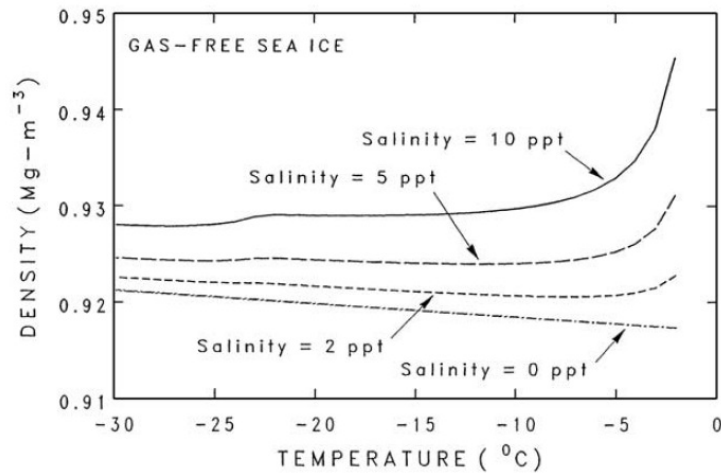


Figure 3.2: Plot of density versus temperature for four different salinities[18]

solid salt dissolves back into liquid phase. This happens approximately when the temperature warms to about $-8\text{ }^{\circ}\text{C}$. Further increase in the temperature will increase the size of the brine pockets rapidly, and "brine drainage channels" will form. This factor gives a thinner and significantly weaker ice.

3.2.4 Ice density

The density is an important parameter for many applications. First of all the density determines the weight of the ice and how much the ice moves out of the sea water. For fixed installations the weight of the ice can be important to determine the load when ice ridges up. The density also determines the buoyancy force as the difference between density of ice and sea water. Buoyancy can be an important factor for a vessel moving through an ice cover. A reasonable density estimate for first-year sea ice is $0.90\text{ (Mg/m}^3\text{)}$.

3.2.5 Tensile strength

Tensile strength is an another important property of the sea ice. The tensile strength defines the maximum tensile stress that the ice can sustain before failure, and is therefore a key failure mode when sea ice interacts with offshore structures and ship. This is an important parameter for an icebreaker proceeding in level ice because the necessary bending force is related to the vertical tensile strength in ice.

The true tensile strength of ice can found through number of tests. Since test of sea ice is time consuming and it is difficult to get reliable results, so few extensive test has been carried out.

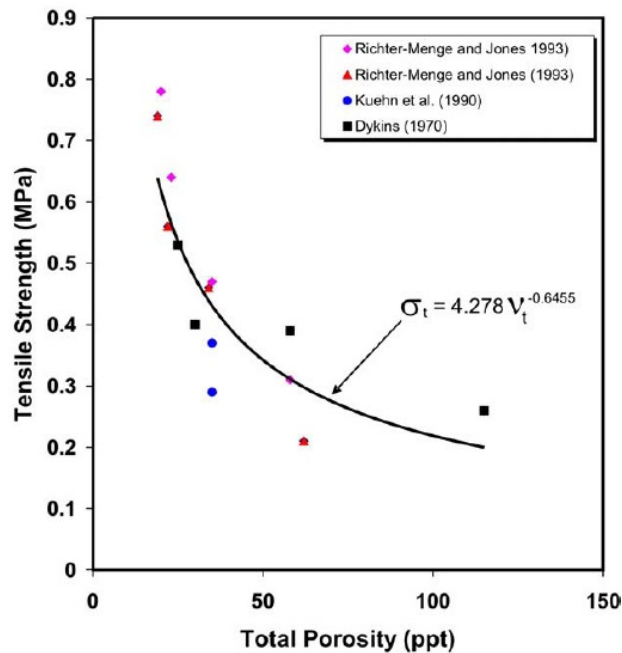


Figure 3.3: Tensile strength of first-year ice as a function of total porosity[18]

A small number of tests of tensile strength of first-year sea ice have been done. In general there is a decrease in tensile strength with increasing temperature, and the strength will drop off with increased porosity, see figure 3.3. The tensile strength in vertical- and horizontal-direction is different because of the growth direction of the sea ice (vertical). Tests of ice under loading with different orientations have showed that the vertical tensile force can be about three times larger.

3.2.6 Flexural strength

Flexural strength is not a basic material property, but many real sea ice failures occur in flexure. For instance is the flexure strength important for pressure ridge formation, ice-breaking and bending of ice on conical-shaped structures. A large number of measurements for this property have been done because of its importance in engineering problems, and because it is easy to measure. The flexural strength of sea ice ranges from about 1Mpa and deceases with brine volume as illustrated in figure 3.4.

3.2.7 Shear strength

Ice sheets interacting with structures or similar are often subjected to biaxial stress conditions involving tensile and compressive stresses or a shear stress. The shear strength is an

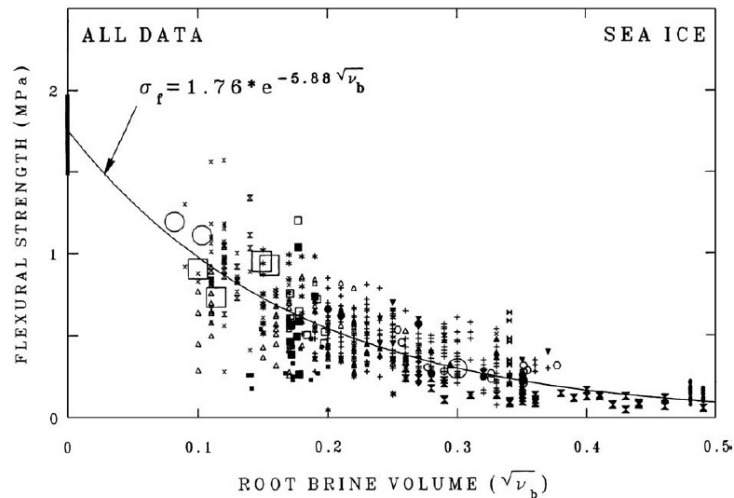


Figure 3.4: Flexural strength versus the square root of the brine volume[18]

important property, but it is difficult to perform experiment to obtain the reasonable values. In engineering practice, the shear strength is not frequently used. This is because the ice tends to fail in tension rather than in shear because of the tensile strength is normally lower.

3.2.8 Compressive strength

Compressive strength is another important property of sea ice. Since sea ice often tends to fail in compression, this property has been extensively studied. Failing in compression of sea ice can occur during formation of pressure ridges and crushing against a platform or ship. As for other sea ice properties many factors affect the compressive strength, for instance; temperature, salinity, density, ice type, crystal size and orientation.

3.3 Summary

Different types of sea ice and their mechanical and physical properties are briefly described. Thickness of sea ice is the key parameter to determine the strength of the ice, and the thickness also directly affects the speed of a vessel in ice. The main parameters deciding thickness of sea ice is the air temperature and freezing time. In addition to the thickness of the sea ice, also temperature, salinity, density, ice type, crystal size and orientation have an influence on the ice strength.

The mechanical properties of sea ice, as an engineering material, are tensile, flexural, compressive and shear stress. Flexural strength is not a basic material property, but an

important property for icebreaking and bending of ice. The tensile strength is also a key failure mode when sea ice interacts with offshore structures and ships. Compressive strength is important property when ice fails in crushing.

3. Types of Sea Ice and their Physical and Mechanical Properties

Chapter 4

Models for Calculation of Contact Pressure

There exist a handful of different methods of describing the ice load and actions from ice on ships and structures. Even given the same input values, the scatter will vary for the different methods. This section will briefly present three different and popular approaches to predict ice loads on structures and ships, namely; empirical pressure relationships, physical models and stochastic models.

4.1 Empirical pressure relationships

A well known approach to predict ice loads on ship hulls and fixed structures was presented by Masterson and Frederking[12]. They collected information from ship impacts, field tests and large scale offshore platforms to develop a design criteria covering a large range of contact areas. The result was a pressure vs. area graph, see Figure 4.1.

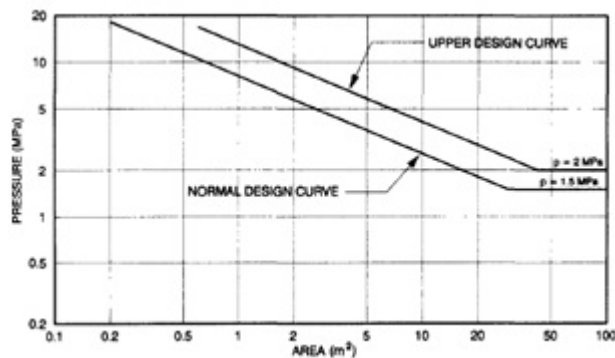


Figure 4.1: Design curve based on contact area[12]

The results indicated a trend that decreasing local ice pressures levels off at larger areas. However, side shell and bow pressures on a ship still present a challenge when designing frames, plates and bracings. As the design curve indicates the pressure on small loaded areas will be high. In case of an impact with a mass such as an iceberg, often with uneven surfaces, the load area may be low, resulting in very high pressure.

An empirical design curve is preferable for most users of design codes because they are user friendly and give often good predictions. Because the curves often are fitted to a large amount of data measured under different conditions, users of design code must check if the conditions are comparable for the new design.

4.2 Physical model

A physical model tries to reproduce the original problem to a model. The idealized physical model is usually based on observations from measurements. In a physical model it is difficult to account for all physical effect, so different models normally are tailor made for the problem. There exists considerable amount of physical models to describe ice interaction with structures, but their range of application is limited. In the later years simplified models, finite element and finite difference approaches has been used to model ice-structure interactions.

Historically, the uniaxial strength of ice has been found using empirical formulas and analytical equations to calculate ice loads on marine structures as described in section 4.1. In recent year, with availability of high power computers, numerical methods are being used more than ever before. A computer simulation based on computational techniques such as finite elements, boundary elements and discrete elements require constitutive models and failure criteria to represent the mechanical behavior of ice[6].

A paper by Derradji-Aouat[6] describes how to formulate a mathematical model for columnar grained ice, on the basis of laboratory test results. The model describes the behavior of ice subjected to any loading, including cycling loading conditions. The paper points in the direction that there is a possibility for the existence of a 'universal and general failure criterion' that can be used for numerical predictions of ice loads on ship and offshore structures.

There is need for this kind of general ice model capable of describing the response of ice to arbitrary loading, unloading and reloading conditions. Suchlike models are needed by finite elements codes to compute impact forces exerted by ice on ships. This does not mean that physical model is the best way of predicting the loads on a structure or ship. So far no physical model has been trusted in prediction of ice loads on a structure[2].

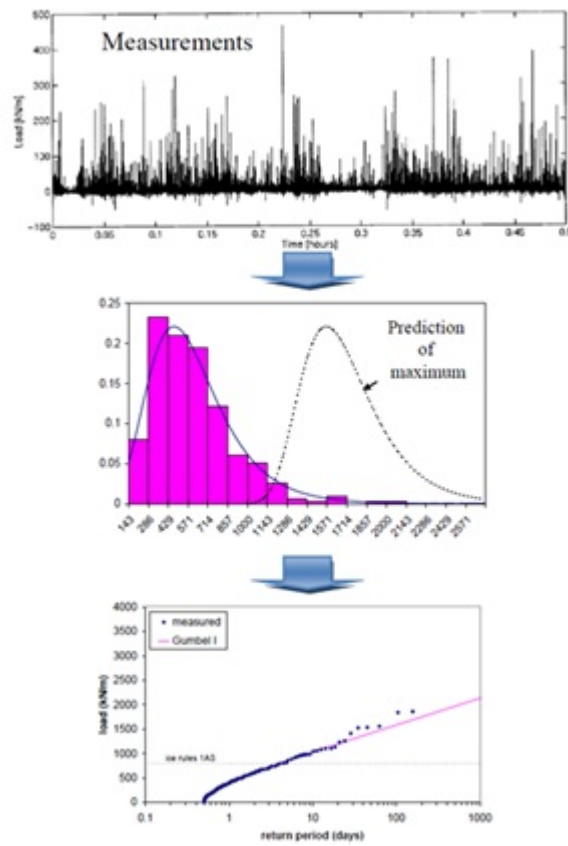


Figure 4.2: Long term response analysis of ice loads[16]

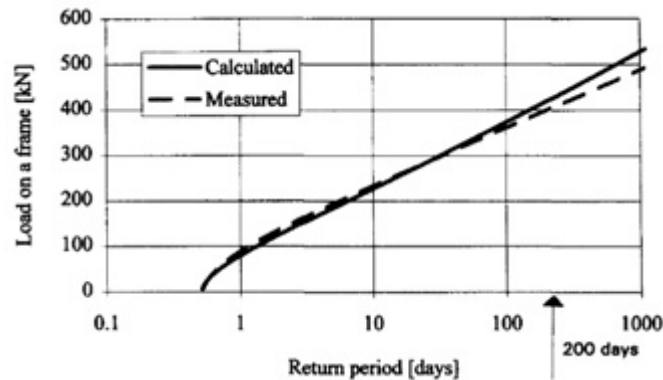


Figure 4.3: Long term distribution of ice load on a bow frame[9]

4.3 Stochastic model

Stochastic models apply probabilistic theories and the ideas with random processes. Instead of dealing with one possible solution of how the ice load may evolve over time, there are many possible solutions, but some are assumed to be more probable than others.

Ice load on ships can be described as individual pulses. The pulses are induced by the bending of ice floes or impact with ice floes. The long term response can be found by first finding the distribution of the maximum ice loads from a given period (for instance 12 hour period). Then the predicted maximum for this period can be established. Further, the maximum from each period be fitted to a Gumbel distribution or similar distribution. The following Figure 4.2 illustrates the step from measurements to a Gumbel distribution of long term ice loads.

Pentti Kujala presented in 1995 a semi-empirical evaluation of long term ice loads on a ship hull[9]. The aim of the project was to give a result that could be used in the development of design codes for ice-strengthened ships. The method Kujala developed for determination of long term ice loads for transverse frames was based on observation that the measured 12 hour maximum ice loads values are approximately piece-wise linearly related to the winter maximum equivalent ice thickness on various sea areas[9].

The model from his work can be useful in design of safe and reliable structures for ship navigating in ice covered waters. With long term distribution of ice loads established, the lifetime loads on various parts of the ship can be evaluated.

Another example of a stochastic model is described in a paper by Qu et al.(2007)[21]. The paper presents an ice force spectrum model for narrow conical offshore structures deployed in ice infested areas. The force spectrum was developed from a spectral analysis of ice load data for a full-scale test for a platform in Bohai Bay.

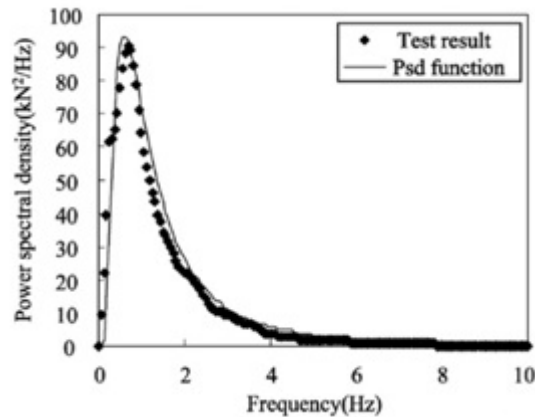


Figure 4.4: The PSD function obtained from test data and model[21]

Statistical methods are well established for wave induced loads on ships. With spectral analyses, various sea states can be described with a few parameters and the statistical characteristics can be established by relating the statistical load parameters to the sea state parameters. These methods can also easily be implemented in commercial finite element software used in structural design. Use of stochastic models to evaluate ice loads is useful because the fluctuating part of ice loads can be represented and applied in design to reveal lifetime loads and fatigue problems due to ice actions[2].

4.4 Summary of contact pressure

Three different approaches for calculations of ice loads were presented. The empirical pressure relations approach is easy to apply, but have limitations that are difficult to control. A physical model is challenging to establish because many details about the ice-structure interaction phenomenon are still unknown[2]. The last approach is to determine ice loads based on a stochastic model. This is a well known method for engineers, as there are similar methods from wind and wave engineering. Based on measurements and observations quite good models can be designed for representing the long term ice loads with this model. The best approach to predict ice forces depends on the problem and what kind of data you have. In general there is still need for more theoretical and empirical research on this problem before a method can be trusted to properly predict realistic ice forces[2].

Chapter 5

Ice Class Rules

Ships operating in areas experiencing seasonal or year round ice covered oceans and seas must take extra precaution to maintain environmental and ship integrity. To ensure safe navigation, ice class rules are implemented by the coastal states for these regions. Normally, ice class rules are developed in cooperation with the coastal state and classification societies. The existence of different sets of ice rules is due to the variations in the design conditions and the assumptions used in the requirements for the different areas. Specific oceans and sea areas are covered by the following ice class rules[8].

Baltic Sea

Bay and Gulf of Bothnia and Gulf of Finland are covered by Finnish and Swedish Finnish Swedish Ice Class Rules (FSICR) while the Russian territorial water in Gulf of Finland is covered by Russian Maritime Register of Shipping (RMRS).

Arctic Ocean

Russian Maritime Register of Shipping (RMRS) Ice Class Rules covers the Russian territorial waters stretching from the Barents Sea to the Chukchi Sea while the Beaufort Sea and Baffin Bay is covered by Canadian Arctic Shipping Pollution Prevention Rules (CASPPR).

Sea of Okhotsk

The Sea of Okhotsk is also covered by the Russian Maritime Register of Shipping (RMRS) Ice Class Rules.

5.1 Introduction

Ice class rules are generally divided in two main groups, requirement for navigation in first-year ice and requirements for navigation in multi-year ice. First-year ice have not

more than one winter growth and can be typically up to 120 cm thick and has typically low ice strength. Multi-year ice is sea ice that has survived at least one summer with melt and can be up to 3 m thick or more and have high ice strength.

Each Classification Society has a set of rules for strengthening during navigation in ice. In an attempt to unify the Ice Class Rules the International Association of Classification Societies (IACS) is in process of introducing Polar Ships Rules. IACS are working for safe ships and clean seas, and to achieve these goals IACS contribute with technical support, compliance verification and research and development. The IACS Polar Rules are created in line with the IMO Guidelines for ships operating in Arctic waters. Due to variations in design conditions and the assumptions used in determination of requirements, Russian Maritime Register of Shipping will retain rules for Arctic vessels and Finnish Swedish Ice Class Rules will also be retained for vessels operating in the Northern Baltic. These rules have been recognized as standard in their areas.

Classification rules are based on the ice thickness the vessel is intended to navigate in. Further are the ice class rules categorized into various levels depending upon the ice condition. Thicker ice requires greater hull reinforcement, propeller increasing and steering gear strengthening to resist the additional loads. The rules also accounts for independent or escorted navigation.

5.1.1 DNV ice class rules

The ice class rules in the DNV rules for ships is applied to vessels intended for navigation in waters with ice conditions. DNV have divided the rules into the three following categories based on service area and expected ice conditions.

1. Basic Ice Strengthening *Pt.5 Ch.1 Sec.2*
2. Ice Strengthening for the Northern Baltic *Pt.5 Ch.1 Sec.3*
3. Vessels for Arctic and Ice Breaking Service *Pt.5 Ch.1 Sec.4*

Table 5.1 and 5.2 gives an overview of the different ice classes in the DNV rules

The vessels requirement will be given by the suitable ice class, where the highest class has highest requirements. The highest ice class is for icebreakers and vessels intended to operate unassisted in ice-infested waters in Arctic and Antarctic regions. The supplementary requirements for relevant vessels deal with hull strength/fatigue, corrosion, coating, machinery and winterization.

<i>Ice Class</i>	Ice conditions	Ice Thickness
ICE-1A*	Difficult ice conditions, without the assistance of icebreakers	1.0
ICE-1A	Difficult ice conditions, with the assistance of icebreakers when necessary	0.8
ICE-1B	Moderate ice conditions, with the assistance of icebreakers when necessary	0.6
ICE-1C	Light ice conditions,with the assistance of icebreakers when necessary	0.4
ICE-C	Light ice conditions,with the assistance of icebreakers when necessary	0.4
ICE-E	Light localised drift ice in mouths of rivers and coastal areas	0.4

Table 5.1: Basic and Ice Strengthening and Ice Strengthening for the Northern Baltic[7]

Throughout this thesis the coast guard vessel KV Svalbard will be used as an example. This vessel is approved according to the Icebreaker POLAR-10 class, shown in table 5.2. The main focus in this part of the thesis is regarding design loads and structural requirements for Vessels for Arctic and Ice Breaking Service, other requirements will not be discussed.

5.1.2 IACS Polar Rules

The IACS Polar Rules are intended for Arctic and Antarctic navigation. In these remote areas Polar rules has to account for limited or no icebreaker assistance and impacts of ice floes. In general the highest Polar rules are used for vessels intended for year round navigation in multi-year ice, while the lower ones PC-6 and PC7 are intended for navigation in ice conditions comparable with the conditions in the Baltic sea.

The IACS Polar Rules are divided in three paramount requirements UR I1 to UR I3. This chapter emphasizes *UR I2 Structural Requirements for Polar Class Ships* which is most relevant. The UR I2 specify structural requirement to enable polar class ship to withstand global and local ice loads. The main scope of UR I2 is to treat plating, framing, plated structures and hull girders strength requirements in addition with material and corrosion allowances. Table 5.3 gives an overview of the different ice classes in the IACS rules.

<i>Class notation</i>	Type of ice encountered	Nominal ice strength σ_{ice} [N/mm^2]	Nominal ice thickness h_{ice} [m]	Limiting impact conditions
ICE-05 ICE-10 ICE-15	Winter ice with pressure ridges	4.2 5.6 7.0	0.5 1.0 1.5	No ramming anticipated
POLAR-10 POLAR-20 POLAR-30	Winter ice with pressure ridges and multiyear ice-floes and glacial ice inclusions	7.0 8.5 10.0	1.0 2.0 3.0	Occasional ramming
Icebreaker	As above	As above	As above	Repeated ramming

Table 5.2: Vessels for Arctic and Ice Breaking Service[7]

<i>Polar Class</i>	<i>Ice Description</i> (based on WMO Sea Ice Nomenclature)
PC-1	Year-round operation in all Polar waters
PC-2	Year-round operation in moderate multi-year ice conditions
PC-3	Year-round operation in second-year ice which may include multi-year ice inclusions.
PC-4	Year-round operation in thick first-year ice which may include old ice inclusions
PC-5	Year-round operation in medium first-year ice which may include old ice inclusions
PC-6	Summer/autumn operation in medium first-year ice which may include old ice inclusions
PC-7	Summer/autumn operation in thin first-year ice which may include old ice inclusions

Table 5.3: Polar Class Description[7]

5.2 Introduction to Structural Requirements

The objective of the structural requirements in ice class rules is to ensure that ship operating in ice infested waters can withstand the effect of ice load and temperature. Strength requirements are generally based on a design scenario, for instance is the Polar Rules based on a glancing impact on the bow for determining the scantlings required to resist ice loads.

The structural resistance to ice action may be assessed by means of elastic or plastic methods of analysis. Both principles are used by ship classification societies. Requirements from DNV are based on elastic theory, while the International Association of ship Classification Societies (IACS) rules is based on plastic methods. Elastic and plastic methods are based on different principles, but the two approaches may give very similar results.

In conventional analysis it is assumed that the response of the structure is elastic to the applied loads. This means that the structure returns to its initial state with no deformation if the load is removed. In plastic methods of analyses the structure is allowed to deform plastically so that permanent deflections will be developed. Plastic methods are therefore generally accepted if the action effects are dominated by a few extremes and not cyclic of nature. Additionally should the structure have redistribution capability of action effects and ductility. This applies notable to resistance of shell plating; the ice action is one side excursion and the plate resistance increases for finite deformations (membrane effects)[1]. In the following chapter, both DNV and IACS ice class rules will be reviewed. The main focus is design loads and plate, stiffener, girder and framing requirements.

5.3 Design loads

The following section is a review of the general principles behind the development of the DNV design loads and IACS design loads.

5.3.1 Rule Methodology

Determination of the extent of reinforcement is closely linked with design scenarios and damage experience. Due to the nature of ice, it is difficult to model and assess every design scenario, and therefore many rules are based on damage statistics to circumvent such a situation. Ships are designed for differing operational uses and will be reinforced in areas that have experienced damage from this, e.g. in areas with icebreaker convoy system vessels will have different damages than areas where ships have limited icebreaker escort.

The extent of reinforcement according to DNV ice class rules and IACS Polar Rules are divided into 7 and 10 different areas based on damage experience, see figure B.11. DNV and

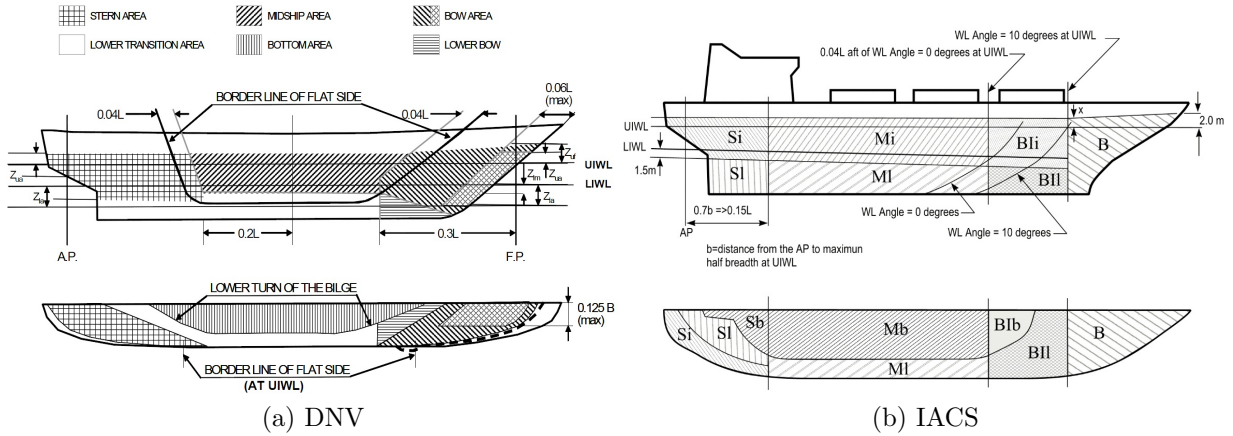


Figure 5.1: Ice reinforced areas from DNV and IACS rules[7]

IACS ice class rules have factors associated with each region which are used to interpolate from the design bow impact pressure.

5.3.2 DNV Design loads

The following section is based on the book *DNV hull structural rules : development, background, motives* by Det Norske Veritas[13]. Research and experience has shown that the loads imposed by ramming and subsequent beaching on large and hard ice ridges and floes may result in critical hull girder stresses.

The evaluation of the vertical bow impact design force is based on studies of the behavior of the hull girder when the ship is ramming an ice floe at a certain speed V_{RAM} , and the kinetic energy is transferred to a sliding/lifting motion of the bow, initially considered as a rigid body motion. In this studies both mathematical formula and a ship hull/ice interaction model were used.

The mathematical study involves simplify the elastic energy model and combine with expression for crushing energy and related to the input energy. The total kinetic energy of the ship is given by:

$$E_k = \frac{1}{2} \Delta \cdot V_{RAM}^2 \quad (5.1)$$

$$E_{IMP} = E_K \frac{\tan^2 \gamma}{\tan^2 \gamma + 2,5} \quad (5.2)$$

The impact energy is equated to the crushing energy, being a function of the nominal ice strength and the contact area. The vertical ice load force is then found and calibrated with

simulations and full scale measurements:

$$P_R = \left(C \frac{E_{IMP}}{\tan \gamma} \right)^{0,6} (\sigma_{ice} \tan \alpha)^{0,4} \quad (5.3)$$

The constant C in this formula has been calibrated by simulations, and this final formula is seen to involve Δ and V as a function of $\Delta^{0,6}V^{1,2}$.

Line load is when a vessel is trapped between moving ice floes and pressure is action simultaneously in the horizontal plane at water level and shall be taken as

$$q = \frac{165}{\sin \beta} h_{ice}^{1,5} \quad (5.4)$$

The basic local pressure is directly proportional to the ice crushing strength, multiplied with a weight factor F_A for the different areas of the hull.

$$p_0 = 1000 \cdot F_A \cdot \sigma_{ice} \quad (5.5)$$

The design pressure shall be applied over a corresponding contact area, given in the correction factor F_B . The area shall reflect the type of load and the design pressure is in general to be taken as

$$p = F_B \cdot p_0 \quad (5.6)$$

The correction factor F_B for size of design area A_C is given as:

$$F_B = \begin{cases} \frac{0,58}{(A_C)^{0,5}} & \text{for } A_C \leq 1,0m^2 \\ \frac{0,58}{(A_C)^{0,15}} & \text{for } A_C > 1,0m^2 \end{cases} \quad (5.7)$$

5.3.3 IACS Design loads

The following section is based on presentation notes of "IACS Requirements for Polar Class Ships, Overview and Background" by Claude Daley[5]. The basis for the Polar Rules is the concept that ice loads can be rationally linked to a design scenario. The design scenario in this case is a glancing collision with an ice edge. Parameters such as ice thickness, ice strength (crushing pressures), hull form, ship size and ship speed are all taken into account in the design code.

The load equation is derived from the solution of a collision model and the maximum impact force is than found by equating the normal kinetic energy of the ship with the ice indentation energy.

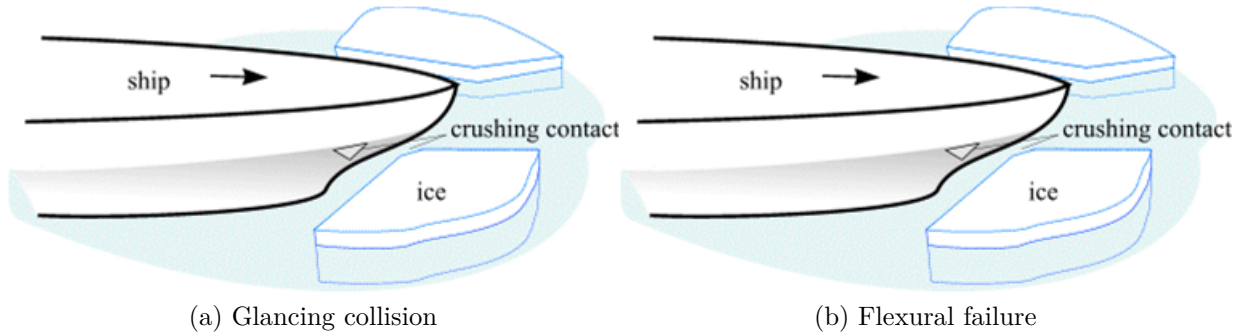


Figure 5.2: Design scenarios for derivation of ice loads[5]

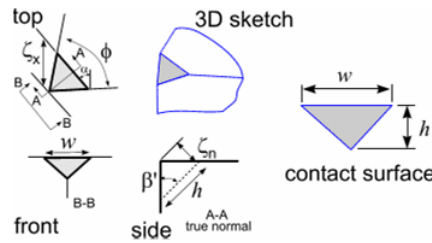


Figure 5.3: Contact area and penetration depth[5]

$$KE_{normal} = IE_{ice} \quad (5.8)$$

The kinetic energy is related to the effective mass and the normal velocity of the ship, this shall be equal to the integral of the normal force over the penetration depth in the ice.

$$\frac{1}{2} M_e \cdot V_n^2 = \int_0^{\delta_m} F_n(\delta) \cdot d\delta \quad (5.9)$$

Penetration geometry and pressure are needed to define the normal crushing force. Figure 5.3 indicates how the contact area is assumed to be a triangle and how the penetration length is found. Further is the equation for the normal ice load simplified, where the f_a factor take into account the bow area load characteristics.

$$F_n = f_a \cdot P_o^{0.36} \cdot V_{ship}^{1.28} \cdot M_{ship}^{0.64}$$

The rule equation is then simplified with class factors that represent the increasingly challenging ice conditions that different ice class are designed for. In deriving these values, ice thickness, strength and ship speed are all take into account.

$$F_n = f_a \cdot CF_C \cdot M_{ship}^{0.64} \quad (5.10)$$

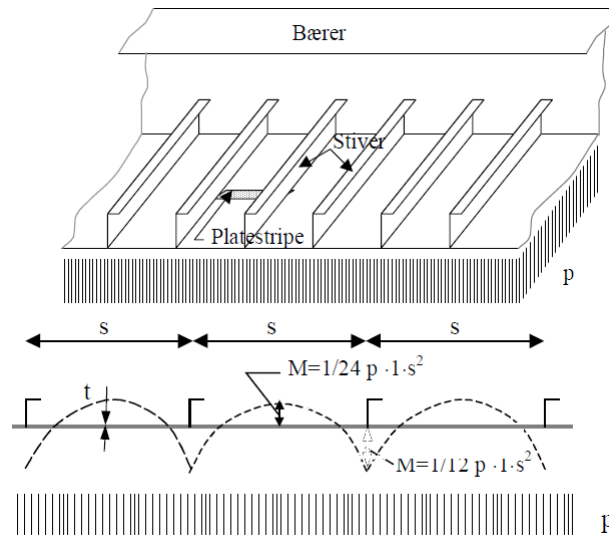


Figure 5.4: Plate strip analogy

From equation 5.10 the other rule equations for pressure P (equation 5.11) and line load Q (equation 5.12) can be derived.

$$P = F_n^{.22} \cdot CF_D^2 \cdot AR^{0.3} \quad (5.11)$$

$$Q = F_n^{.61} \cdot CF_D \cdot AR^{-0.35} \quad (5.12)$$

F_n = rule force

CF_D = Load patch dimensions class factor

AR = Aspect ratio

The aspect ratio is given as $AR = 7.46 \sin \beta'$ for the bow region. For the other areas than the bow the design load is taken as portion of the bow load. The different areas are defined based on the shape and waterlines of the vessel.

5.4 Plating requirements

5.4.1 DNV requirements

The DNV plating requirement is based on elastic methods of analysis and plate stripe analogy as shown in figure 5.4. When a plate is subjected to uniform pressure over a continuous plate field, the plate boundaries may be assumed clamped. The stripe analogy

is applicable for plates with large aspect ratio to predict the plate stresses. The thickness formula developed by DNV is based on the general formula for plate thickness derived in equation 5.15. According to the rules the bending stress is evaluated at the mid-span of the plate strip and not at the boundaries where the bending stresses is largest. This is probably to account for the increase in resistance of the plate at finite deformations due to development of membrane stresses.

$$W = \frac{1}{6}t^2 \quad (5.13)$$

$$M = \frac{p \cdot s^2}{m} \quad (5.14)$$

$$\sigma = \frac{M}{W} = 6 \frac{p \cdot s^2}{m \cdot t^2} \rightarrow t = \frac{77.4 s \sqrt{p}}{\sqrt{m \sigma}} \quad (5.15)$$

The plating requirement in ice is based on a wheel load patch area expression where an aspect ratio factor k_a and pressure distribution factor k_w is added to the thickness expression based on a plate strip.

$$t = \frac{77.4 k_a \sqrt{k_w c s p}}{\sqrt{m \sigma}} \quad (5.16)$$

This formula is then modified for determination of plate thickness for plates exposed to loads from ice, and the final rule expression for plate thickness should not be taken less than:

$$t = 23 k_a \frac{s^{0.75}}{h_0^{0.25}} \frac{\sqrt{k_w p_0}}{\sqrt{m_p \sigma_f}} + t_k \quad (5.17)$$

where

- k_a = aspect ratio factor
- k_w = pressure distribution factor
- m_p = bending moment factor
- h_o = height of contact area
- p_0 = basic pressure
- s = stiffener spacing

5.4.2 IACS requirements

The analysis model that IACS uses for polar ships is shown in figure 5.5. It is based on a yield line model where the plate folding is based on a perfectly plastic hinge formation. The method is further evaluated by equate internal plastic work with external work.

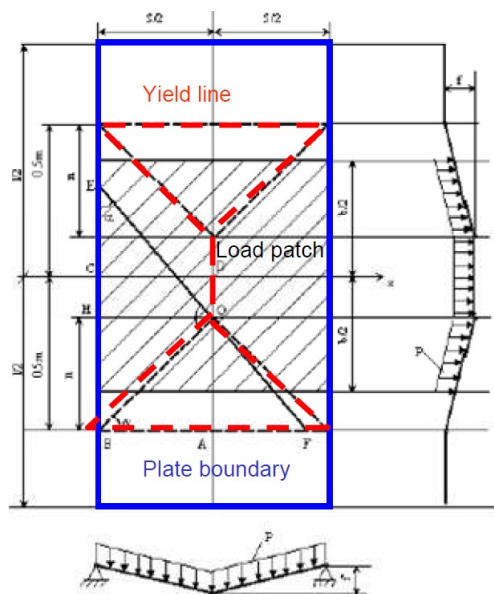


Figure 5.5: Yield line analysis according to IACS Polar ships

Introducing some simplification in the expression for the collapse resistance, and assuming the plate is loaded over the entire length the required plate thickness can be written as

$$t = 0.5 s \sqrt{\frac{p}{f_y}} \cdot \frac{1}{1 + s/(2b)} \quad (5.18)$$

The first term in this solution is recognised as the plate strip solution and the second part represents the plate aspect ratio effect. The formulation as it is expressed in the rules, the equation is simplified with tabulated values

$$t_{net} = 500s \sqrt{\frac{AF \cdot PPF_p \cdot P_{avg}}{\sigma_F}} \frac{1}{1 + s/(2b)} \quad (5.19)$$

where

- AF = Hull Area Factor
- PPF_p = Peak Pressure Factor
- P_{avg} = average pressure
- σ_F = material yield
- s = frame spacing
- b = height of design load patch

5.5 Framing requirements

5.5.1 DNV Stiffeners and Girder requirement

The formula for stiffener and girders are based on elastic bending of beams. Using basic mechanics the general expression for section modulus to a fixed beam can be found.

$$Z = \frac{M}{\sigma}, M = \frac{p \cdot s \cdot l^2}{m} \quad (5.20)$$

$$Z = \frac{p \cdot s \cdot l^2}{m\sigma} \quad (5.21)$$

This is the general expression for a uniform beam with length l . To make this equation valid for ice loads factors are included to cover size and distribution of the patch load. The rule formulation for longitudinal stiffeners shall not be taken less than:

$$Z = \frac{41h_0^{1-\alpha}l^{2-\alpha}p_0w_k}{\sigma \sin \beta} [cm^3] \quad (5.22)$$

- w_k = section modulus corrosion factor
- β = angle of web
- σ = 0.9 of material yield
- h_o = height of contact area
- p_0 = basic pressure
- l = stiffener span

5.5.2 IACS Stiffeners and Girder requirement

Stiffeners and girders formulation in the IACS rules are based on a simplified plastic collapse mechanism. For the framing requirement a 3 limit states is checked, two involving shear/bending and the third is pure shear. Figure 5.6 illustrates the three different following limit states; 3 hinge formation, shear panel formation and end shear.

A real structure would have substantial reserve at design load levels because of mechanisms are simplified and membrane stresses and strain hardening is ignored. The derivation of the formulation is based on energy methods which gives useful design equations. The rule requirement for a frame with ice load acting at the midspan of the transverse frame is given as

$$Z_{pt} = \frac{100^3 LL \cdot Y \cdot s \cdot (AF \cdot PPF_t \cdot P_{avg}) a \cdot A_{1A}}{4 \cdot \sigma_F} \quad (5.23)$$

- LL = length of loaded portion of span

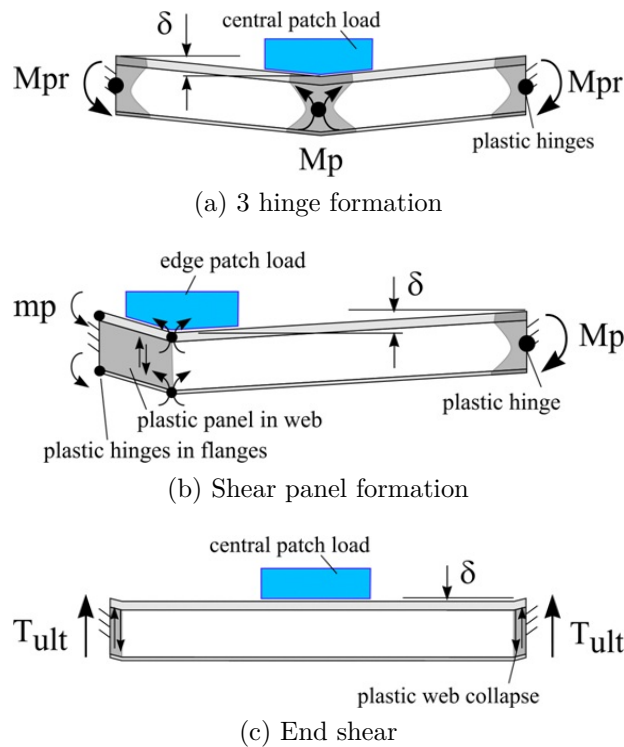


Figure 5.6: Three limit states for a frame

- $Y = 1 - 0.5(LL/a)$
 s = transverse frame spacing
 AF = Hull Area Factor
 PPF_t = Peak Pressure Factor
 P_{avg} = average pressure
 a = frame span
 σ_F = upper yield stress

5.6 Comparison of DNV and IACS rules

Through the last chapter two different ice-class rules, DNV and IACS, are reviewed with respect to design pressure from ice and the resulting hull scantlings. Both of these ice-class rules are being used today for ships navigating in ice.

The two rules are based on different principles, but the approach may give very similar results. DNV rules are based on the elastic methods of analyses, while IACS polar rules are based on the plastic method of analyses. Comparing the rules using only rule equations is difficult when the method of analysis is different. A numerical study between the two rule sets will give a better understanding about the difference.

Chapter 6

Numerical Comparison of Rule Requirements

In chapter 5, a review of the DNV and IACS rules were presented. To get a better understanding of the difference between the two rule set a short numerical study is presented in this chapter. The numerical study will focus on comparing design loads and plate thickness for the two different rule sets. The comparison will be performed only for the bow area.

The class rule requirements is functions of different hull parameters such as displacement, frame spacing and hull shape angels. In this comparison geometry from KV Svalbard has been used to give numerical values to the equations. However, since KV Svalbard already has a given class, some of the input parameters are made up.

It is important to keep in mind that the two rule sets are based on different approach of analysis, and the results are therefore not expected to be directly comparable. All rule requirements given are net requirements, i.e. additional requirements due to corrosion etc. are not included. The classes that is used in this numerical comparison is PC-1, PC-2, PC-3, PC-5 and PC-7 from the IACS rules, and POLAR-30, POLAR-20 and POLAR-10 with and without *Icebreaker* notation from the DNV rules.

6.1 Design load

The design loads from DNV and IACS are based on two completely different theories, and it is therefore of interest to see how the two different requirements compares. Local ice pressure is the governing factor for scantlings requirement, and will be the main focus in this section.

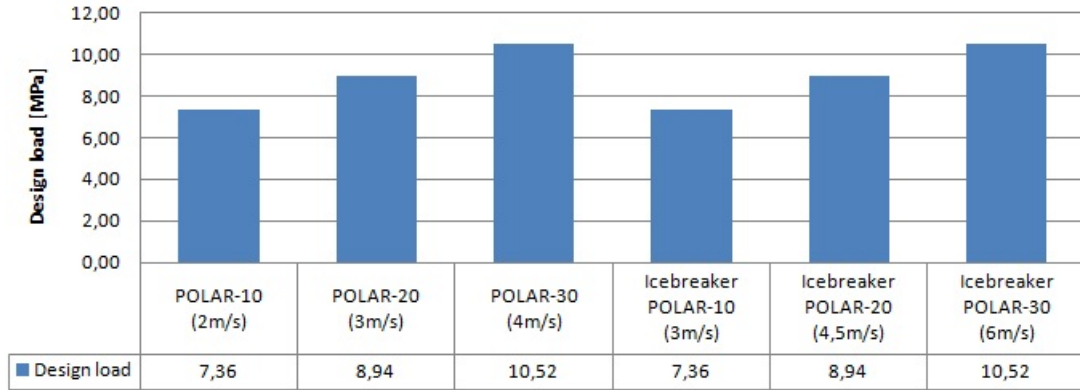


Figure 6.1: DNV design loads

6.1.1 DNV design load

The design pressure is a function of the basic local pressure, and from equation 5.5 in previous chapter we can see that the basic local pressure is directly proportional to the ice crushing strength. Ice crushing strength σ_{ice} is only dependent on the ice class, this can be found in table 5.2. Applied design load is therefore only dependent on the selected ice class.

Considering equation 5.6 for design pressure, the factor F_B accounts for the effect of contact area and is defined in equation 5.7. The size of the contact area has an important influence on the design load, and the contact area will vary from different vessels. If considering only one specific plate field the design load is only depending upon the class.

Figure 6.1 shows the DNV design load when considering a specific plate field from KV Svalbard. Higher ice class results in higher design loads which again results in higher structural requirements. The same plate field is used when calculating the different loads design loads using IACS rules. Since ice crushing strength for vessels with and without class notation *Icebreaker* is equal, the design pressure is equal for both notations.

6.1.2 IACS design load

Local ice pressure in the IACS rules is given by equation 5.11 in previous chapter. However, the pressure used in the scantling requirement are only depending on P_{avg} as defined in equation 6.1. b and w in the equation defines contact area. To simplify the different formulas IACS has introduced many class factors that is listed in tables, and the average pressure is depending upon all the class factors given in table C.6 except the Longitudinal Class Factor (CF_L). The factors take into account all the different parameters such as ice thickness, ice strength, hull form, ship size and speed. The main focus in this section is

Polar Class	Crushing Failure Class Factor (CF_C)	Flexural Failure Class Factor (CF_F)	Load Patch Dimensions Class Factor (CF_D)	Displacement Class Factor (CF_{DIS})	Longitudinal Strength Class Factor (CF_L)
PC-1	17.69	68.6	2.01	250	7.46
PC-2	9.89	46.8	1.75	210	5.46
PC-3	6.06	21.17	1.53	180	4.17
PC-4	4.5	13.48	1.42	130	3.15
PC-5	3.1	9	1.31	70	2.5
PC-6	2.4	5.49	1.17	40	2.37
PC-7	1.8	4.06	1.11	22	1.81

Table 6.1: Class factors used in IACS rules

limited to local ice pressure.

$$P_{avg} = \frac{F}{b \cdot w} \quad (6.1)$$

Figure 6.2 shows the design loads for the polar class using IACS rules. As opposed to the DNV rules, design load is proportional to the displacement when using IACS rules, and design pressure is therefore presented versus vessel displacement. It is clearly that displacement influences the design load, this is because they have used a energy model based on kinetic energy to find the design pressure.

6.1.3 Comparison of DNV and IACS design loads

Figure 6.3 show a comparison of DNV and IACS design loads for the selected classes. As mention, DNV design load will be constant when considering a specific plate field. Despite that the rules are based on two completely different design principles, the applied design load is in the same range.

The DNV design load seems to be somewhat smaller than the IACS loads, especially for vessels with large displacement. Comparing the design loads for KV Svalbard that have a Icebreaker POLAR-10 class in DNV, a class between PC-2 and PC-3 from IACS is comparable, illustrated in figure 6.3. The difference in design load could be explained with the fact that DNV rules are based on elastic analysis, and will typically underestimate the resistance compared with a plastic analysis.

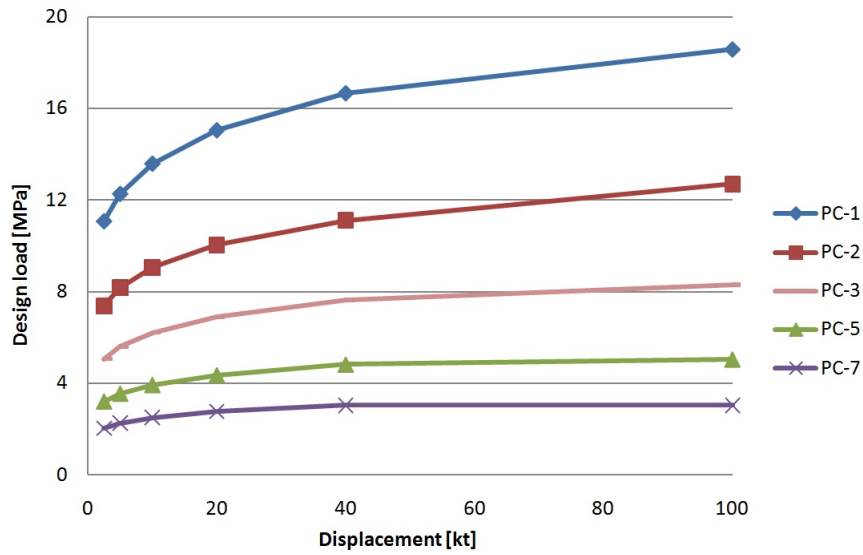


Figure 6.2: IACS design load

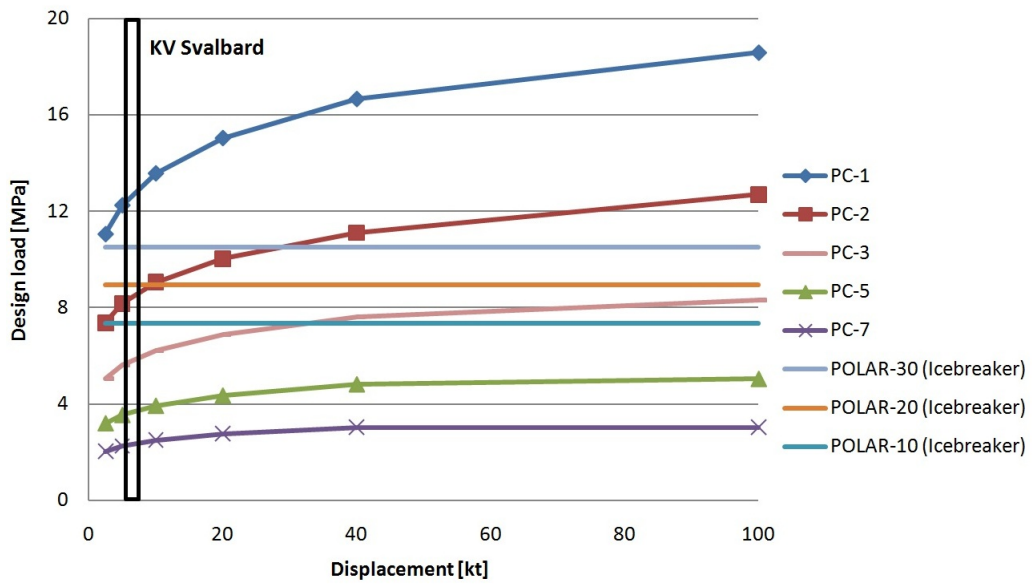


Figure 6.3: Comparison of DNV and IACS design load

6.2 Plate thickness requirement

The plate thickness requirement is derived to resist design pressure for selected class. DNV and IACS uses different theories of analysis to find the thickness requirement, as described in chapter 5.4.

Figure 6.4 shows the comparison of plate thickness as function of vessel displacement. Only the higher class from IACS is covered in this figure, the lower one has obvious smaller thickness than the ones given. The plate used for investigation is taken from KV Svalbard together with geometry such as hull shape angels.

The DNV plate thickness requirement is as given in equation 5.17

$$t_{net} = 23k_a \frac{s^{0.75}}{h_0^{0.25}} \frac{\sqrt{k_w p_0}}{\sqrt{m_p \sigma_f}} \quad (6.2)$$

The IACS plate thickness requirement is as given in equation 5.19

$$t_{net} = 500s \sqrt{\frac{AF \cdot PPF_p \cdot P_{avg}}{\sigma_F}} \frac{1}{1 + s/(2b)} \quad (6.3)$$

If we first consider a vessel with small displacement ($<20[\text{kt}]$) the requirements from DNV is quite high compared with the rules from IACS. For a vessel with larger displacement the plate thickness is comparable. The space between different DNV classes are considerably smaller compared with the IACS rules.

For both class rules, it seems that the design pressure is the governing factor. The shape of the required thickness curve in figure 6.4 from the IACS rules are similar to the design load curve.

6.3 Summary

This chapter presented a short numerical comparison of design loads and required plate thicknesses using class rules from DNV and IACS. The two sets of rules depends on two different design principles, and a numerical comparison is therefore more suitable to illustrate the difference between the rule sets.

Design load using the two different rules as illustrated in figure 6.3, shows that the IACS rules are generally higher for vessels with large displacement. The dependence of the vessel displacement is notable in the IACS rules, while for the DNV rules design load is independent on displacement. The IACS rules are typically most conservative for larger vessels

6. Numerical Comparison of Rule Requirements

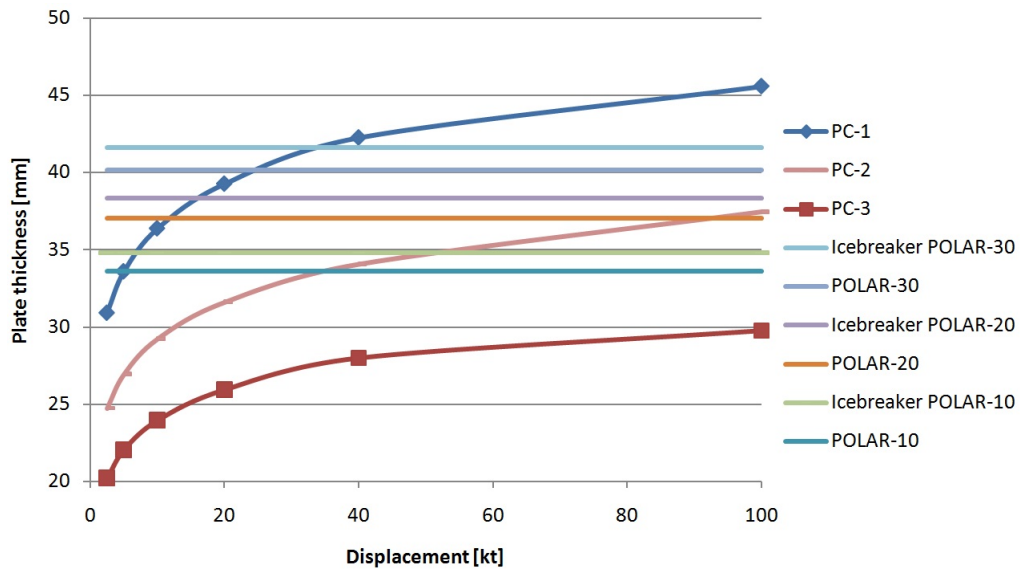


Figure 6.4: Comparison of plate thickness DNV and IACS

with large displacement, while the DNV rules are conservative for smaller vessels with small displacement.

Chapter 7

Estimation of Ice Resistance of Ships

The literature has provided a wide range of equations to estimate ship resistance in ice, but the quality of these formulas can be discussed. In general they are based on experience and observation of ships in service.

In this section a review of two formulations for estimation of ice resistance for ship will be presented. The methods is based on parameters that is easy accessible. The first formulation is collected from the paper *a straightforward method for calculation of ice resistance of ships* (Lindqvist, 1989)[11]. This paper also describes the ice breaking process in a physical and understanding way by identifying and simplify the problem. The second is a modification of the previous formulations given in the report *performance of merchant vessels in ice in the Baltic* (Kaj Riska, 1997)[17]. These two formulations will later be quantified and compared with resistance estimations from KV Svalbard that is a later part of this thesis.

Usage of these inexpensive analytical models can give an early estimation of the ice re-



Figure 7.1: KV Svalbard in ice

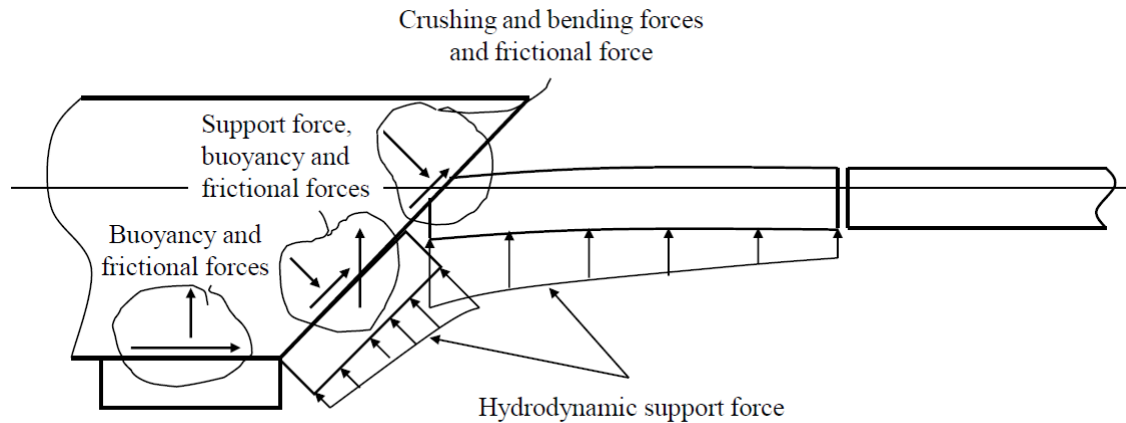


Figure 7.2: The forces acting in Ice breaking

sistance and most important, the power requirement. In future, as the knowledge of the physics behind icebreaking advances and more experience has been gathered, one can expect greater reliability from these types of formulation.

7.1 Lindqvist

This is a short review of the formulation Lindqvist published in his paper[11]. The approach used by Lindqvist is to identify the main components in the resistance and approximate the contribution with simple physical formulas. With this simplified approach, it is also easy to show how resistance is affected by main dimensions and hull form.

Lindqvist has not included all resistance components to describe the ice breaking process, but he has chosen the components that are generally accepted as dominating. The components that are included in his formulation of ice resistance are breaking, crushing and resistance due to submersion (buoyancy and frictional forces) together with the effect of speed.

7.1.1 Crushing

Crushing of ice occur almost continuous at the stem for a wedge-shaped icebreaker. It is observed that the force never grows large enough to break the ice in bending at the stem. This is due to the geometry of the bow and the undamaged ice, whereas further astern we will have cracks due to the interaction with the stem. It is difficult to determine the

magnitude of this force, and no exact formulation appears to exist.

$$F_v = \frac{1}{2} \sigma_b \cdot H_{ice} \quad (7.1)$$

In Lindqvist method this force is based on an intelligent guess. He estimates the average vertical force acting on the ice based on bending strength of ice, equation 7.1. With analysis of the force components Lindqvist came up with the following resistance force due to crushing

$$R_c = F_v \cdot \left(\tan \phi + \mu \cdot \frac{\cos \phi}{\cos \psi} \right) / \left(1 - \mu \cdot \frac{\sin \phi}{\cos \psi} \right) \quad (7.2)$$

7.1.2 Breaking by bending

Ice is best broken in bending, and it is clearly that this will happen at the bow some distance from the stem. The bending failure of the ice is initiated by crushing and shearing. As the ship hits a sharp edge of ice, the edge is crushed until the force is big enough to shear away a small piece of ice. The plane of failure is close to the contact area and the crushing of the edge will continue. The process with crushing and shearing continues and results in increased contact area with the ice. This process will continue until the force transmitted through the area is big enough to cause the ice to fail in bending.

The method by Lindqvist tries to describe the breaking process (as mention above) mathematical by using different assumptions. The mathematical calculation of the process will not be presented here, but the calculation is generally based on simplifying the problem. The required vertical force for breaking the ice is assumed and the force acting will increase linearly. The average vertical force necessary to break off one ice piece is then derived based on the assumption mentioned. Further this expression is used to find the total breaking resistance for the whole ship.

$$R_b = 0.003 \cdot \sigma_b \cdot B \cdot H_{ice}^{3/2} \cdot \left(\tan \psi + \mu \cdot \frac{\cos \phi}{\sin \alpha \cdot \cos \psi} \right) / \left(1 + \frac{1}{\cos \psi} \right) \quad (7.3)$$

The resulting expression for the breaking resistance gives some interesting values. First, the resistance is proportional to the ice thickness to the power of 1.5, which is very realistic value. Further is the resistance very dependent on the breaking angle psi which makes a bad performance to a wedge-shaped bow in thick ice.

7.1.3 Submersion

When a ship is running in level ice and the ice starts to break at the bow, ice floes starts to flow along the buttock lines of the ship. As ice is lighter than water, the buoyancy force

starts to create motion upwards. When the ice floes are lifted against the hull they give resistance through normal forces and friction.

When calculating the friction part of the submersion resistant, Lindqvist has assumed that the bow will be completely covered in ice and the bottom to be covered 70% of the length of ship. This knowledge is obtain threw observation of model tests and underwater observations of full-scale tests.

The mathematical expression for the submersion resistance is calculated by separate the loss of potential energy and frictional resistance. Loss of potential energy is estimated based on that the ice is evenly distributed along the ship. Further is the submersion draft for the ice floes under the ship equal to the ship draft, and the submersion draft for the side is assumed to be half the draft. When energy is described as force times distance Lindqvist made an approximation for the loss of energy.

The frictional resistance that is caused by the floes sliding along the hull is estimated by the lifting force from the density difference between water and ice and the frictional coefficient. Using approximation for the contact area described above an approximation of the submersion resistance is obtained:

$$R_s = (\rho_w - \rho_i) \cdot g \cdot H_{ice} \cdot B \cdot \left\{ T \frac{B+T}{B+2T} + \mu \left[\left(0.7 - \frac{T}{\tan \varphi} - \frac{B}{4 \tan \alpha} \right) + T \cos \varphi \cos \psi \sqrt{\frac{1}{\sin^2 \varphi} + \frac{1}{\tan^2 \alpha}} \right] \right\} \quad (7.4)$$

7.1.4 Speed

The breaking and submersion resistance have been estimated using relatively simple theory. How the speed will affect the resistance components are more uncertain. Many factors are suggested to influence the total resistance due to speed of the vessel. Such factors are: increase of breaking resistance, increase of submersion resistance, acceleration of ice floes, ventilation of ice floes and viscous drag. How much each factor influences the resistance is not known, but the resistance seems to increase fairly linearly with the speed. The total resistance is then obtained:

$$R_{ice} = (R_c + R_b) \cdot \left(1 + 1.4 \cdot \frac{v}{\sqrt{g \cdot H_{ice}}} \right) + R_s \cdot \left(1 + 9.4 \cdot \frac{v}{\sqrt{g \cdot L}} \right) \quad (7.5)$$

The method presented by Lindqvist gives an easy method of calculating the ice resistance. This formula is not a scientific explanation of the icebreaking process but a tool in the design process. The formula takes account of friction and hull geometry of the ship, which differs from many earlier formulations.

7.2 Riska

The ice resistance formulation published by Kaj Riska et al.[17] aimed to obtain the required powering for vessels operating in the Baltic Sea. With sufficient powering the transportation in winter time can be quick and continues without extensive use of ice-breakers. The work was a result of a five year program supported by the Finnish and Swedish Maritime Administrations.

The work was carried out together with an extensive collecting campaign during the five years of the program. The resulting formulation of ship resistance in level ice was then developed based on earlier formulations and calibrated with the new data obtained from observations of Finnish vessels.

The aim of the program was not only finding the resistance in level ice but an extensive effort was also put into developing formulation of resistance in old navigation channel. This is of great importance in the Baltic where the most common ice condition is navigating in these old channels. This section will only focus on the resistance in level ice.



Figure 7.3: Ferry breaking ice in the baltic sea

7.2.1 Level ice resistance

The formulation of ice resistance in level ice that Riska(1997) published are based on the assumption that the open water and ice resistance components can be separated and superimposed to obtain the total resistance.

$$R_T = R_{ow} + R_i \quad (7.6)$$

The open water resistance is usually very small compared with the ice resistance in ice-breaking speed so ignoring the cross coupling between ice and hydrodynamic forces does

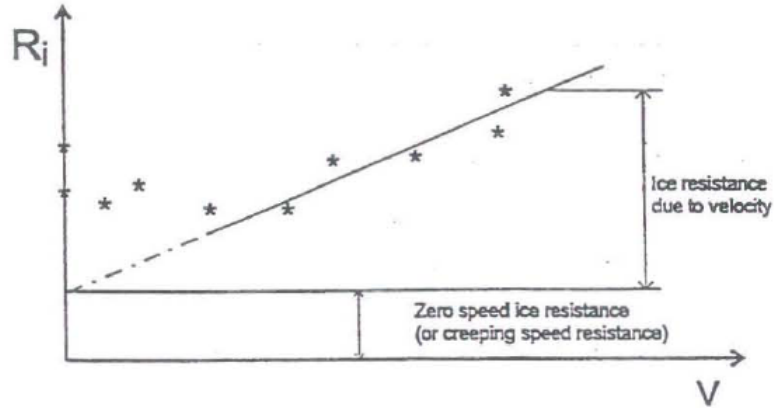


Figure 7.4: Ice resistance versus ship speed deduced from full scale tests

not lead into significant error.

Ice resistance is defined as the average value of towing force. When testing ship, the thrust is increased until the ship starts to move, then if the thrust is not reduced, the ship will speed up to a higher speed. This is because the ice resistance is higher at zero speed than at very low speeds. As the thrust further increases, the ship speed increases approximately linearly, as illustrated in figure 7.4.

The main ice parameter that will influence the level ice resistance is the ice thickness. Ice strength, density and friction between the ice and ship will also naturally influence, but the values of these can be assumed to be constant when estimating ice resistance for a area.

The parameters used in Riska's formulation can be divided into three groups. The first is the external parameters: ice thickness and ship speed. The two other groups describe the shape and size of the ship. The resulting equation for ice resistance is split into parts and the parameter dependency of each part is determined. The ice resistance and functions is as given

$$R_i = C_1 + C_2v \quad (7.7)$$

where

$$C_1 = f_1 \frac{1}{2\frac{T}{B} + 1} B L_{par} H_i + (1 + 0.021\phi)(f_2 B H_i^2 + f_3 L_{bow} H_i^2 + f_4 L_{bow} H_i)$$

$$C_2 = (1 + 0.063\phi)(g_1 H_i^{1.5} + g_2 H_i) + g_3 H_i \left(1 + 1.2 \frac{T}{B}\right) \frac{B^2}{\sqrt{L}}$$

$$f_1, f_2, f_3, f_4, g_1, g_2, g_3 = \text{constants}$$

To find the constants in the formula above Riska has modified already existing formulations from Ionov and Lindqvist. As the formulations shows, the speed dependency is assumed to be linear. If this is a good assumption is not mention, but Riska emphasizes that based on the scatter in the data available at the time no other form is appearing.

The formulations derived by Riska can be important when deciding the design requirements and power requirements. This formulation is based on previous formulations but modified, and does not give a scientific explanation of the icebreaking process. Simplifications is also made in order to only be dependent on main dimensions and the stem angle.

7.3 Comparison

The formulas presented will give a good prediction of the ice resistance. This kind of formulations can be a important tool when estimating required power consumption in a early stage of the design process. Riska's method is based on different formulation, among them is Lindqvist's formulation. To see how the formulations perform and if they are comparable, a numerical comparison is done. The main parameter from the coastal vessel KV Svalbard is used in this connection to quantify the ice resistance, see table 7.1. The main difference between Riska's and Lindqvist's formulation is the ice parameters, Riska has fixed these parameters based on experience while in Lindqvist's formulation they can be given by the user. When comparing the formulations the ice parameters are selected according to those given in Riska's study.

Looking at figure 7.5 and 7.6 the calculated results are comparable in most cases when the ice is thin ($h_i < 1m$). When the ice is thicker Lindqvist's formulations give a slightly higher resistance. It is possible that Lindqvist overpredicts the resistance, but without the true ice resistance for vessel it is not to possible to make a conclusion. Riska's formulation is of newer date and has been modified through an extensive validation program in the Baltic. Since the formulation by Riska is developed and validated in the Baltic, it is also expected a slightly difference in the result because of local conditions.

Description	Symbol	Value
Ship length between perpendiculars [m]	L_{pp}	89
Length of parallel midbody [m]	L_{bow}	27.2
Length of the bow at waterline [m]	L_{par}	36.3
Ship breath [m]	B	19.1
Ship depth [m]	D	10.8
Ship draft [m]	T	6.5
Ship displacement [t]	Δ	6530
Bow shape angles [deg]	α	35.0
	ϕ	34.0
	ψ	34.3
Hull/ice friction	μ	0.15
Ice strength [kPa]	σ	500
Difference in density (water/ice) [kg/m ³]	ρ_{Δ}	125

Table 7.1: Main properties of KV Svalbard used in the comparison

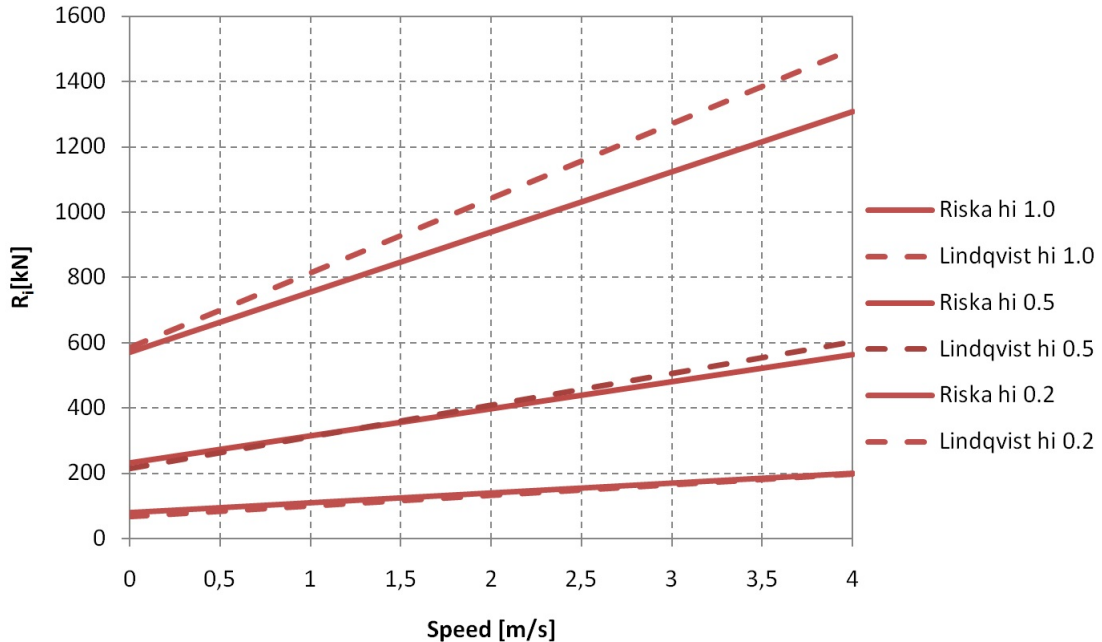


Figure 7.5: Ice resistance comparison Riska vs Lindqvist, different ice thickness

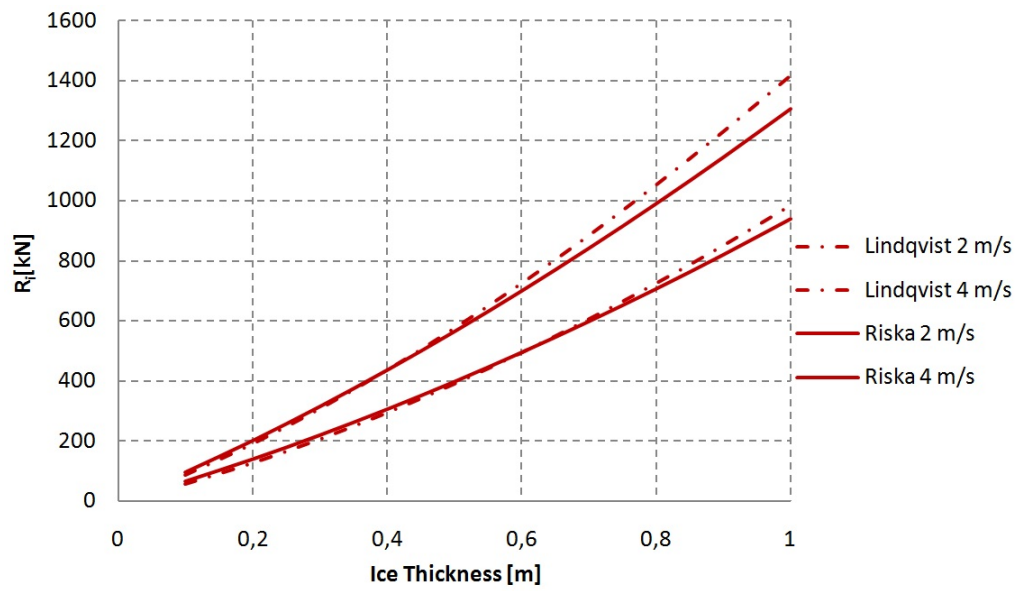


Figure 7.6: Ice resistance comparison Riska vs Lindqvist, different speed

Chapter 8

Measurement System for KV Svalbard

This chapter contains a short presentation of the Ice Load Monitoring system (ILM) mounted onboard the coast guard vessel KV Svalbard illustrated in figure 8.1. The system was mounted as a part of the project run by Det Norske Veritas. Other measurement systems which are not a part of the ILM system, but are used later in this thesis is also mentioned.

The hull monitoring system installed on KV Svalbard is a prototype of a planned Ice Load Monitoring system. The system installed during the voyage in March 2007 included only the three first components of the five following items.

1. Fiber Optic sensors to measure the strain at selected frames. The actual ice load is then possible to measure.
2. Electro Magnetic equipment to measure the thickness of the ice at the bow.
3. Necessary software and a computer to analyse and display measured data at bridge.

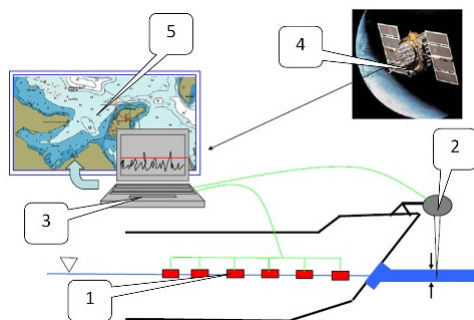


Figure 8.1: The Ice Load Monitoring system (ILM)

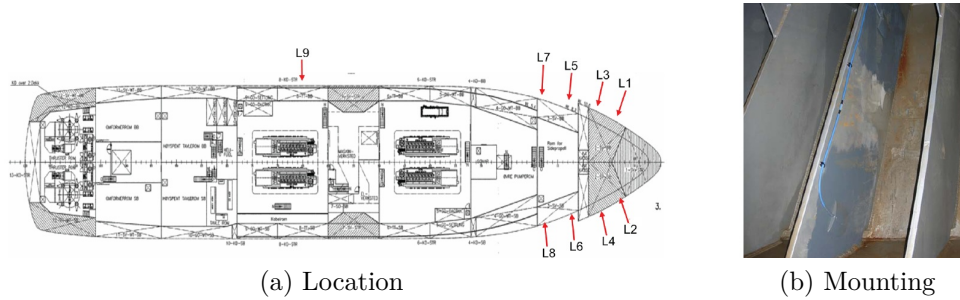


Figure 8.2: Frames instrumented with sensors

4. Utilize meteorological and satellite data and apply this data on the electronic chart.
5. Update and display the ice information continuously.

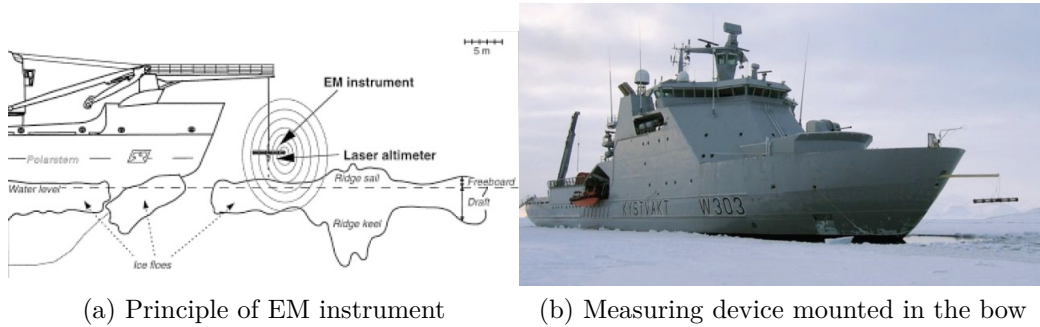
8.1 Fiber Optic strain sensors

Evaluation of the actual load on the hull is identified as one of the major uncertainties when operating a ship in ice. To measure the actual load, fiber optic strain sensors have been mounted onboard KV Svalbard. Fiber optic strain sensors are used because the advantages over an electrical alternative. This sensors offer high sensitivity and sampling rate, they are also relatively easy to install and have good resistance toward water, chemicals and electromagnetic interference. A total of 66 strain sensors where installed on 9 critical frames mainly in the bow area. The location of the strain sensors is indicated in figure 8.2.

8.2 Electro magnetic ice thickness measuring device

This section gives a short review of the technical report *Ship-borne sea ice thickness electro-magnetic measurements*[15] with emphasize on method description and accuracy. A more detailed explanation of the system can be found in the reference.

The ice thickness measurement system is composed of two instruments, an Electro Magnetic (EM) instrument to measure the distance between the EM system and the water surface d_{EM} , and a laser or a sonic altimeter to determine the height of the EM system above the ice surface d_{Sonic} , shown in figure 8.3. The ice thickness Z_i is then obtained as the difference between those two measurements. The thickness measured is the sum of snow plus ice thickness since the sonic measures the distance to the surface.



(a) Principle of EM instrument

(b) Measuring device mounted in the bow

Figure 8.3: Measuring of ice thickness[15]

$$Z_i = d_{EM} - d_{Sonic} \quad (8.1)$$

8.2.1 Method description

The EM instrument sends out an EM sound to measure the electrical conductivity structure of the underground. The underground is composed of a sea ice layer above a deep sea water layer. Since the conductivity of sea ice is very low the EM field penetrates the ice layer almost unaffected into the underlying sea water. Sea water has high conductivity which will be sensed by the EM instrument.

8.2.2 Accuracy over level ice

The accuracy of the EM ice thickness measurement depend on the sensitivity of the instrument, the actual ice thickness, instrumented height above the water surface and problems due to special situation in front of the ship. Thickness measurements is also strongly dependent on accurate calibration. The calibration will only be valid for a certain area, and open water of at least 50 meter in diameter is recommended to calibrate the EM.

The sensitivity of the instrument decreases with increasing instrument height above the water. This means a higher installation height or greater ice thickness results in a weaker signal. With an instrument height of 4m above ice surface and a thickness of 2m still can be measured with an accuracy of 0.1m.

In front of the ship, ice conditions are normally very variable. The ship passes often small floes or cracks which can result in numerous deviations of the ice thickness from the real ice thickness. Cracks in front of the ship might be seen by the sonic instrument, but not by the EM. These can under- or overestimate the true ice thickness. The thickness of pressure ridges gives the most inaccurate measurements over deformed ice. Because

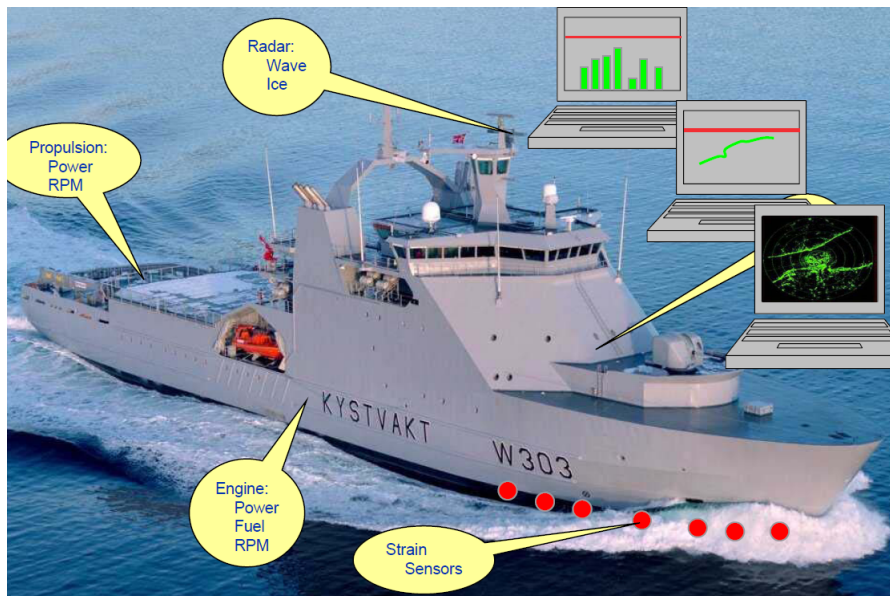


Figure 8.4: Different parameters measured onboard KV Svalbard

pressure ridges is rafted ice blocks that are unconsolidated they have a large porosity and a mixture of ice blocks and water. This highly increases the conductivity resulting in an underestimating in the maximum thickness.

8.3 Other measurements

KV Svalbard is equipped with many other sensors in addition to the ILM system. The most important parameters that used in this thesis are

- Vessel speed over ground
- Course over ground
- Ice thickness
- Power from Azipods
- Angles of Azipods

RPM, sea water temperature and ship motion is other parameters that also is available but not used in this thesis.

Chapter 9

Collected Data from KV Svalbard

This chapter presents the collected data that is used further in this thesis. They were collected in connection with research work done with KV Svalbard around Spitsbergen for a total of two weeks in late March 2007(19.March - 31.March 2007). During seven of this days from 22nd to 28th March 2007 KV Svalbard was operating in ice covered waters in Storfjorden and the Barents Sea. This chapter picks out data sequences of interest from the collected data. Additionally a section discussing the quality of the collected data and variations in ice thickness measurements. This chapter is inspired by Chapter 5 - Collected Data from Ice Action and Response Monitoring of Ships by Øyvind Espeland[22].

9.1 Sequences of Interest

In order to find data of particular interest for further analysis, a screening of the collected data is necessary. Favourable sections should have speed, power, heading and ice conditions that are not fluctuating. For this reason, the screening process focused on finding intervals with acceptable stable conditions.

9.1.1 Screening

The screening tries to separate interesting parts of data from parts with less relevance for estimation of resistance. Each day from March 22nd to March 28th is shortly described based on field reports and measured data, and sequences of interest are pointed out. The sequences of interest is presented in 10min length with mean values and standard deviation.

March 22nd

KV Svalbard transit northward through Storfjorden March 22nd, ice condition consist of refrozen polynya with low ice concentration and mostly nilas with small thickness[15]. Since the thickness sensor was not calibrated correctly until this day, no investigation of measurements from March 22nd is done.

March 23rd

This day the ice conditions are reported as rafted and ridged nilas with ice thickness around 50cm. After investigating the measurements from this day no interesting sequences was found, only small transfer in low speed was registered. No data from this day will be included in further analysis.

March 24th

The morning on March 24th KV Svalbard navigated through concentrated fast ice with a thickness around 60 cm[14]. Several promising intervals were found during the first hour, but the best interval found is between 05:08-05:38. The mean ice thickness from this interval is registered between 47–89cm, which agrees with the observed ice conditions.

Interesting shorter periods were also found scattered throughout the day. The ice conditions changed during the day, and mean ice thickness higher than 1.5m was measured. Reported ice conditions described heavily ridged ice resulting in that the vessel gets stuck with all engine running at full speed[15]. The speed is relative constant for each sequence, but the mean speed is varying from 0.71–3.39m/s for all sequences of interest from March 24th. Mean power is also constant for many of the sequences apart from the first two, and it generally seems that mean power increases with higher thickness. The selected sequences of interest with standard deviation is given in table 9.1, used further in the analyses.

March 25th

In the start of the day maneuver tests were carried out in fast ice in Freemansund. The speed and heading is therefore not stable, and this part of the day is not included further in the analysis. The rest of the day ice conditions were varying from thin pancake ice to parts that were heavily ridged[14]. Mean speed for the selected sequences varied between 2.23–3.32m/s with low standard deviation. Further is the mean power very stable with low

March 24th	Mean power	Std	Mean speed	Std	Mean ice	Std
05:08-05:18	1953	937	1.96	0.38	0.47	0.44
05:18-05:28	2997	710	2.29	0.18	0.63	0.48
05:28-05:38	3479	34	1.82	0.24	0.89	0.43
14:04-14:14	3231	65	3.18	0.17	0.45	0.20
14:29-14:39	3556	47	3.39	0.21	0.53	0.34
14:40-14:50	3587	73	1.26	0.56	1.32	0.25
14:50-15:00	3617	30	1.22	0.41	1.22	0.42
15:30-15:40	6656	121	0.71	0.15	1.68	0.34
15:55-16:05	9671	179	1.31	0.58	1.53	0.25

Table 9.1: Sequences of interest for March 24th

standard deviation, and the mean ice thickness is spanning from 5–131cm. The interesting sequences that was found is included in table 9.2.

March 25th	Mean power	Std	Mean speed	Std	Mean ice	Std
16:00-16:10	2546	24	3.13	0.07	0.41	0.19
16:10-16:20	2743	178	3.12	0.10	0.39	0.21
16:20-16:30	2854	39	3.17	0.11	0.45	0.22
16:45-16:55	3597	100	2.33	0.25	1.21	0.58
16:55-17:05	3557	115	2.23	0.30	1.31	0.64
17:05-17:15	3716	20	3.02	0.10	0.87	0.37
17:32-17:42	1976	31	3.32	0.11	0.05	0.22

Table 9.2: Sequences of interest for March 25th

March 26th

Through March 26th the ice conditions was varying, but the best data are found between 19:00 and 21:15. The speed for the different sequences are varying from 2.05–3.17m/s with with general low standard deviation. Ice thickness is stretching from 41–141cm, and the mean power seems to increase with ice thickness. Sequences of interest are given in table 9.3.

March 27th

The vessel stayed anchored to the floe the whole day, so no thickness data were measured this day[15].

March 26th	Mean power	Std	Mean speed	Std	Mean ice	Std
19:00-19:10	5330	761	2.33	0.60	1.41	0.82
19:10-19:20	2331	73	2.60	0.25	0.92	0.43
19:20-19:30	2250	56	2.35	0.12	0.94	0.42
19:30-19:40	2407	59	2.85	0.18	0.65	0.36
19:40-19:50	2470	29	3.05	0.09	0.51	0.26
19:50-20:00	2466	47	3.07	0.11	0.44	0.29
20:00-20:10	2488	64	3.17	0.19	0.41	0.49
20:10-20:20	2292	39	2.49	0.13	0.95	0.37
20:20-20:30	3144	679	2.41	0.26	1.14	0.39
20:30-20:45	3727	136	2.79	0.28	0.93	0.55
20:45-20:55	4717	714	2.33	0.51	1.33	0.82
20:55-21:05	4422	1365	2.12	0.38	1.29	0.77
21:05-21:15	2934	752	2.05	0.22	1.04	0.69

Table 9.3: Sequences of interest for March 26th

March 28th

March 28th was the last day of the voyage, KV Svalbard headed north through 90-100% first year ice mainly with big level floes. The speed variations made it difficult to find usable sequences, and therefore no measurements are used from this day.

9.2 Quality of measurement

This section discusses shortly the quality of measurement used from KV Svalbard collected during the voyage in late March 2007. Power, speed and ice thickness measurements makes the basis for resistance formulation presented in chapter 10, and the quality of data should therefore be discussed.

9.2.1 Power measurements

Measurements of power output is assumed to be quite accurate, and the measured values are stable and does not fluctuate much. When the vessel is at rest the recorded power still gives a positive value, but in comparison with recorded power at full speed, a error around 1% is neglectable.

9.2.2 Speed measurements

Speed is measured with GPS, where speed is calculated based on positions. This means the speed over ground is quite exact, but in many cases this is not equal to the relative speed due to drift. The contribution from drift to the relative speed is assumed to be neglectable. Measured speed over ground is therefore a good approximation for the relative speed.

9.2.3 Ice Thickness Sensor

Ice thickness is one of the most important parameter when dealing with resistance in ice, but also the one most difficult to measure. The validity of the ice thickness measurements done during the voyage in March 2007 is questionable. For instance is negative values found which is physical impossible and should be investigated. This section will discuss the validity of the collected ice thickness and present possible explanations.

Calibration error and sensor uncertainties is a natural source of error. The accuracy of the electro magnetic ice thickness measuring device was discussed in section 8.2. Assuming an instrument height of 4 meters over an area between $12 m^2$ and $16 m^2$ a accuracy of the measurements is about 0.1m in level ice. The accuracy is expected to be lower for pack ice. Other source of error, also mention in section 8.2, is motion of the ice sensor, uneven ice sheet, submerged ice features or ice crack in front of the measuring device.

The model outlined to describe resistance in ice, reviewed in chapter 10, is based on average ice thickness. Small errors or deviation will therefore not influence the average value notable. Calibration errors or other source of measuring error that gives a constant deviation is on the other hand not desirable, and can result in bad results. Based on the data available it is difficult to give an estimate of the total error of the measurements. In many cases ice thickness can be measured relatively good, but it should be kept in mind that ice is not only a length parameter also strength parameter.

Distribution of ice thickness

To illustrate how much the ice thickness can vary for a given time, the sequences from March 26th were picked and plotted in a density plot, see figure 9.1. This sequence selected was chosen due to stable speed and relative constant ice thickness. The figure displays all the ice thickness samples obtain between 19:00 and 21:15, and the mean ice thickness is equal to 0.92 m with standard deviation 0.63 of for the hole sequence. Observing negative values in the time series is clearly measurement error, but they are few and the deviation from zero small.

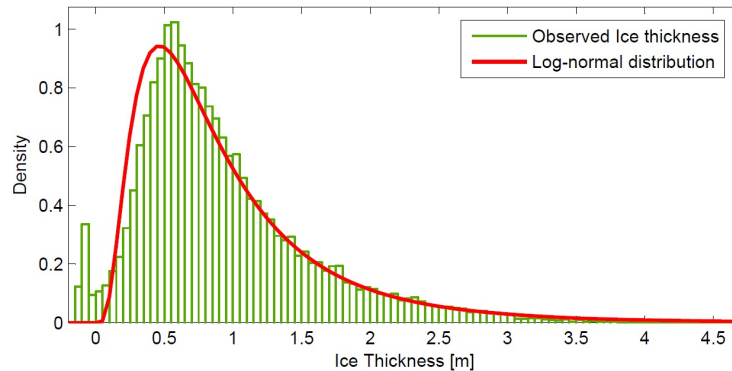


Figure 9.1: Ice observations from March 26th

A log-normal distribution is fitted to the positive data. This is suggested as a model for level ice observations[22]. The suggested distribution is skewed to the left, this indicates that the observations are slightly higher than the level ice model.

9.2.4 Summary of screening and quality of measurements

The screening process of this data has identified different intervals of interest from the voyage. Sequences from three of the days were pointed out based on stable conditions and reported ice conditions. These sequences are recommended for further analysis. Since the measurements are used for estimating the resistance in ice, the quality of the measurements used is discussed.

Power and speed measurement is found to be quite accurate, while the ice thickness measurements are questionable. In calm weather with level ice and correct calibrated measurement equipment the accuracy should be good, but the conditions during the voyage with ice ridges and different types of floes and openings the accuracy is lowered. If the ice thickness is underestimated or overestimated is difficult to conclude, but studying the mean thickness and density distribution of ice thicknesses for the different sequences and compare with manual observations, it seems like the mean ice thickness is over predicted for some sequences. The ice thickness is however been regarded as applicable for this thesis, but an uncertainty to the results of the ice thickness measurements should be kept in mind.

Chapter 10

Resistance Formulation

As the growing Russian oil and gas market opens to western markets the number of ships strengthened for ice breaking operations will increase. This include ship types as ice breakers, offshore support ships, oil tankers, LNG transport, bulk carriers, and to some extent also container carriers and passenger cruise vessels. The ice resistance can be an important parameter e.g. in order to estimate the additional transportation cost for arctic as compared to non-arctic areas. The following chapter presents how ice resistance can be estimated based on available measurements of ice thickness, speed and power.

When a ship proceeds in ice a resistance arises when the ship crushes and breaks ice floes, turns them parallel to the ship hull and forces them to slide down and eventually up along the hull. The forces have large variations in time partly because the breaking process is not continuous. Ice resistance is defined as the average value of the instantaneous total force, see figure 10.1.

The parameter that can be measured continuously is the power required to proceed in a certain ice condition with a constant average speed. The propulsion power is a good

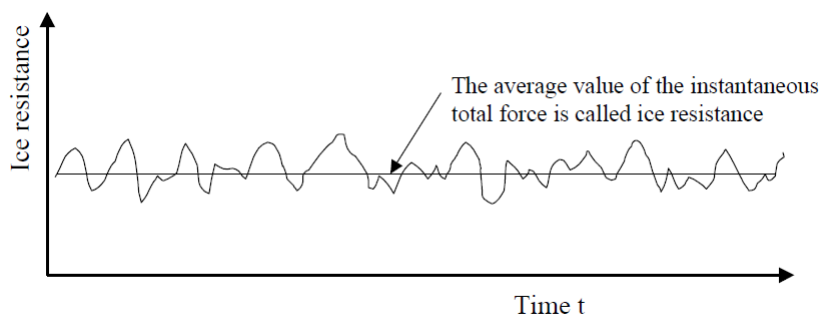


Figure 10.1: Ice resistance is an average force

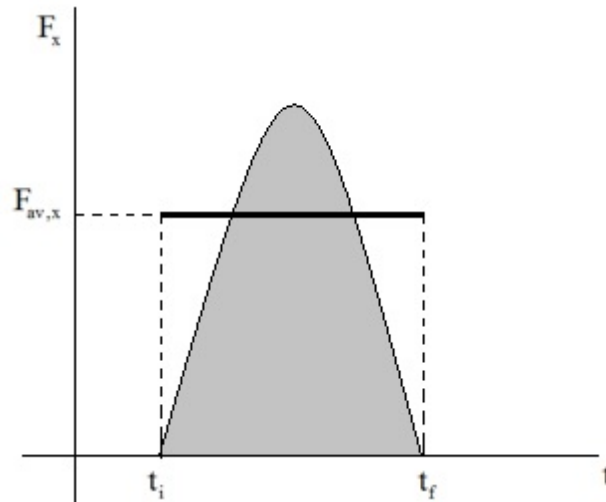


Figure 10.2: Time variation of force during collision and average force

parameter to use when estimating ice resistance because the ship performance in ice is strongly related to the output power.

10.1 Conservation of energy

The law of conservation of energy is an empirical law of physics. It states that the total amount of energy remains constant over time in an isolated system. This means that energy can neither be created or destroyed, it can only be transformed from one state to another. A way to transfer energy into or out of a system is do work on the system from the outside. Assuming this is the only method of energy transfer the law of conservation of energy becomes

$$W_{ext} = \Delta E_{sys} \quad (10.1)$$

Where W_{ext} is the work done on the system by external forces and ΔE_{sys} is the change in the system's total energy. This theorem is a powerful tool for studying a wide variety of systems.

10.2 Average Force

Figure 10.2 shows the time variation of the magnitude of a typical impulse load. During the time of the impulse load $\Delta t = t_f - t_i$ the force is large. The impulse \vec{I} of the force is

defined as

$$\vec{I} = \int_{t_i}^{t_f} \vec{F} \cdot dt \quad (10.2)$$

The average force for the interval $\Delta t = t_f - t_i$ is defined as

$$\vec{F}_{av} = \frac{1}{\Delta t} \int_{t_i}^{t_f} \vec{F} \cdot dt \quad (10.3)$$

The average force is the constant force that gives the same impulse as the actual force in the time interval Δt . Ice breaking induces impulse forces when the ice sheet repeatedly breaks, and based on equation 10.3 the average force can be calculated. The proposed formulation in this chapter uses the average force delivered by the propulsion system with corresponding ice thickness to estimate the average resistance force.

10.3 Resistance Formulation

Using the law of conservation of energy for estimating resistance in ice of a ship, an isolated system has to be defined. Choosing the ship as the system makes it is easy to determine the energy into or out of the system. The total forces done by all the forces W_{Total} equals the change in kinetic energy of the system $\Delta E_{K,sys}$.

$$W_{Total} = \Delta E_{K,sys} \quad (10.4)$$

The change in kinetic energy in the system can be derived from Newton's second law of motion, equation 10.5. Net force is allowed to change magnitude as long as the system is rigid. M is the displacement of ship, and v is the velocity of the ship at a given point in time.

$$\begin{aligned} W_{Net} &= \int_{s_0}^{s_1} F_{Net} \cdot ds = \int_{s_0}^{s_1} Ma \cdot ds \\ &= \int_{s_0}^{s_1} Mv \cdot \frac{dv}{ds} \cdot ds = \int_{v_0}^{v_1} Mv \cdot dv \\ &= M \int_{v_0}^{v_1} v \cdot dv = M \cdot v^2 \Big|_{v_0}^{v_1} \\ &= \frac{1}{2} Mv_1^2 - \frac{1}{2} Mv_0^2 \end{aligned} \quad (10.5)$$

The total work done on the system is equal to the difference between work from propeller and work from resistance.

$$W_{Total} = W_{Thrust} - W_{Resistance} \quad (10.6)$$

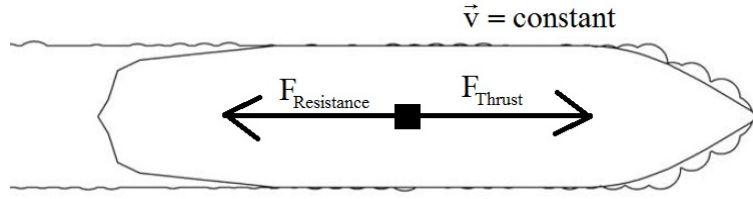


Figure 10.3: Equilibrium between resistance and thrust when speed is constant

Thrust from the propellers is not usually measured because it requires advanced measuring instruments, however power delivered to the shaft is common available parameter. The power describes the rate at which work is performed or energy converted. For a ship driven by propeller thrust, power is the rate which the mechanical work from the shaft is converted. The integral of the power usage for a period of time gives the amount of work performed to overcome the resistance for that period. Work done by the resistance is assumed equal to the work done by the thrust

$$W_{Thrust} \approx \int_{t_0}^{t_1} P_{Output} \cdot dt \quad (10.7)$$

Inserting equation 10.8 into equation 10.6 and inserting the change in kinetic energy for W_{Total} which describes net work, we get the following relation.

$$\int_{t_0}^{t_1} P_{Output} \cdot dt - W_{Resistance} = \frac{1}{2}M (v_1^2 - v_0^2) \quad (10.8)$$

Relocating equation 10.8 to get the resistance term, resistance now is equal to the sum of work done by the thrust and the change in kinetic energy.

$$W_{Resistance} = \int_{t_0}^{t_1} P_{Output} \cdot dt + \frac{1}{2}M (v_0^2 - v_1^2) \quad (10.9)$$

A formulation of the work done by the resistance for a sequence is found in equation 10.9. Dividing the work done by the resistance with the distance the system has moved gives the average resistance force for the selected sequence as given in equation 10.10. The distance the system has moved can be calculated by integrating the vessel speed over the sequence time, as in equation 10.11.

$$F_{Resistance,seq} = \frac{W_{Resistance,seq}}{\Delta S_{seq}} \quad (10.10)$$

$$\Delta S_{seq} = \int_{t_0}^{t_1} v(t) \cdot dt \quad (10.11)$$

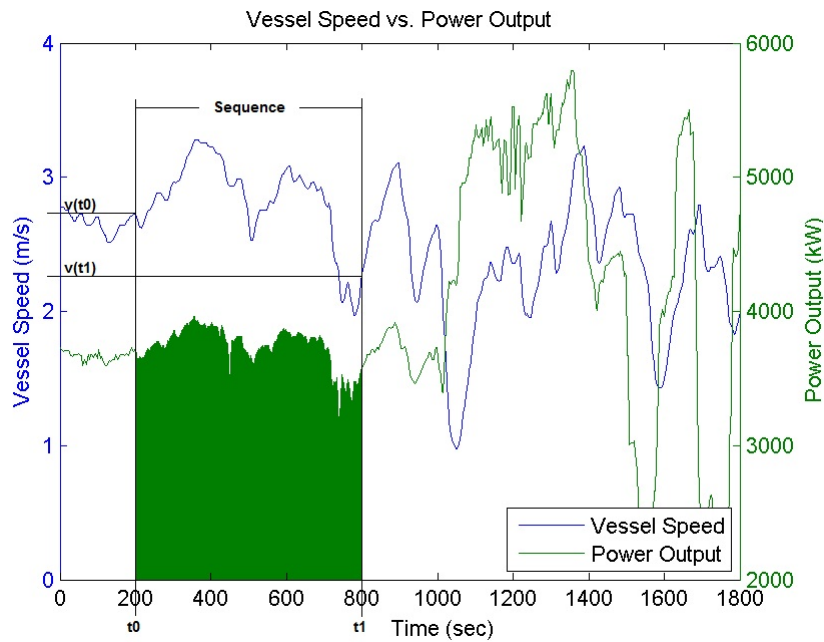


Figure 10.4: Time sequence illustrated

Figure 10.4 shows briefly how the resistance can be calculated from available measurements. In this illustration a sequence length of 10 minutes or 600 seconds is selected.

10.4 Summery

Based on the law of conservation of energy a formulation is outlined to estimate the resistance for a particular case. The formulation uses the parameters ice thickness, speed and power in the estimation, parameters that also is measured onboard KV Svalbard during the voyage in March 2007. The formulation outlined simplifies the ice breaking problem, but the estimations should give reasonable prediction for a given ship if the quality of measurements is good.

Chapter 11

Processing of Collected Data

The previous chapter derived a formulation using energy conservation to estimate resistance in ice based on measurements of speed, ice thickness and power. During the scientific voyage with KV Svalbard late in March 2007 measurement from the Ice Load Monitoring system (ILM) were saved for later processing and related research. The measurements collected during this voyage is summarized in chapter 8, further is sequences of interest picked out as described in chapter 9. This chapter will use the sequences of interest found in chapter 9 and the proposed model to estimate the resistance for KV Svalbard in ice.

11.1 MATLAB System

Data that was received contained measurements from different sensors on board KV Svalbard. The different storage files received and belonging parameters is given in table 11.1. Measurements were collected at different frequency, and due to relatively high sampling frequency MATLAB was used to handle the large amount of data. The following section gives a short description of how the data was managed in MATLAB.

11.1.1 Screening

A simple screening script was made to visualise the measurements and find sequences of interest for further analysis. The screening process was done manually and therefore time consuming. Sequences of interest was found, and different scripts was made to analyse the data further.

Sensor	Parameter
<i>Azipod sensor</i>	AZ1RPMSetpunkt
	AZ1RPMAktuell
	AZ1Angleactual
	AZ1AngleCommand
	AZ1Power
	AZ2RPMSetpunkt
	AZ2RPMAktuell
	AZ2Angleactual
	AZ2AngleCommand
	AZ2Power
<i>Ice sensor</i>	IceThickness
<i>Navigation sensor</i>	Latitude
	Longitude
	Speed Over Ground
	Course Over Ground

Table 11.1: Measurements received

11.1.2 Loading and selecting data

To process the measured data it was loaded from files into MATLAB, a simple script was made for this purpose. All measurements was further loaded into different matrix's where they were easy accessible for other scripts. Despite that the measurement have different sampling frequency, a time and date tag is linked to the measurements to keep track. Using the tag made it easy to find sequences of interest and pick them out from the different matrixes.

11.1.3 Processing and analysing

No additional processing or filtering is done with the data received. An attempt to down-sample the measurements was done, but it was concluded that is was unnecessary. Further is different scripts and functions made for generation of plots and other repeated tasks.

The script used to analyse the sequences of interest using the proposed formulation from previous chapter saves the results to an excel file for further process of the result. To solve the integrals in the proposed formulations a trapezoidal rule that is implement in MATLAB was used.

11.2 Results

This section will present the results from the analysis run in MATLAB. The result is presented for each day of the voyage with sequences of interest. The results from each day will be shortly commented. Further in next section, the results are compared with existing formulation of ice resistance. Fitting of statistical models to the calculated data is discussed in later chapter 12.

11.2.1 March 24th

The results using sequences of interest from March 24th are illustrated in figure 11.1 and 11.2. 10 minutes long sequences were used in the first analysis, while in the second analysis the sequence length was reduced in half. The resulting resistance force that is calculated shows a clear trend to increase with increasing mean ice thickness. As commented in chapter 9 and as illustrated in the figures, the vessel encounter heavily ridged ice during this day which resulted in high resistance. Since the vessel got stuck in ridged ice, it is uncertain if the results from the sequences with heavy ridges can be used later as a model for continuous resistance in ice.

Dividing the already 10 minutes long sequences into 5 minutes long sequences can be useful in many ways. First, the number of data points increases which is an advantage for statistical analysis of the data. On the down side it is expected that further dividing will increase the scatter of the data. The length of the sequences should be chosen in such way that a clear trend is formed. Inspecting the results from March 24th, sequences with length of 5 minutes is acceptable. Further dividing into shorter sequences is investigated and do not give any particular new information, and the results seems to be rather more scattered.

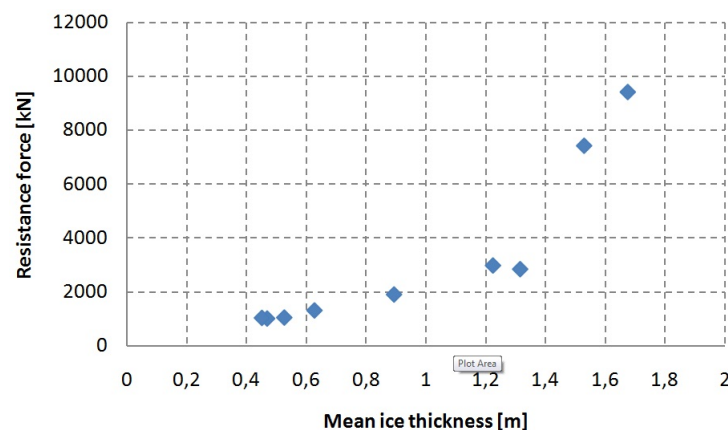


Figure 11.1: March 24th - Resistance vs mean ice thickness, 10 min sequences

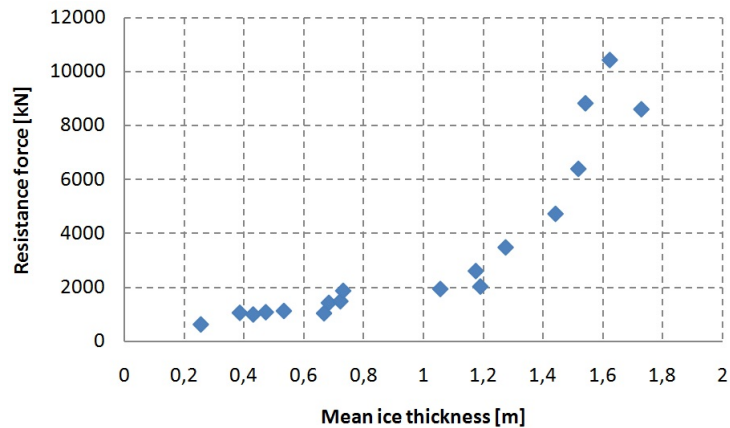


Figure 11.2: March 24th - Resistance vs mean ice thickness, 5 min sequences

11.2.2 March 25th

The first to notice comparing the results from March 25th in figure 11.3 and 11.4 with the previous results from March 24th is that the resistance looks noticeable lower. The difference is obvious a result in different ice properties. As mention the vessel experienced heavily ridges during March 24th while the ice conditions during March 25th was more moderate. Yet for lower ice thicknesses (<1.2m) the results are comparable and follows an apparently straight line. Also for March 25th it looks acceptable to split into 5 minutes long sequences, but it is noted that data is grouping for some ice thicknesses.

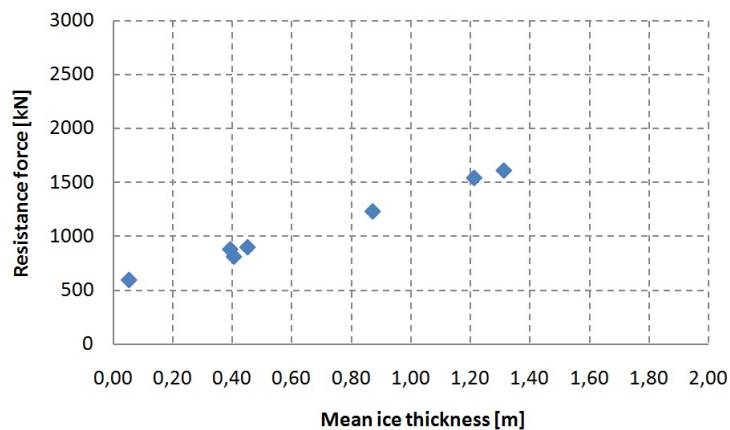


Figure 11.3: March 25th - Resistance vs mean ice thickness, 10 min sequences

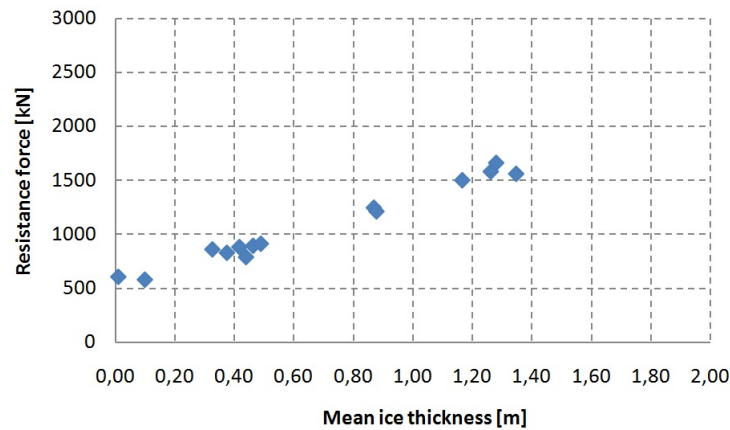


Figure 11.4: March 25th - Resistance vs mean ice thickness, 5 min sequences

11.2.3 March 26th

The last day with measurements the same trend as the previous results appears, increasing mean ice thickness gives a corresponding increase in the resistance force. Compared with the two other days, the number of data points is nearly twice from March 26th which is a good basis for further analyses. The plot with 5 minutes sequence length in figure 11.6 indicate that the results is more scattered compared with the 10 minutes sequence length in figure 11.5. A good regression line is more difficult to draw if the results is scattered, this will be discussed in the next chapter.

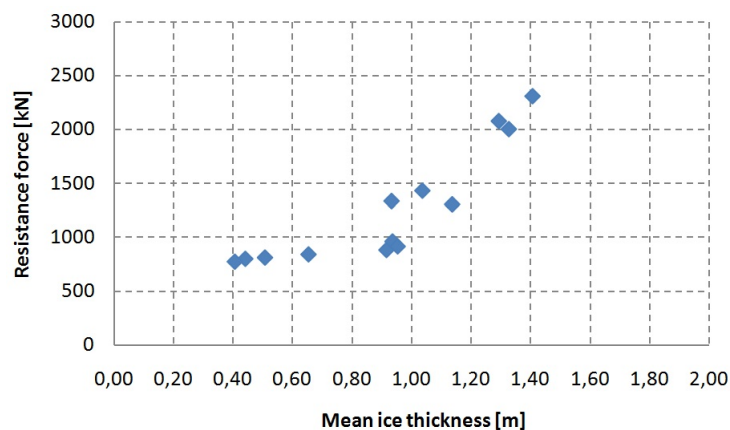


Figure 11.5: March 26th - Resistance vs mean ice thickness, 10 min sequences

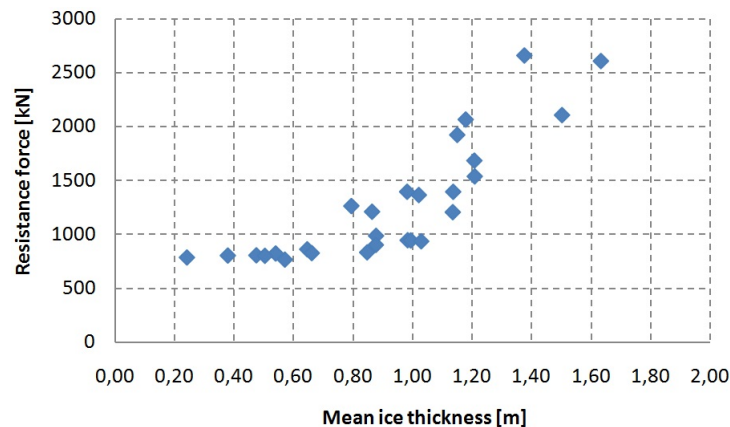


Figure 11.6: March 26th - Resistance vs mean ice thickness, 5 min sequences

11.3 Comparison and summary

Figure 11.7 and 11.8 shows the results from all three days compared. It should be noted that some of the highest values from March 24th are left outside the range of the axis. As commented, the highest values from March 24th are not comparable with results from the other days. It seems to be a clear correlation between the three days for lower ice thicknesses, while for higher ice thicknesses there is a wider range of scatter in the results. This scatter is obvious from different ice properties or small error from ice thickness measurements. While the results from March 25th and 26th compares quite good, the results from March 24th indicate a slightly higher resistance for increasing ice thickness.

Reducing the length of the sequences from 10 minutes to 5 minutes gives obvious additional data points, but as illustrated the scatter becomes larger. How long sequences that is necessary to give a good trend depends much on the quality of the measurements and how much data that is available. Based on the amount of sequences of interest and the quality of the data, sequences with length between 5-10 minutes is preferable for the data set used in this thesis.

11.3.1 Comparison with existing formulation

In chapter 7, two different formulations for ice resistance was presented. Comparing the estimated resistance in ice with already existing formulation gives a possibility to compare the results with models based on research and tests results. The resistance obtained by using formulations from literature gives the ice resistance, and to get the total resistance, open water resistance should be added. The estimated resistance using measurements from KV Svalbard gives the total resistance in ice. It is therefore expected that the formulations from literature gives a lower value compared with the calculated.

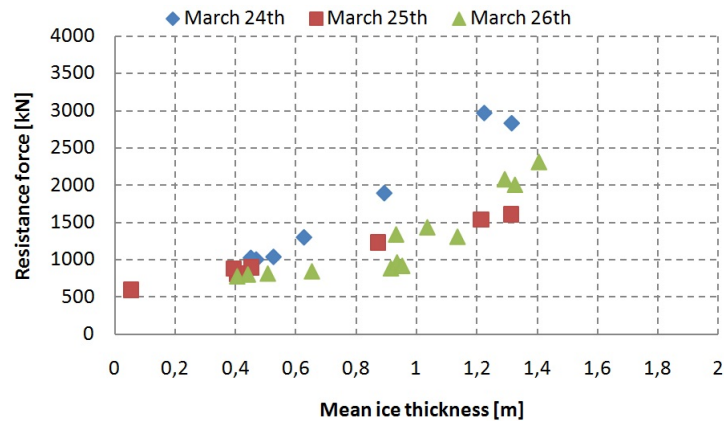


Figure 11.7: March 24th–26th - Resistance vs mean ice thickness, 10 min sequences

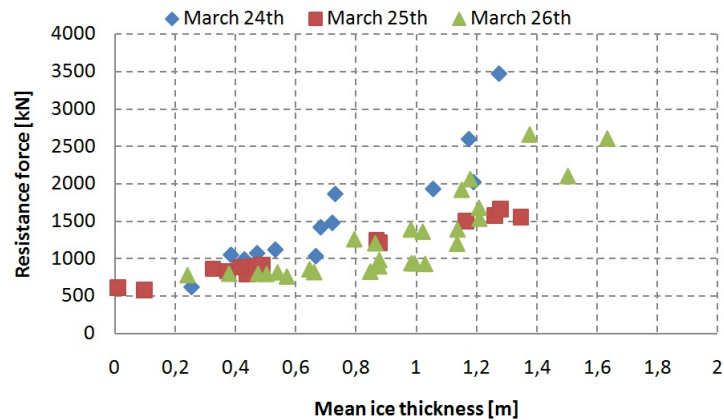


Figure 11.8: March 24th–26th - Resistance vs mean ice thickness, 5 min sequences

Comparing the formulations with the estimated resistance as illustrated in figure 11.9 it appears that the estimated resistance is higher than the one calculated from formulations. As commented the open water resistance is not included in the equations by Riska and Lindqvist. To illustrate the effect of open water resistance an intelligent guess of this resistance components is done. Using the measurements where the ice thickness is about zero an open water resistance is estimated to be around 500 [kN]. With a shift of the axis to the resistance from literature set equal to 500 [kN] gives the figure 11.10. Comparing the estimated data with the formulations with a shift indicate nearly the same trend and resistance level. The results from March 24th show a slightly higher resistance than the highest resistance from using Lindqvist's formulation.

The formulations by Riska and Lindqvist is illustrated in figure 11.9 and 11.10 is a function of constant speed. The speed during the voyage with KV Svalbard in late March 2007 is measured around 2-4 m/s, and the curves is in the same range. Comparing the estimated

11. Processing of Collected Data

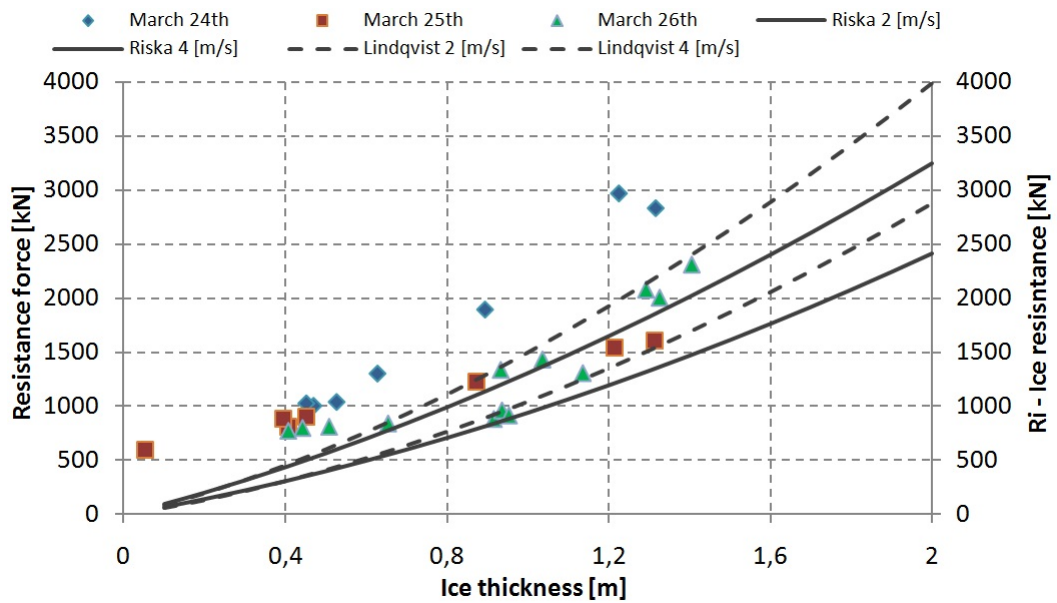


Figure 11.9: Results compared with Riska and Lindqvist formulations

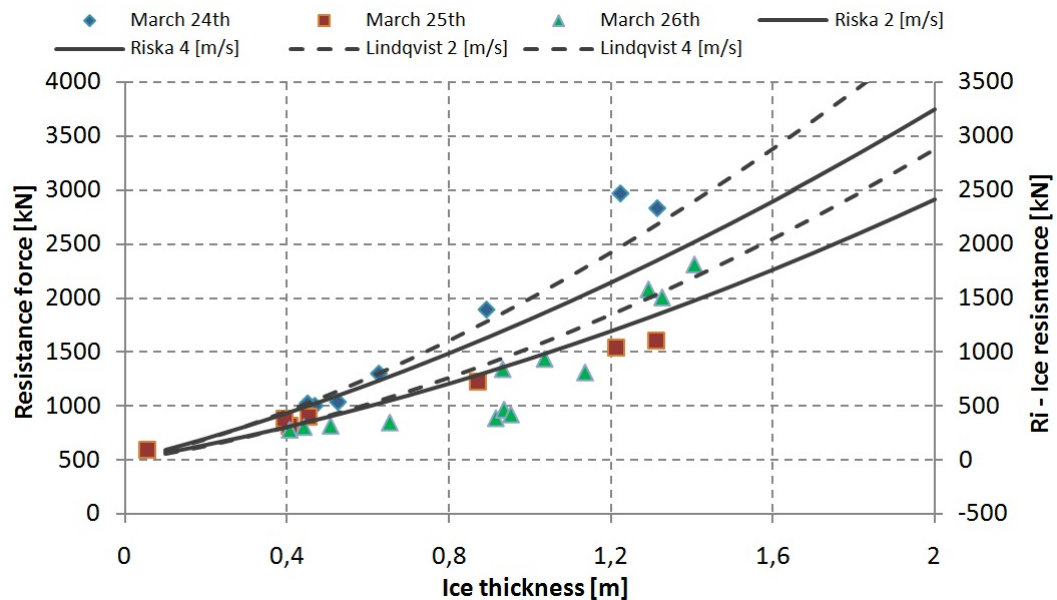


Figure 11.10: Results compared with Riska and Lindqvist formulations with 500kN shift

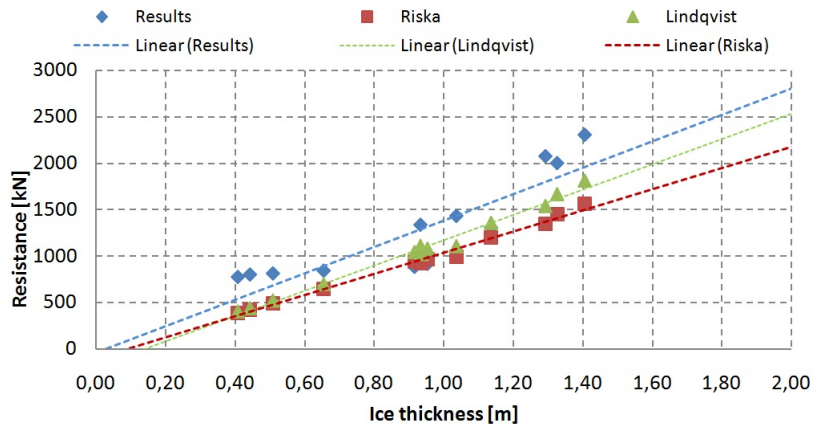


Figure 11.11: Results from March 26th compared with Riska and Lindqvist using equal speed and ice thickness

resistance with Riska and Lindqvist with equal speed and ice thickness gives the results as given in figure 11.11. The linear trend is comparable for the results from March 26th, the result from March 25th fits also good while the results from March 24th indicates a steeper trend.

Using the sequences of interest from the screening process and the outlined formulation ice resistance is estimated. Examine the scatter of calculated data shows that the resistance increases with ice thickness. The estimated resistance is compared with the two reviewed formulations from literature, and it seems to agree. Some of the sequences of interest were found too poor, and was removed in further analysis.

Chapter 12

Curve Fitting

Curve fitting, also known as regression analysis, is used to find the "best fit" line or curve for a series of data points. The curve fitting will produce an equation that can be used to find points anywhere along the curve. In some cases, instead of finding an equation, a curve fit is used to smooth the data to improve the appearance of a plot.

To find an equation that can be used to find resistance for different ice thicknesses can be of interest. In chapter 11, resistance values for different ice thicknesses was estimated. Using curve fitting to this series of data points can produce an applicable model that can predict future resistance given the ice thickness. The model obtain is not a universal model that fits for every vessel, but a model to determine the resistance for a specific vessel, in this case KV Svalbard. To choose the right curve fit model to the estimated resistance in ice for KV Svalbard, a study is necessary. There are many different types of curve fits, and this chapter will give a overview of some Least Square curve fits and will try to suggest the best fit to the analysed data.

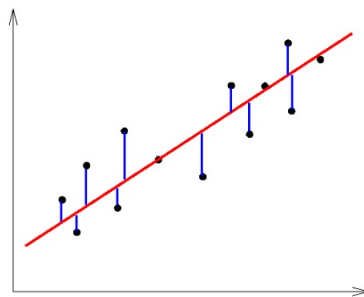


Figure 12.1: Illustration of Least Squares method

12.1 Least Squares method

Least Squares is a method of curve fitting that has been popular for a long time. The method tries to minimize the square of the error between the original data and the values predicted by the equation, see figure 12.1. The method has the advantage that it is simple and easy to understand, but the method is not the most statistically robust method of fitting a function to a data set. The weakness of the Least Squares method is that it is sensitive to outliers in the data. For instance if a data point is widely different from the majority of the data, the result from the regression can be bad. The data should for this reason always be examined before fitting. The most common Least Square fits are: Linear, Polynomial, Exponential, Logarithmic and Power.

In the following section theory is collected from *Probability and statistics for engineers and scientists*[20] and only linear theory is reviewed.

12.1.1 Linear curve fitting

The simplest regression is linear, and many natural processes follow this linear relationship. When dealing with natural independent variables or regressors, a linear form of relationship between the response Y and the regressor x is given as

$$Y = \alpha + \beta x \quad (12.1)$$

where, α is the intercept and β is the slope. If this relationship is exact, then it is a deterministic relationship between two scientific variables and there is no random or probabilistic component to it. In general in scientific and engineering studies, the relationship is not deterministic which means a given x does not always give the same value for Y .

To estimate the parameters α and β is very simple using least square method. The fitted line is an estimated of the true regression line, and the fitted line should be closer to the true regression line when large amount of data are available. When dealing with estimation it is important to know the concept of residual. A residual is an error in the fit of the model. If a set of n residual is large, it is obviously that the fit of the model is not good. Small residuals are a sign of a good fit.

Given a set of regression data (x_i, y_i) and a fitted model, $\hat{y}_i = a + bx_i$ the residuals is given by

$$e_i = y_i - \hat{y}_i, \quad i = 1, 2, \dots, n \quad (12.2)$$

When using the method of Least Squares, a and b shall be found as estimates for α and

Functional form relating y to x	Proper transformation
Exponential: $y = \alpha e^{\beta x}$	$y^* = \ln y$
Power: $y = \alpha x^\beta$	$y^* = \log y; x^* = \log x$
Reciprocal: $y = \alpha + \beta \left(\frac{1}{x}\right)$	$x^* = \frac{1}{x}$
Hyperbolic function: $y = \frac{x}{\alpha + \beta x}$	$y^* = \frac{1}{y}; x^* = \frac{1}{x}$

Table 12.1: Transformations to Linearize

β so that the sum of squares of the residuals is a minimum. The residual sum of squares is often called the sum of squares of the errors about the regression line and is denoted by SSE

$$SSE = \sum_{i=1}^n e_i^2 = \sum_{i=1}^n (y_i - a - bx_i)^2 \quad (12.3)$$

12.1.2 Linearizing

A model which x or y is transformed should not be viewed as a nonlinear regression model. We normally refer to a regression model as linear when it is linear in the parameters. If the complexion of the data suggest that we could regress y^* against x^* where each is a transformation of the natural data x and y . Then the model of the form

$$y_i^* = \alpha + \beta x_i^* + e_i \quad (12.4)$$

is a linear model since it is linear in the parameters α and β . A example is the log-log model.

$$\log y_i = \alpha + \beta \log x_i + e_i \quad (12.5)$$

This model in is not linear in x and y , but is linear in the parameters and is thus treated as a linear model. A truly nonlinear model is

$$y_i = \beta_0 + \beta_1 x_i^{\beta_2} + e_i \quad (12.6)$$

Several function are given describing relationships between y and x that can produce linear regression through the transformation given in table 12.1.

12.1.3 Coefficient of Determination

The coefficient of determination, R^2 , is a measure of quality of the fit. It is a measure of the proportion of the variability explained by the fitted model. The analyses of variance uses

the error sum of squares SSE and the total corrected sum of squares SST . SST describes the variation in the response values that ideally would be explained by the model, while SSE is the variation due to error. The R^2 is given as:

$$R^2 = 1 - \frac{SSE}{SST} \quad (12.7)$$

If the fit is perfect, all residuals are zero, and thus $R^2 = 1.0$. But if SSE is only slightly smaller than SST, $R^2 \approx 0$.

The reliability of R^2 is function of the size of the regression data set and the type of application. Clearly, $0 \leq R^2 \leq 1$ and the upper bound is archived when the fit to data is perfect. So what is an acceptable value for R^2 ? When using high-precision piece of equipment a very high R^2 value is expected (perhaps exceeding 0.99), while dealing with data impacted by variability in human behavior an R^2 value of 0.70 is accepted. Based on experience in model fitting it is possible to evaluate when a value is large enough.

For fitting of the estimated resistance for KV Svalbard, what is an acceptable value for R^2 ? The measurements of speed and power output are assumed to be good, while the thickness measurement have a lower precision in predicting the true ice thickness. An R^2 value larger than 0.8 is in this case assumed to be acceptable, depending of numbers of data points that used in the fit.

The R^2 criterion is dangerous to use for comparing different fitting models for the same data set. If adding additional terms to the model, it decreases SSE and thus increases R^2 . In this way the R^2 can be made artificially high by overfitting.

12.2 Choosing a Curve Fit Model

There exist a number of different curve fit types and choosing the right model for a particular data set can be a difficult task. When deciding a curve fit model, knowledge of the underlying properties associated with the data helps to make a good fit. If the fit to use is unknown, a scatter plot is useful to find the general shape of the curve. Some general shape of various fits are illustrated in figure 12.2.

Earlier formulation of ice resistance can give a good indication of what kind of fit that is used on regular basis. In the review of two different formulations from literature described in chapter 10 a power equation was used to describe ice resistance for different ice thicknesses. A power fit should therefore be included in this study.

In the following part linear, exponential and power will be attempt to fit the estimated

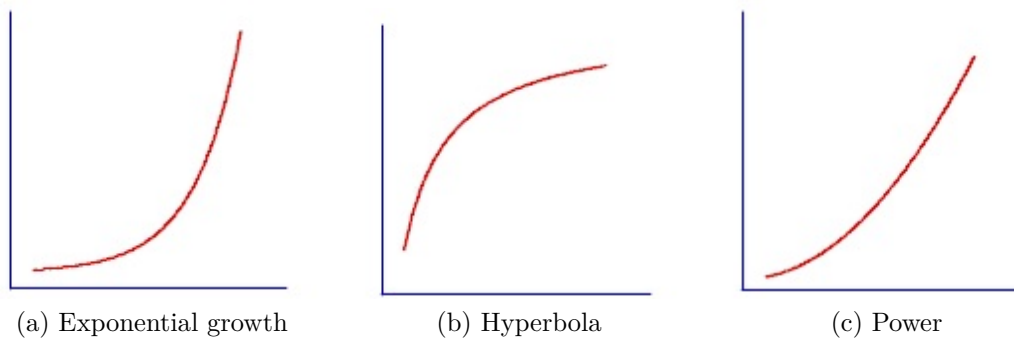
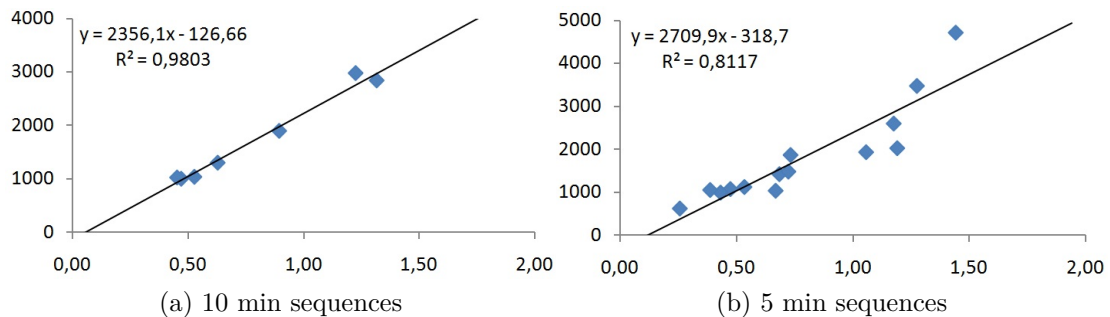


Figure 12.2: General shape of various curve fits

Figure 12.3: March 24th - Linear regression with formula and R^2

resistance in ice. Each day from the voyage is presented separately. For each day, both sequences with length of 5 and 10 minutes is discussed and compared. Since numbers of data points with sequence length of 10 minutes are few, fitting using 5 minutes sequences is more emphasized.

12.2.1 March 24th

Some of the estimated results from March 24th was quite high compared with the majority of the data sets, and they are not included in further regression. The first choice is to use the simplest regression, the linear fit. A simple linear regression fit to the data, figure 12.3a and 12.3b, produces the fitted models and the coefficient of determination

$$10 \text{ min seq.: } \hat{y} = -126.7 + 2356x \quad (R^2 = 0.9803) \quad (12.8)$$

$$5 \text{ min seq.: } \hat{y} = -318.7 + 2710x \quad (R^2 = 0.8117) \quad (12.9)$$

Equation 12.8 is the fitted line from the data with sequence length of 10 minutes. A linear fit seems to fit this data good. The residuals are low and the coefficient of determination

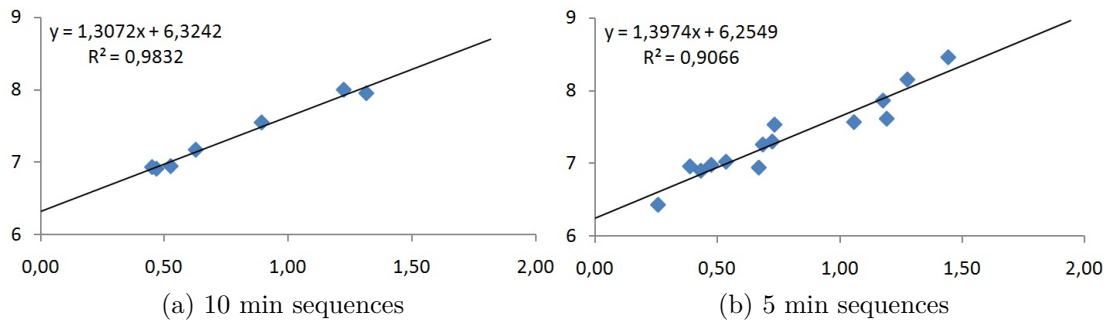


Figure 12.4: March 24th - $\ln(y)$ transformation with formula and R^2

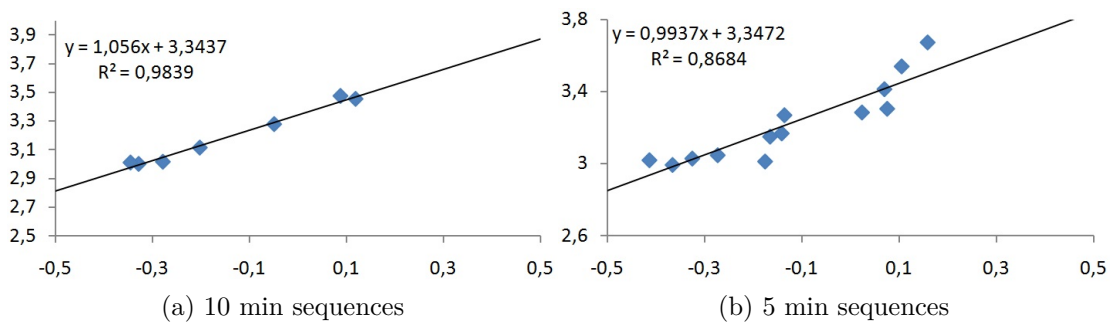


Figure 12.5: March 24th - $\log(x)-\log(y)$ transformation with formula and R^2

R^2 emphasize this to be a good fit. On the other hand number of data points are quite low and the span of thicknesses is low. A linear model looks to fit good for a narrow collection of ice thicknesses.

Decreasing the sequence length from 10 to 5 minutes gives a linear regression equal to the equation 12.9. This results in wider span of thicknesses and increased number of data points, see figure 12.3b. In this case a linear fit does not seem to be the best fit, and R^2 is also now lower. Looking at the residuals, this is not an ideal set of residuals because they do not show a random scatter around the fitted line. Clusters of positive and negative values might suggest that a curvilinear trend in the data should be investigated.

The general shape of the scattered data with 5 minutes length indicates that an exponential or a power curve may fit better. Starting with a \ln transformation to see if the estimated resistance fits better to an exponential curve. Regressing $\ln(y)$ against x produces the regression

$$5 \text{ min seq.: } \ln \hat{y} = 6.25 + 1.40x \quad (R^2 = 0.910) \quad (12.10)$$

Figure 12.4b shows that the data fits better to an exponential curve than a linear, the residuals are more evenly distributed and R^2 is also higher. The last model to test is the power fit. Using a log-log transformation as viewed in figure 12.5b, and regressing $\log(y)$ against $\log(x)$ produces the following regression

$$5 \text{ min seq.: } \log \hat{y} = 3.35 + 0.99 \log(x) \quad (R^2 = 0.8684) \quad (12.11)$$

A power fit seems to be better than the linear regression, but compared with the exponential fit a power fit is not that good. A power fit will start from the origin while the exponential curve will cross the horizontal axis. If the resistance was supposed to be equal to zero at zero ice thickness a power fit would have been a better fit. Since my model includes all resistance the resistance at zero thickness is always larger than zero. The best fit for the estimated data is found to be the exponential, and writing it in the true functional form

$$10 \text{ min seq.: } \hat{y} = 558 e^{1.31x} \quad (R^2 = 0.983) \quad (12.12)$$

$$5 \text{ min seq.: } \hat{y} = 521 e^{1.40x} \quad (R^2 = 0.910) \quad (12.13)$$

The equation 12.12 is fitted to the sequences with 10 minutes length and the equation 12.13 is fitted to 5 minutes length. Despite that the equations are different, figure 12.6 shows that they are nearly identical for small ice thickness values ($<1.5\text{m}$).

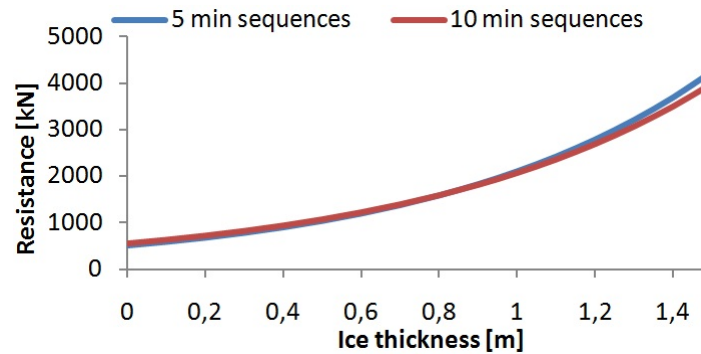


Figure 12.6: Comparison of fitted curves

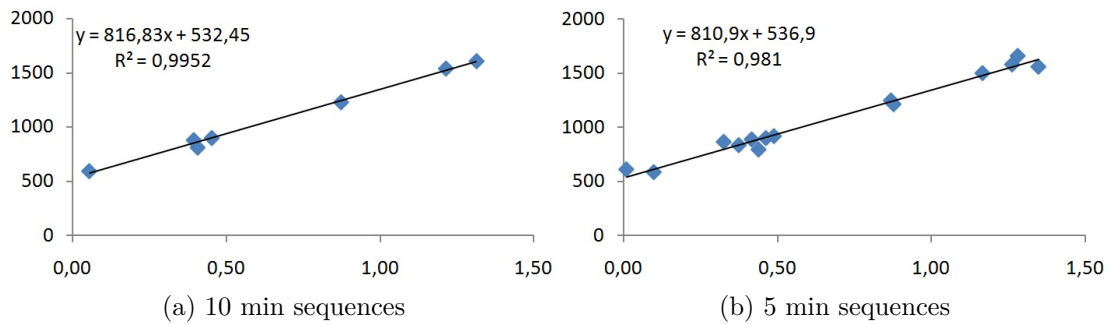


Figure 12.7: March 25th - Linear regression with formula and R^2

12.2.2 March 25th

Starting with linear regression fitted to the data form March 25th as illustrated in figure 12.7a and 12.7b gives the following expressions

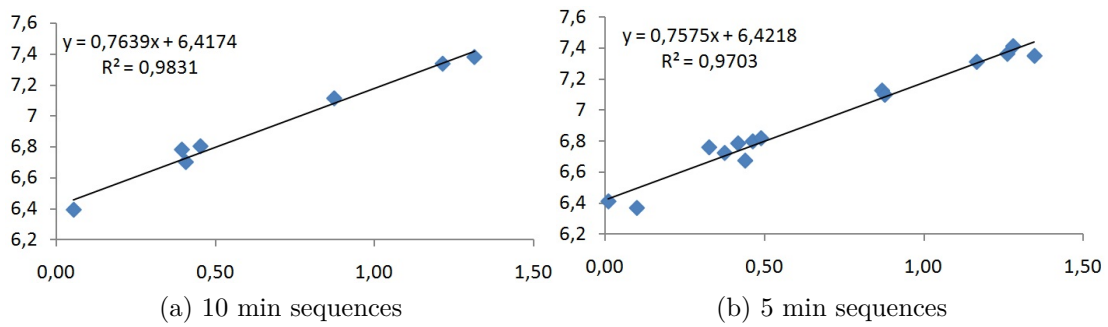
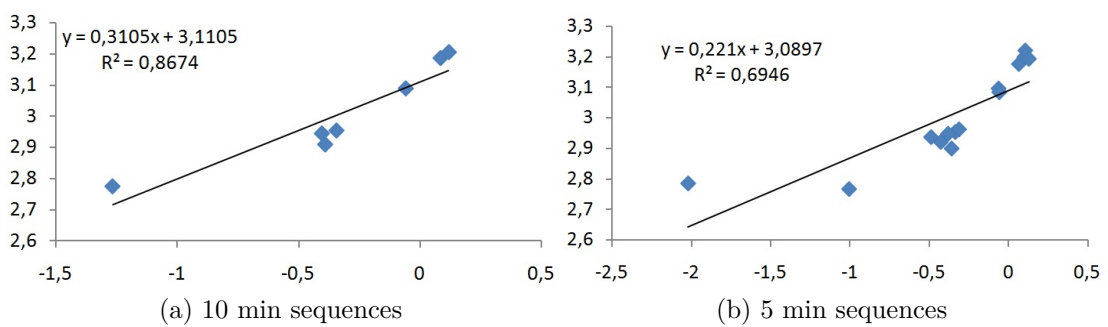
$$10 \text{ min seq.: } \hat{y} = 532.5 + 817x \quad (R^2 = 0.995) \quad (12.14)$$

$$5 \text{ min seq.: } \hat{y} = 536.9 + 811x \quad (R^2 = 0.981) \quad (12.15)$$

Both equation 12.14 and 12.15 seems to fit very good to a linear fit. The residuals are low both for the equation with 10 and 5 minutes long sequences. The span of estimated data varies also from nearly no ice thickness up to nearly 1.5m, this is good because data is available in the thickness span of interest. Even though the linear fit is good, also the other fits are tested.

Using \ln transformation to see how the data fits to an exponential curve gives the regression when $\ln(y)$ is regressed against x

$$5 \text{ min seq.: } \ln \hat{y} = 6.42 + 0.76x \quad (R^2 = 0.970) \quad (12.16)$$

Figure 12.8: March 25th - $\ln(y)$ transformation with formula and R^2 Figure 12.9: March 25th - $\log(x)$ - $\log(y)$ transformation with formula and R^2

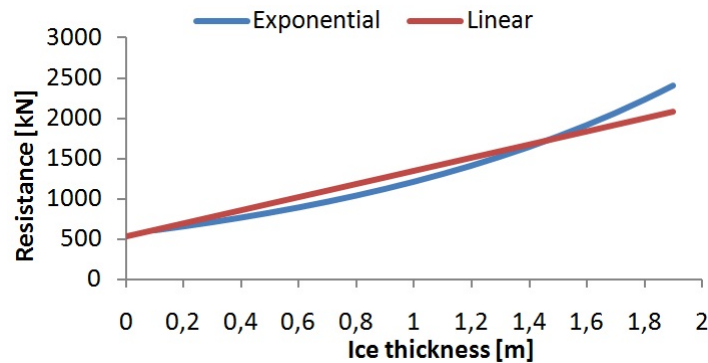


Figure 12.10: Comparison of fitted curves

Equation 12.16 gives the linear regression for data with sequence length of 5 minutes when using the \ln transformation. This model seems to fit quite good, despite that the power fit is a curved fit. The exponential function is nearly equal to the linear regression line in the ice thickness range of interest, a linear fit is therefore a simpler model that gives the same results.

The figure 12.9 shows that the power fit is not a good model in this case. Since the power model starts at zero resistance at zero ice thickness this model will not fit good else we introduce more parameters, but this is not looked into.

The best fit to the results from March 25th is either the linear equation 12.17 or the exponential equation 12.18. The linear and the exponential functions are illustrated in figure 12.10, and they compare quite good.

$$10 \text{ min seq.: } \hat{y} = 536.9 + 811x \quad (R^2 = 0.981) \quad (12.17)$$

$$5 \text{ min seq.: } \hat{y} = 615 e^{0.76x} \quad (R^2 = 0.970) \quad (12.18)$$

12.2.3 March 26th

Linear regression of the estimated ice resistance from March 26th, see figure 12.11, gives the following regression for 5 and 10 minutes long sequences

$$10 \text{ min seq.: } \hat{y} = -39.1 + 1423x \quad (R^2 = 0.765) \quad (12.19)$$

$$5 \text{ min seq.: } \hat{y} = 2 + 1386x \quad (R^2 = 0.708) \quad (12.20)$$

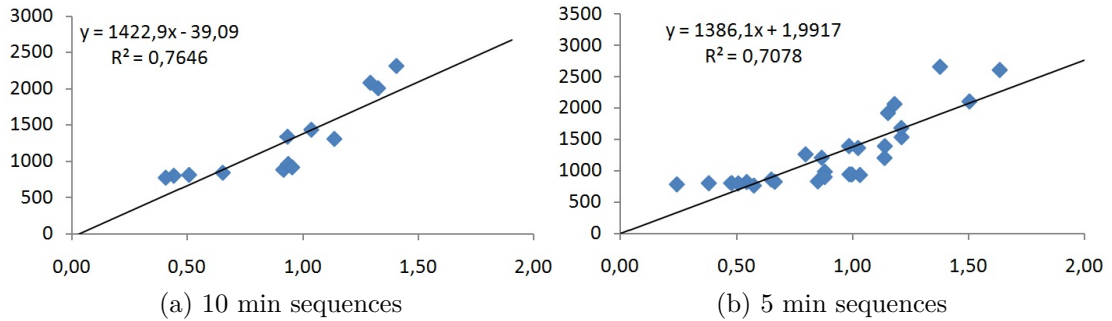


Figure 12.11: March 26th - Linear regression with formula and R^2

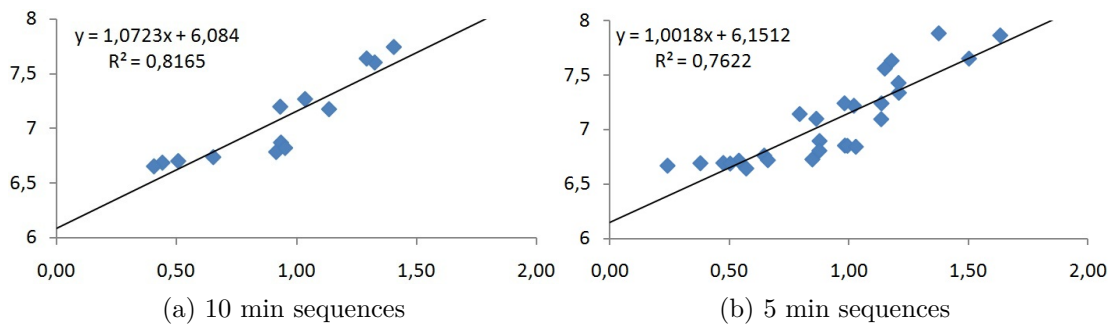


Figure 12.12: March 26th - $\ln(y)$ transformation with formula and R^2

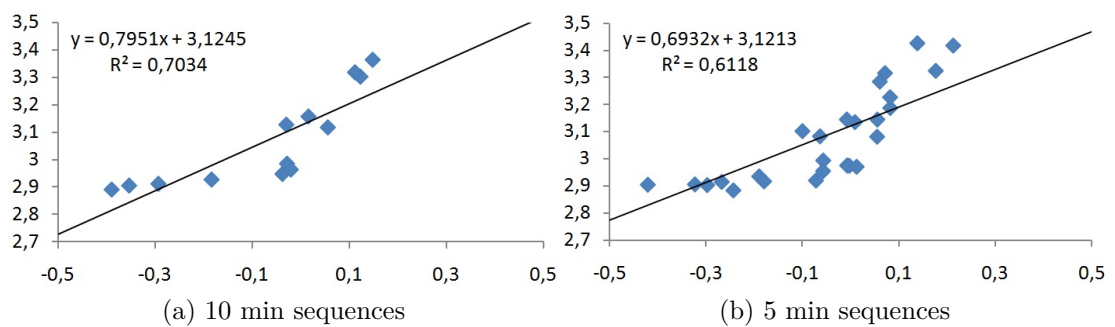


Figure 12.13: March 26th - $\log(x)$ - $\log(y)$ transformation with formula and R^2

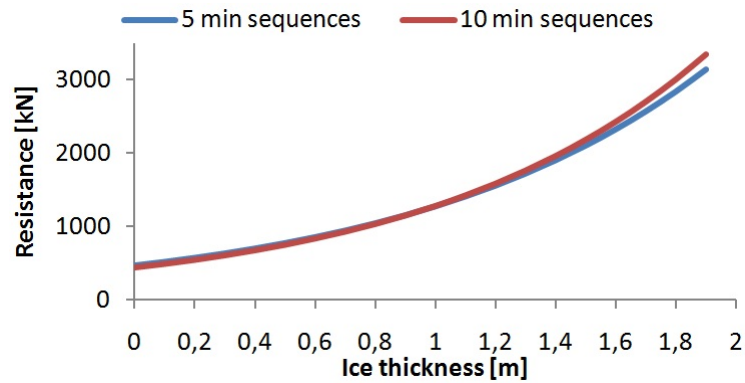


Figure 12.14: Comparison of fitted curves

Figure 12.11 illustrates that a linear fit is possible not the best fit. The set of residuals is not ideal because they do not show a random scatter around the linear regression line. Clusters of positive and negative values indicates that a curvilinear fit to the data should be investigated.

Using transformation, the new linearized models is shown in figure 12.12. Regressing the parameter $\ln(y)$ against x produces the regression line

$$5 \text{ min seq.: } \ln \hat{y} = 6.15 + 1.00x \quad (R^2 = 0.762) \quad (12.21)$$

For both the 5 and 10 minutes long sequences a better fit is obtain. There are still some scatter around the fitted curve, but the residuals are better. Comparing with a power fit as illustrated in figure 12.13 a exponential fit is best. The exponential fit seems to be the best fit even though that it not is perfect and due to the scatter around the fitted curve. The best fit found for the estimated resistance from this day written in the true functional form

$$10 \text{ min seq.: } \hat{y} = 439 e^{1.07x} \quad ((R^2 = 0.817) \quad (12.22)$$

$$5 \text{ min seq.: } \hat{y} = 469 e^{1.00x} \quad (R^2 = 0.762) \quad (12.23)$$

For small values of ice thickness ($<1.5\text{m}$) both the equations 12.22 and 12.23 resulting in nearly equal resistance force. Figure 12.14 illustrates the two fitted models.

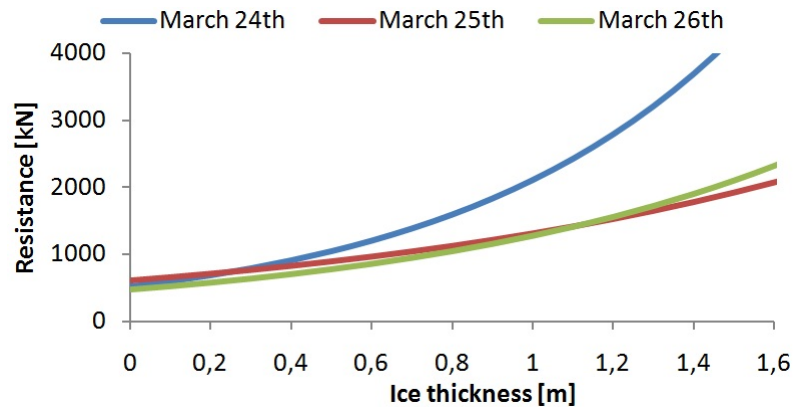


Figure 12.15: Comparison of fitted curves

12.3 Comparison and summery

Three different days with data are tried fitted with different curve models. Sequences split in 5 and 10 minutes length are studied with linear, exponential and linear fit for each of the three days. Linear fit seems to be good in most cases, but clusters of negative and positive values is observable and suggest a more curved fit. The exponential fits best to the data in most cases. The coefficient of determination R^2 measure the quality of the fit. This value are for the majority of the data higher when fitting with an exponential curve. Residuals are also more randomly scattered around the exponential fit compared with the linear which indicates that the exponential curve fits is best. A power curve was also tried fitted to the data sets, but it seems to be a poor fit. The reason for this is the fact that a power fit are fitted threw the origin.

Looking at the fitted models for each of the three days, as illustrated in figure 12.15, it seems that the fitted curve from March 24th stands out from the two other days. The cause to the large deviation from the two other days is probably due to heavy ice conditions this day. According to the technical note for the sea ice thickness measurement equipment[15], EM measurements will dramatically underestimate the total thickness of unconsolidated pressure ridges. The actual thickness of ice may for this reason be underestimated, and the report indicate a underestimating by a factor of 2 or more is possible for keels of pressure ridges. How much the mean thickness will be underestimated is difficult to say without physical measurements of the ice thickness. The size of floes and ice strength may also influence, this because the measurements are collected at different areas. Due to lack of detailed information of ice conditions a conclusion is difficult to make.

The fitted models for March 25th and 26th seems to fit quite good. The gradient is different, but in the range of ice thickness with interest they are quite comparable. Comparing this fitted curve with ice resistance formulations developed by Riska and Lindqvist, see figure 12.16, proves that the shape of the fitted models are similar to the formulations. Adding

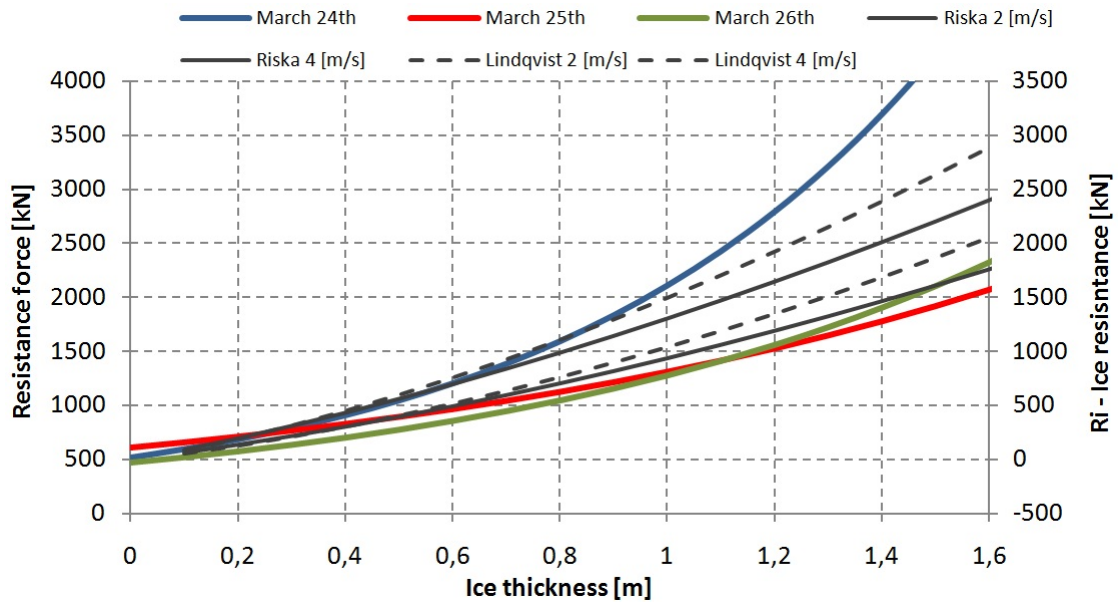


Figure 12.16: Fitted curves compared with Riska and Lindqvist

an open water resistance equal to 500[kN] on the top of the ice resistance calculated from Riska and Lindqvist, the total resistance in ice is now comparable.

Chapter 13

Conclusion

Different types of sea ice and their mechanical and physical properties are briefly described. Thickness of sea ice is the key parameter to determine the strength of ice, and the thickness also directly affects the speed of a vessel in ice. The main parameters to decide the thickness of sea ice is air temperature and freezing time. In addition to the thickness of sea ice, also temperature, salinity, density, ice type, crystal size and orientation have an influence on the ice strength.

Three different approaches for calculating contact pressure due to ice are reviewed. Empirical pressure relations are often fitted to a large number of data measured under different conditions and is therefore preferred by class societies. Physical models can give good result, but is often tailor-made and not applicable for all conditions. Stochastic models is good to establish long term distribution of ice loads and can therefore be used to find the lifetime of different part of the ship or structure.

Ice class rules for vessels operating in ice infested waters are reviewed, and the requirement deals with hull strength/fatigue, corrosion, coating, machinery and winterization. This thesis has in general looked at ice induced load and strengthening in Arctic areas by comparing ice class rules from DNV and IACS. The main difference between the two is that IACS use a plastic method of approach, while DNV uses an elastic method. Despite the difference in method of analyses, the numerical comparison shows they are relative similar. The IACS rules are typically most conservative for larger vessels with large displacement, while the DNV rules are conservative for smaller vessels with small displacement.

A review of two different formulations for estimating ice resistance for ship is given. This is inexpensive analytical models that can give an early estimation of the ice resistance and power requirement. Using main properties from KV Svalbard the two different formulations is compared, and they seem to compare quite well for thin ice ($h_i < 1m$) when the vessel speed is low. For higher vessel speeds the results differs more from each other.

During research work with KV Svalbard for a total of two weeks in late March 2007 operating in ice covered waters around Spitsbergen, measurement from the ILM-system was stored for later usage. The screening process of this data has identified different intervals of interest from the voyage. Sequences from three of the days is pointed out based on stable conditions and reported ice conditions. These sequences are recommended for further analysis. Since the measurements are used for estimating the resistance in ice, the quality of the measurements used is discussed. Power and speed measurements are found to be quite accurate, while the ice thickness measurements are questionable. In calm weather with level ice and correct calibrated equipment the accuracy should be good, but the conditions during the voyage with ice ridges and different types of floes and openings, the accuracy is lowered. If the ice thickness is underestimated or overestimated is difficult to conclude, but by studying the mean thickness and the density distribution of ice thicknesses for the different sequences and compare with manual observations, it seems like the mean ice thickness is over predicted for some sequences. The ice thickness is however been regarded as applicable for this thesis, but an uncertainty to the results of the ice thickness measurements should be kept in mind.

Based on the law of conservation of energy a formulation is outlined to estimate the resistance for a particular case. The formulation uses the parameters ice thickness, speed and power in the estimation. The formulation outlined simplifies the ice breaking problem, but the estimations should give reasonable prediction for a given ship if the quality of measurements is good.

Using the sequences of interest from the screening process and the formulation outlined, ice resistance is estimated. Examine the scatter of calculated data shows that the resistance increases with ice thickness. The estimated resistance is compared with the two reviewed formulations from literature, and the trend in the results seems to agree well. Some of the sequences of interest were found to poor, and was removed in further analysis.

A regression analysis was used to find the "best fit" line or curve to the estimated resistance of KV Svalbard. Different Least Square curves was evaluated and discussed and it was found out that an exponential curve fitted best to the estimated data.

Chapter 14

Recommendation for Further Work

The resistance formula proposed in this thesis contains all resistance components. Many ice formulations are based on the assumption that the open water and ice resistance can be separated and superimposed to obtain the total resistance. In this thesis an intelligent guess of the open water resistance was proposed based on measurements with very thin ice and no ice. The open water resistance should be studied more thoroughly to see how large the open water resistance is compared with the pure ice resistance.

The ice resistance depends on many parameters such as thickness, floe size and ice strength. During the voyage in late March 2007 with KV Svalbard only ice thickness was measured. Manually observations of concentration and prevailing ice conditions were also noted, but the manual observations are not complete and not good enough to get a clear picture of the ice conditions. For further work with the same data set or with new measurements ice conditions should be more thoroughly looked into, and ice resistance should be compared based on ice conditions, rather than only thickness.

Generally during ice breaking the vessel speed is low, also the measurement during the voyage in March 2007 shows that the speed was low. How the resistance is dependent on speed could be looked into. In this thesis the speed dependency is not emphasized, and this could be done with the available data set. The amount of data from the voyage is quite large, but the number of sequences with interest found was relative small. A more thoroughly examination of the measured data should also be done to get a larger data set.

14. Recommendation for Further Work

Bibliography

- [1] Jørgen Amdahl. *Buckling and Ultimate Strength Analysis of Marine Structures*. Norwegian University of Science and Technology, 2008.
- [2] Morten Bjerås. *Ice actions on offshore structures*. PhD thesis, Norwegian University of Science and Technology, 2006.
- [3] R. Bridges, S. Hasolt, MS. Kim, and K. Riska. Current hull and machinery ice class rules requirements and impact of iacs polar class. Technical report, LLOYD's register and Helsinki University of Technology, 2004.
- [4] Lars Børshem. Ship hull monitoring of ice-induced stresses. Master's thesis, Norwegian University of Science and Technology, 2007.
- [5] Claude Daley. Lecture notes, iacs requirements for polar class ships, overview and background.
- [6] Ahmed Derradji-Aouat, Nirmal K. Sinha, and Erman Evgin c. Mathematical modelling of monotonic and cyclic behaviour of fresh water columnar grained s-2 ice. Technical report, Institute for Marine Dynamics, National Research Council of Canada, 1999.
- [7] DNV. Rules for classification of ships, ships for navigation in ice, 2004.
- [8] BS Duggal and Sanko Kisen. Ice strengthened ships and ice rules. *Seaways, August 2006*, 2006.
- [9] Pentti Kujala. Semi-empirical evaluation of long term ice loads on a ship hull. Technical report, Helsinki University of Technology, 1995.
- [10] STORE NORSKE LEKSIKON. Arktis. <http://www.sn1.no/Arktis>, Updated: March 2009.
- [11] Gustav Lindqvist. A straightforward method for calculation of ice resistance of ships. *The 10th International Conference on Port and Ocean Engineering under Arctic Conditions, Luleå*, 1989.

- [12] D.M. Masterson and R.M.W. Frederking. Local contact pressures in ship/ice and structure/ice interactions. Technical report, Sandwell Inc and National Research Council of Canada, 1993.
- [13] Christian Mürer. *DNV hull structural rules : development, background, motives*. Det Norske Veritas, 1995.
- [14] A. Pfaffling. Sea ice observations on kv svalbard. Technical report, PFAFFLING geophysics, Det Norske Veritas, 2007.
- [15] A. Pfaffling. Ship-borne sea ice thickness electromagnetic measurements. Technical report, PFAFFLING geophysics, Det Norske Veritas, 2007.
- [16] Kaj Riska. Lecture notes, ice actions on ships - ice ii, 2009.
- [17] Kaj Riska, Max Wilhelmson, Kime Englund, and Topi Leiviskä. Performance of merchant vessels in ice in the baltic. Technical report, Helsinki University of Technology, 1997.
- [18] G.W. Timco and W.F. Weeks. A review of the engineering properties of sea ice. Technical report, Canadian Hydraulics Centre, National Research Council of Canada, 2009.
- [19] Walpole and Ronald E. *Probability statistics for engineers scientists*. Pearson Prentice Hall, 2007.
- [20] G. Wilkman and A.-C. Forsén M. Elo. Ice trials of kv svalbard. *Port and Ocean Engineering under Arctic Conditions*, 2003.
- [21] Qianjin Yue, Yan Qu, Xiangjun Bi, and Kärnä Tuomo c. Ice force spectrum on narrow conical structures. Technical report, 2007.
- [22] Øyvind Espeland. Ice action and response monitoring of ships. Master's thesis, Norwegian University of Science and Technology, 2008.

Appendix A

Ice Conditions

Tables :

Table 1: Ship operation modes

Ship operation mode:	
0	channel
1	lead
2	floe ice
3	breaking
4	ramming

Table 2: Open water types

Open water	
0	No openings
1	Small cracks
2	Very narrow breaks, <50m
3	Narrow breaks, 50-200m
4	Wide breaks, 200-500 m
5	Very wide breaks >500m
6	Lead
7	Polynya

Table 3: Ice types

Ice type	
10	Grease
20	Pancakes
50	Grey Ice
60	First Year 30-70
70	First Year 70-120
80	First Year >120
85	Multiyear
90	Brash
95	Fast Ice

Table 4: Floe sizes

Floe size	
100	Pancakes
200	New sheet ice
300	Brash
400	Cake ice (<20m)
500	Small floes 20-100 m
600	Medium floes 100-500 m
700	Large floes 500-2000m
800	Vast floes >2km

Table 5: Ice topography classes

Topography	
100	Level ice
200	Rafted pancakes
300	Cemented paca
400	Finger Rafting
5xy	New, uncon-solidated ridges
6xy	New, snow filled ridges
7xy	Consolidated ridges
8xy	Old ridges

x values

- 0 0-10% areal coverage
- 1 10-20 %
- 2 20-30 %

... ..

y values

- 1 0.5 m av. Height
- 2 1.0 m
- 3 1.5 m

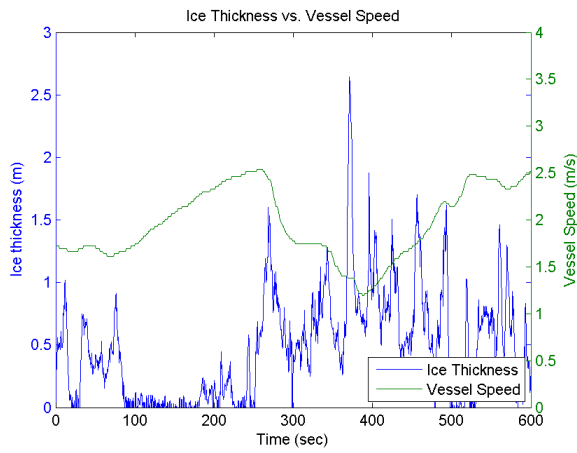
... ..

Appendix B

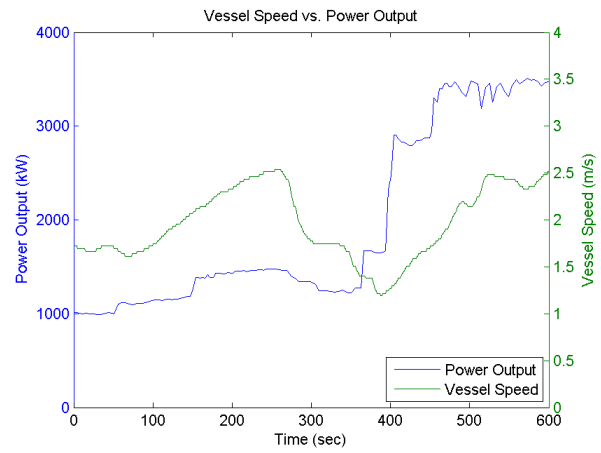
Sequences of Interest

This section contains plots of the sequences of interest found in chapter 9. The plots are presented for each sequence with ice thickness versus vessel speed and vessel speed versus power output.

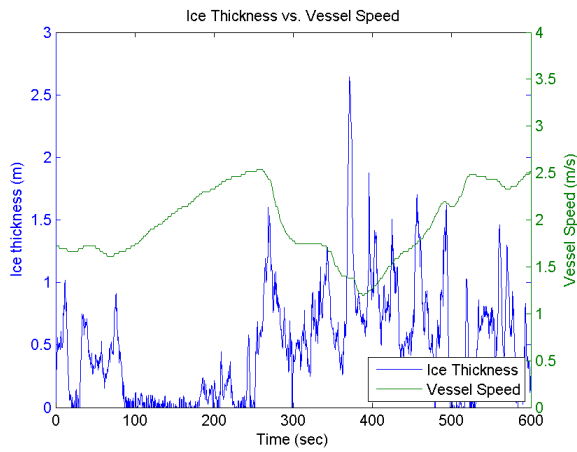
B. Sequences of Interest



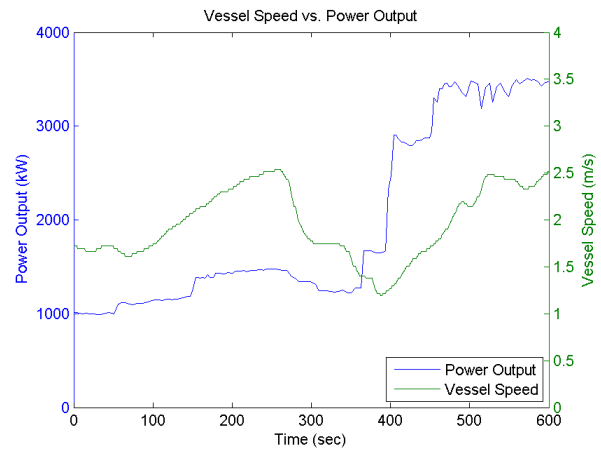
(a) 05:08–05:18



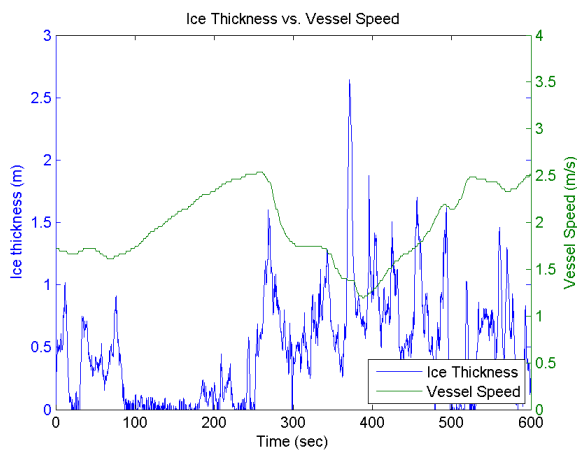
(b) 05:08–05:18



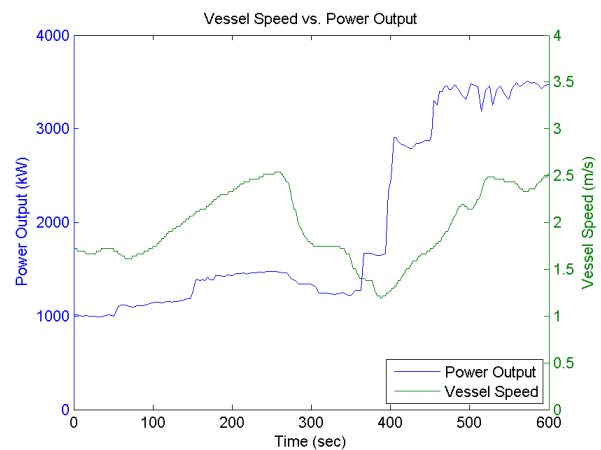
(c) 05:18–05:28



(d) 05:18–05:28

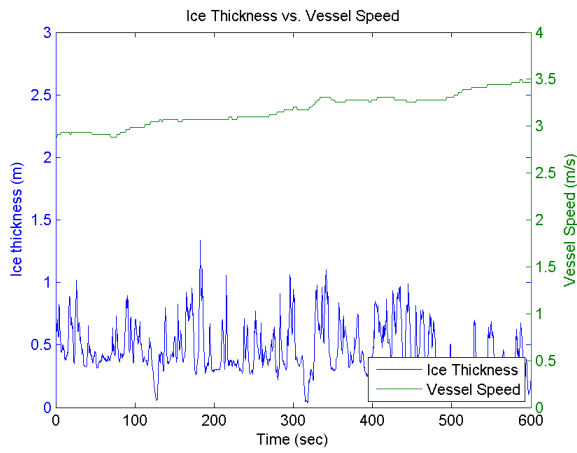


(e) 05:28–05:38

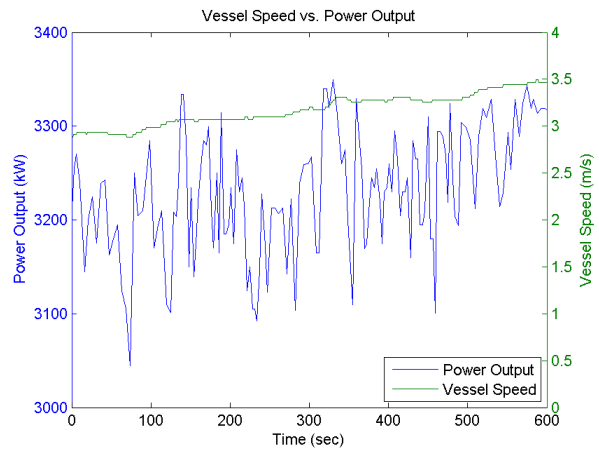


(f) 05:28–05:38

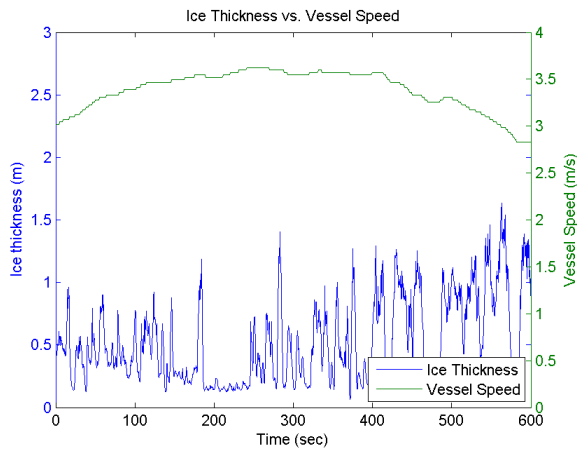
Figure B.1: March 24th



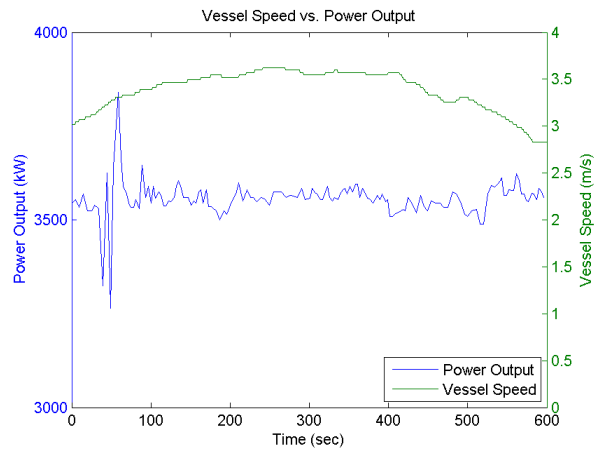
(a) 14:04–14:14



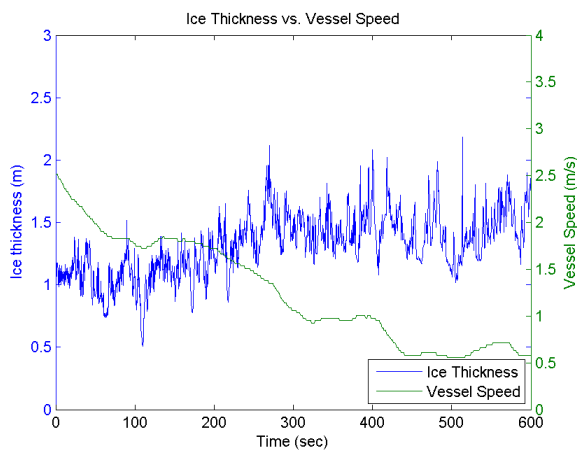
(b) 14:04–14:14



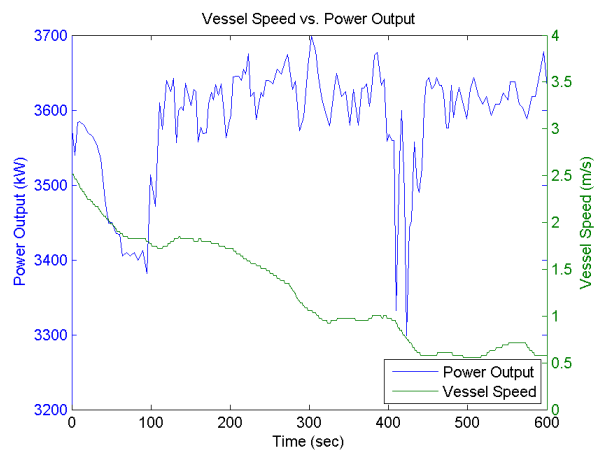
(c) 14:29–14:39



(d) 14:29–14:39



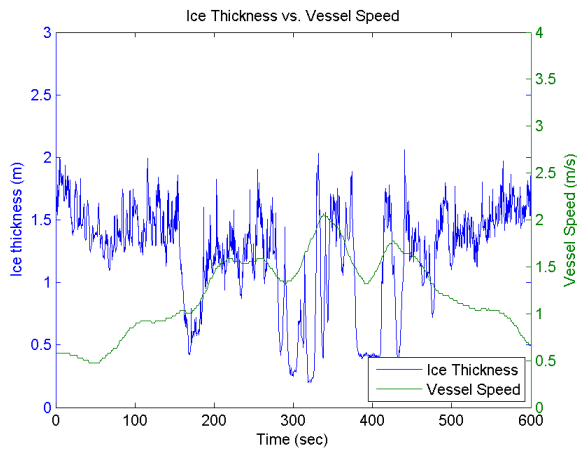
(e) 14:40–14:50



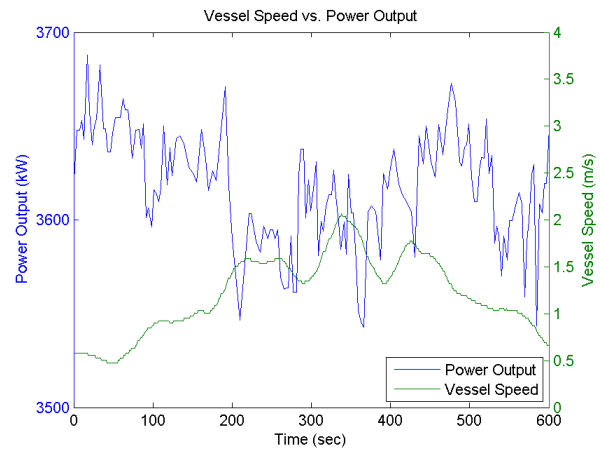
(f) 14:40–14:50

Figure B.2: March 24th

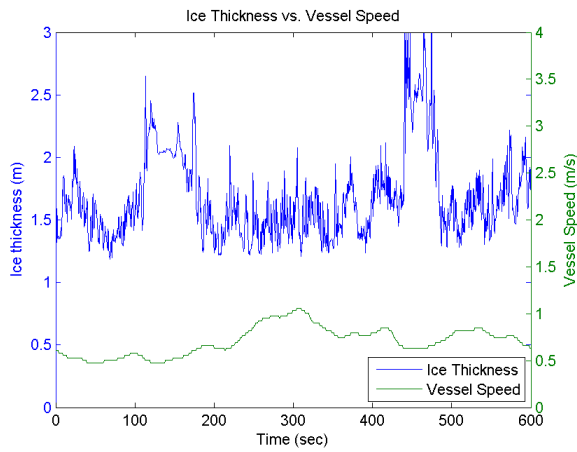
B. Sequences of Interest



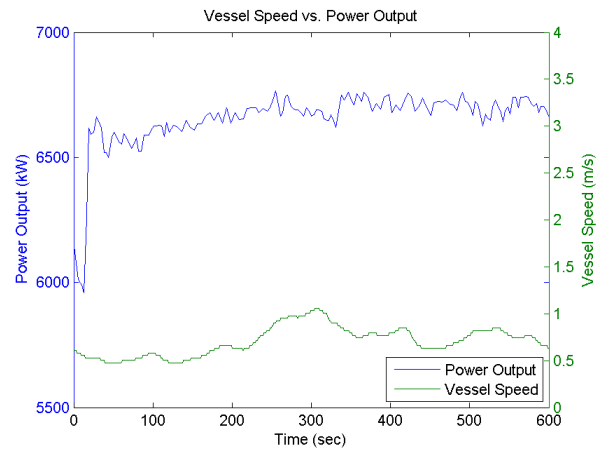
(a) 14:50–15:00



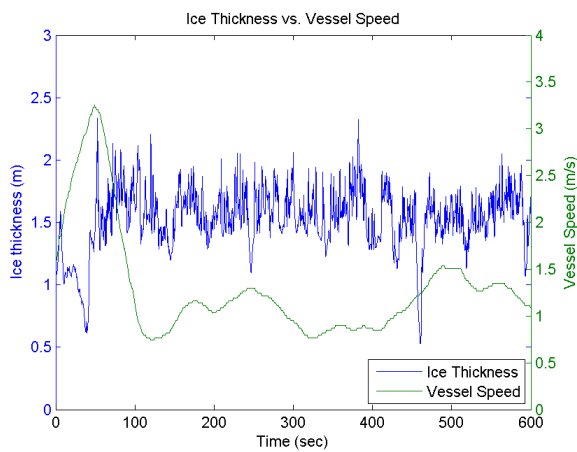
(b) 14:50–15:00



(c) 15:30–15:40



(d) 15:30–15:40

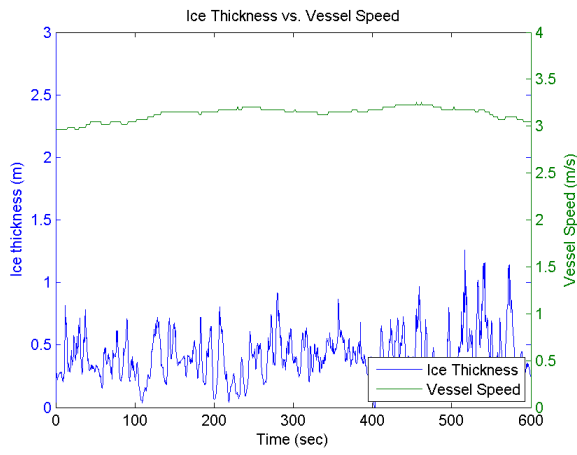


(e) 15:55–16:05

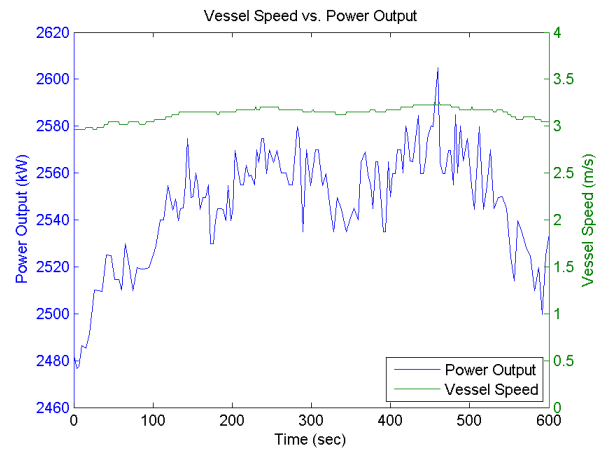


(f) 15:55–16:05

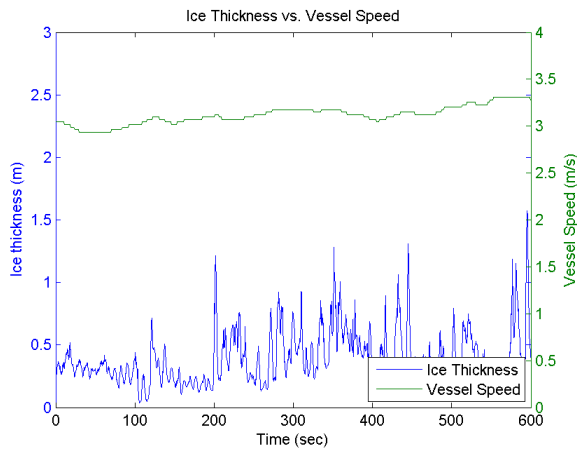
Figure B.3: March 24th



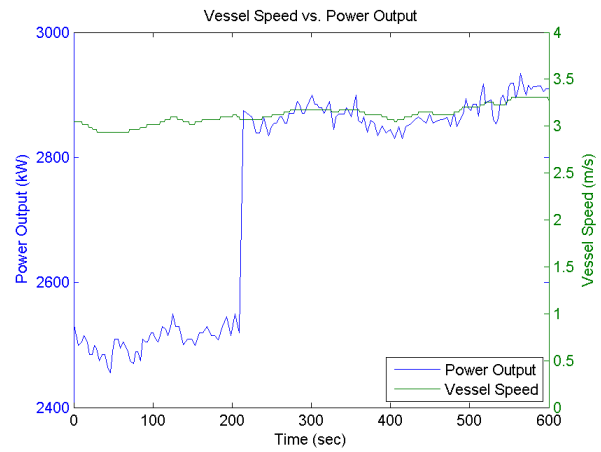
(a) 16:00-16:10



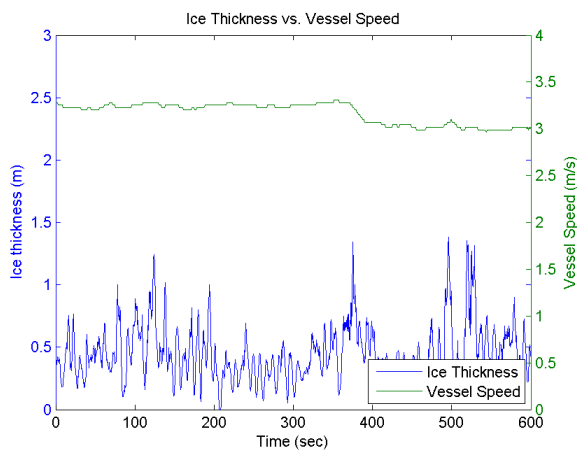
(b) 16:00-16:10



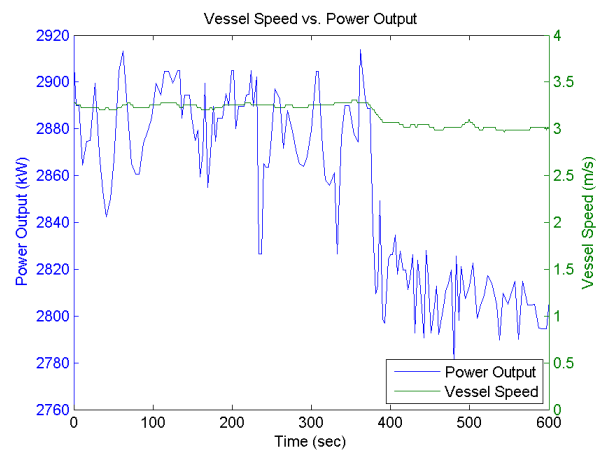
(c) 16:10-16:20



(d) 16:10-16:20



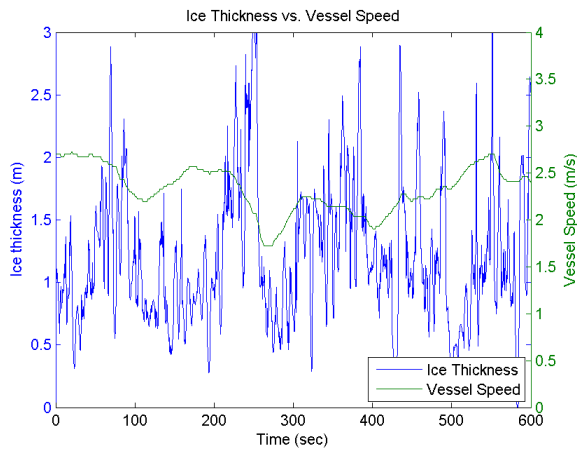
(e) 16:20-16:30



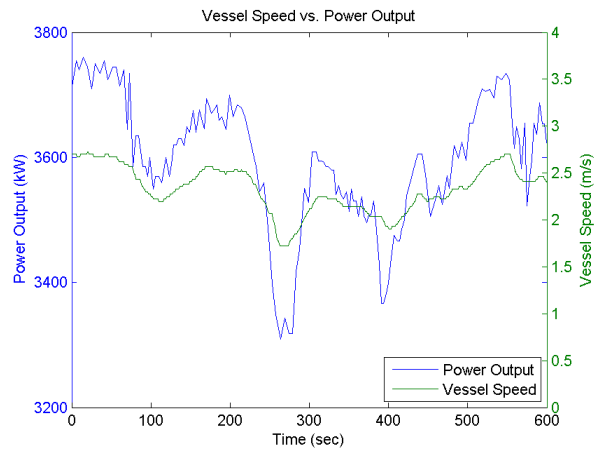
(f) 16:20-16:30

Figure B.4: March 25th

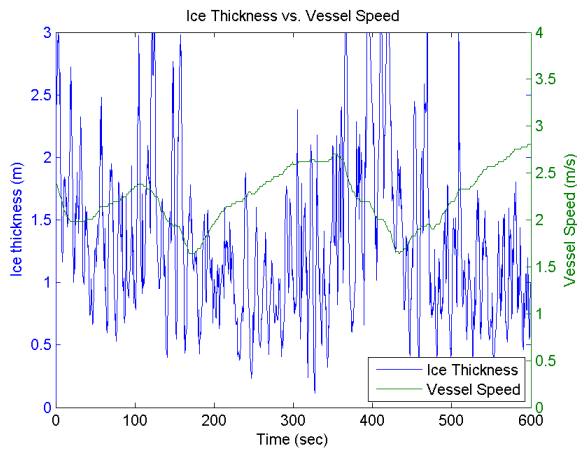
B. Sequences of Interest



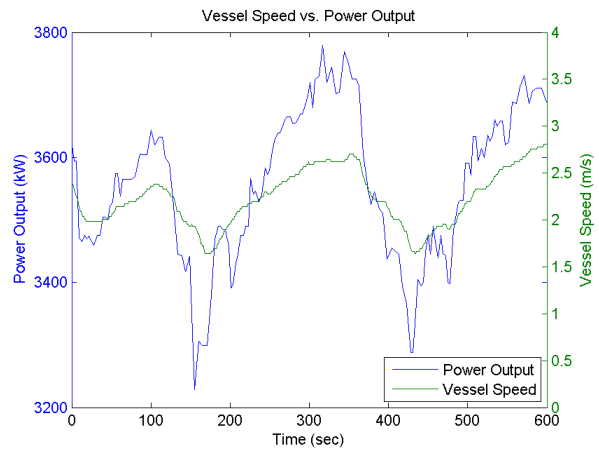
(a) 16:45-16:55



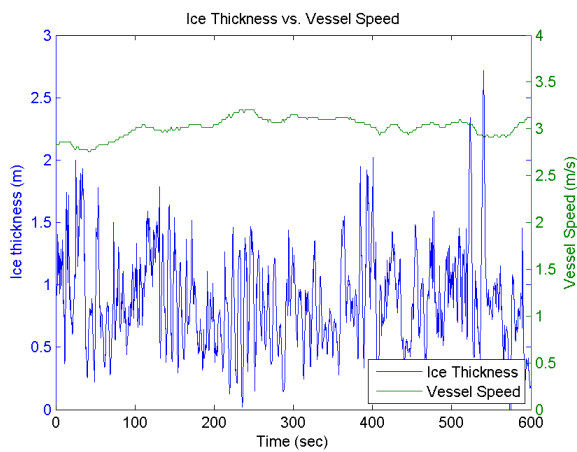
(b) 16:45-16:55



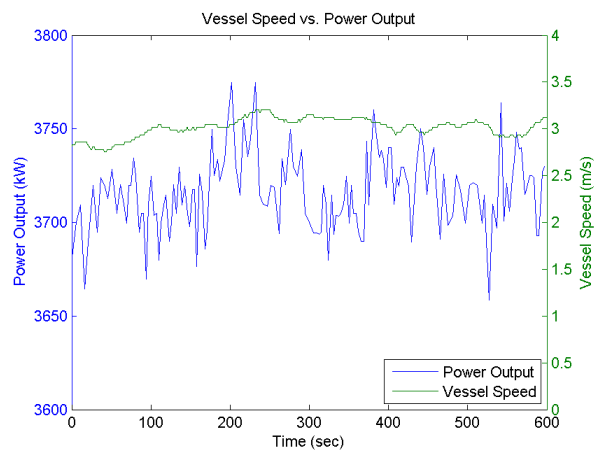
(c) 16:55-17:05



(d) 16:55-17:05

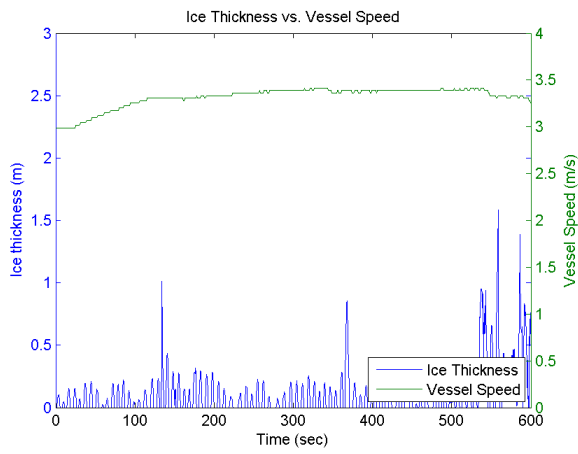


(e) 17:05-17:15

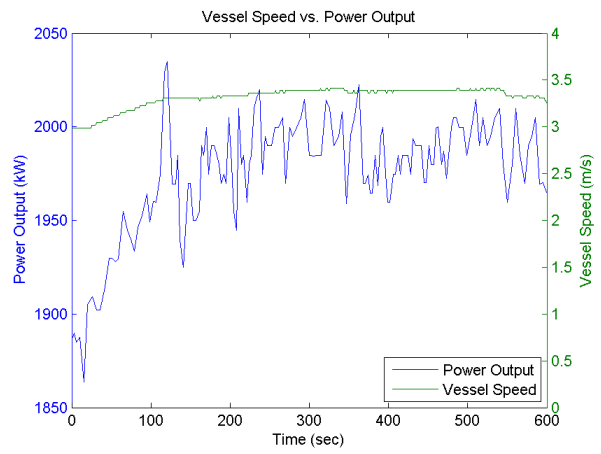


(f) 17:05-17:15

Figure B.5: March 25th



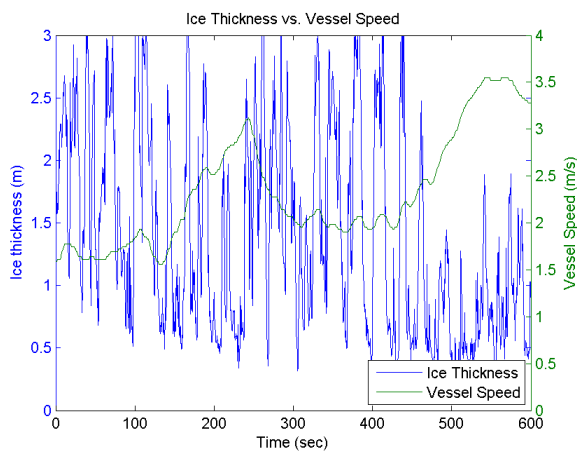
(a) 17:32-17:42



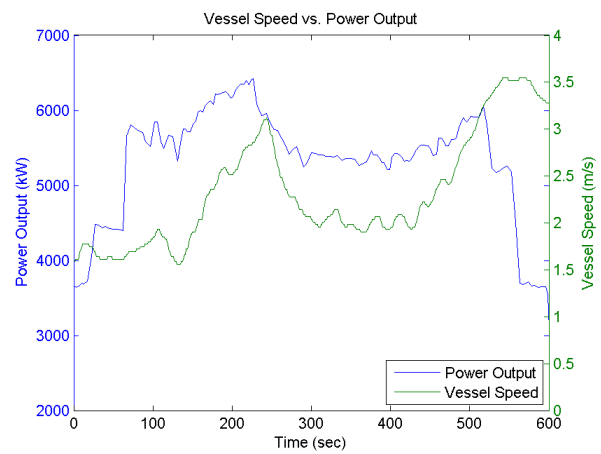
(b) 17:32-17:42

Figure B.6: March 25th

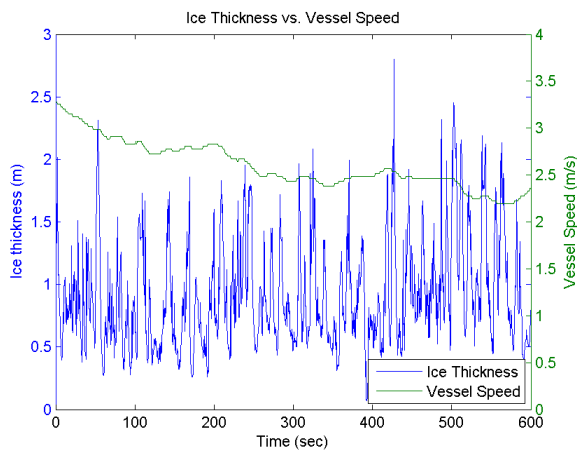
B. Sequences of Interest



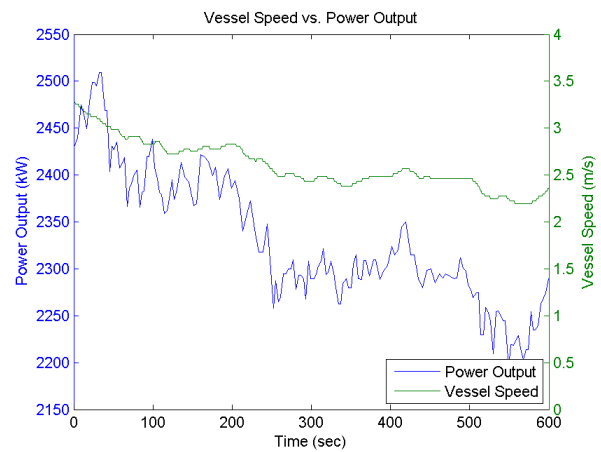
(a) 19:00-19:10



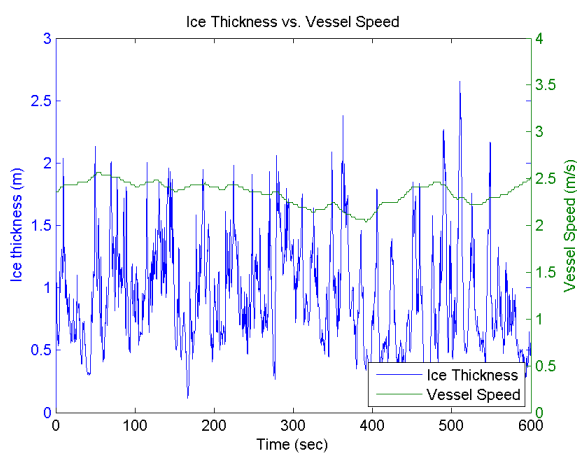
(b) 19:00-19:10



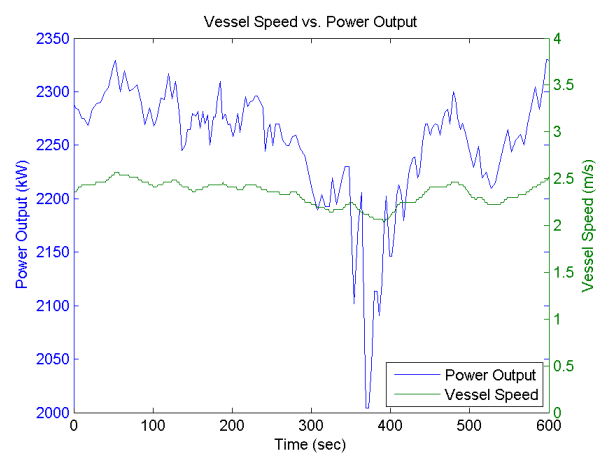
(c) 19:10-19:20



(d) 19:10-19:20

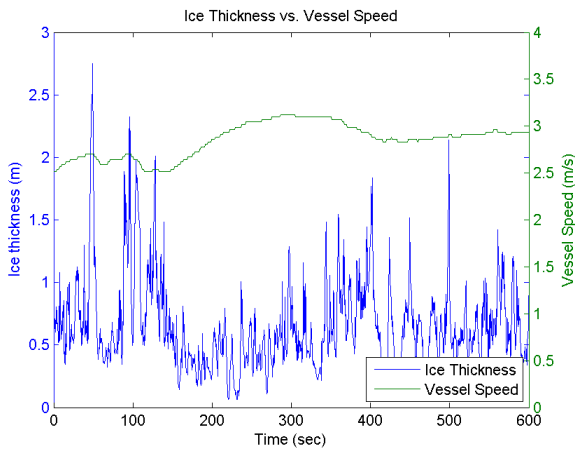


(e) 19:20-19:30

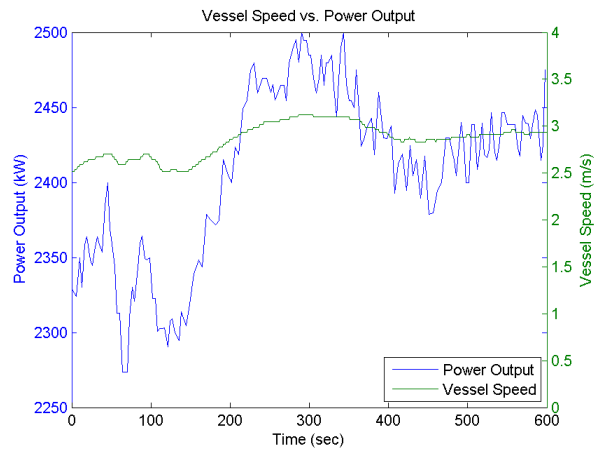


(f) 19:20-19:30

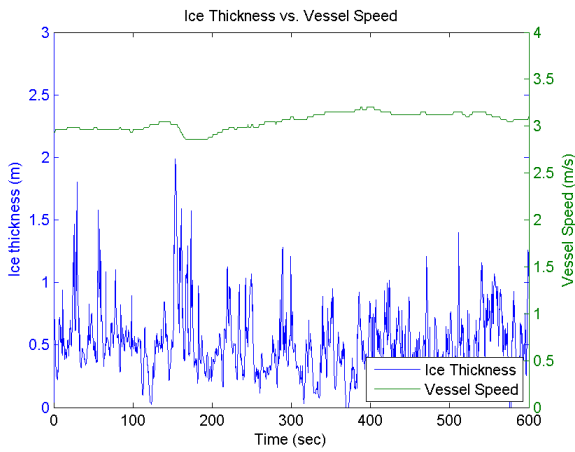
Figure B.7: March 26th



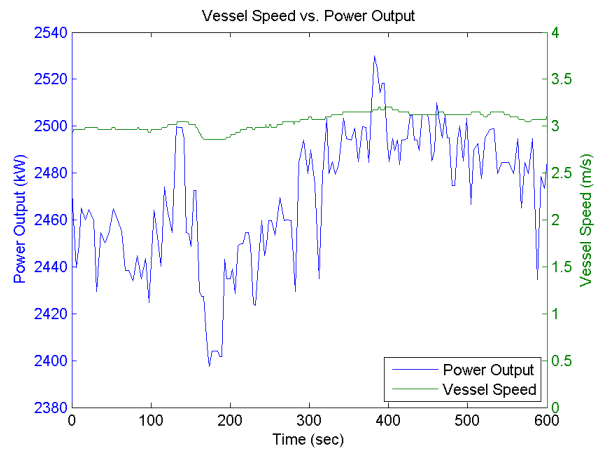
(a) 19:30-19:40



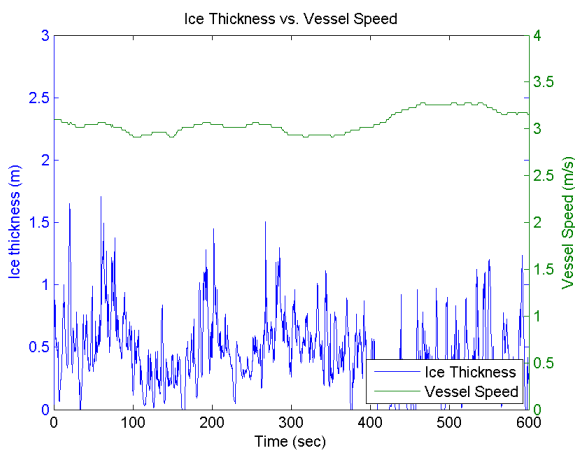
(b) 19:30-19:40



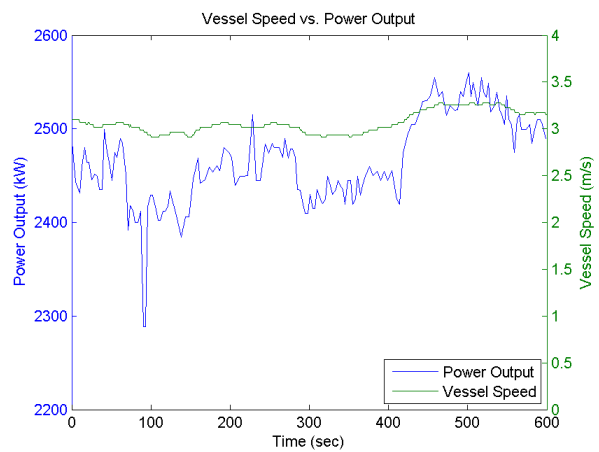
(c) 19:40-19:50



(d) 19:40-19:50



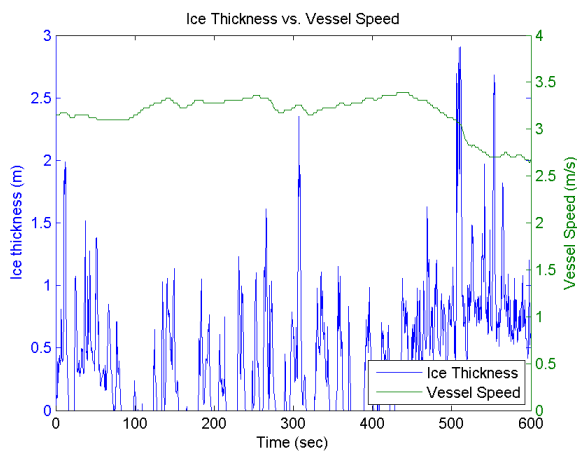
(e) 19:50-20:00



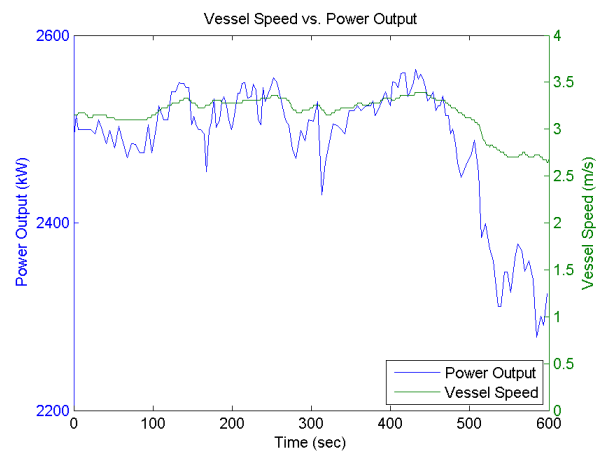
(f) 19:50-20:00

Figure B.8: March 26th

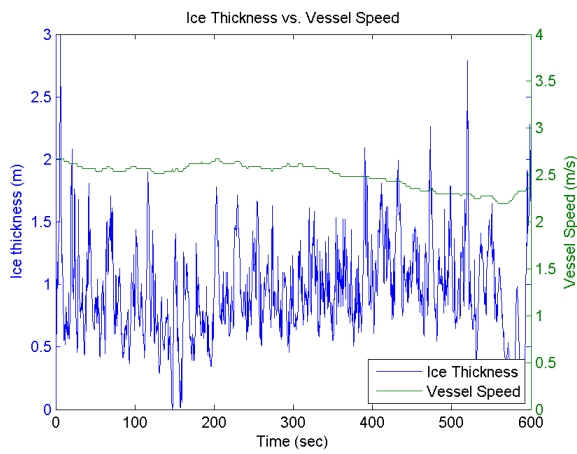
B. Sequences of Interest



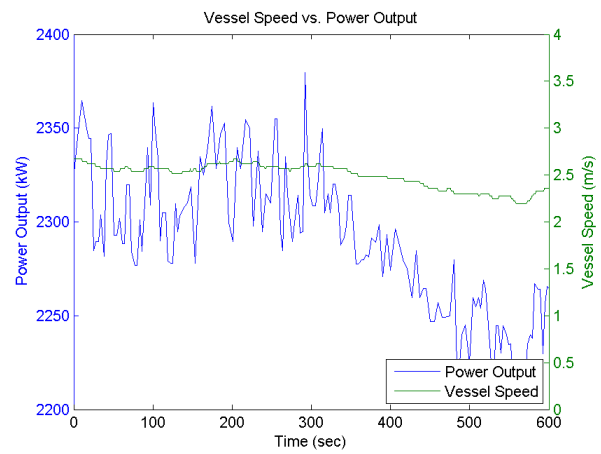
(a) 20:00-20:10



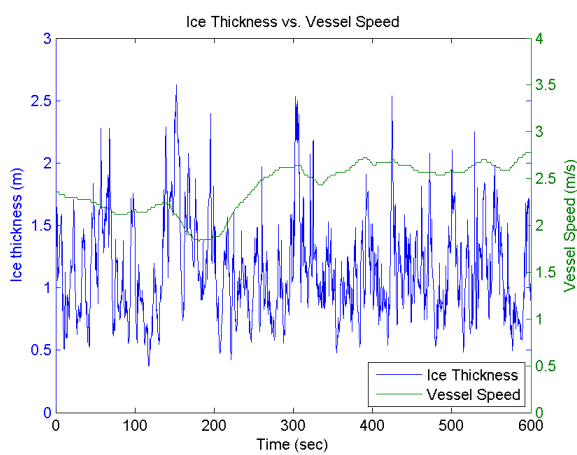
(b) 20:00-20:10



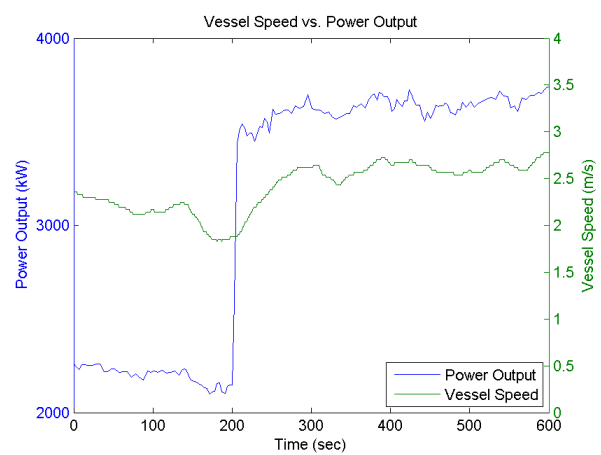
(c) 20:10-20:20



(d) 20:10-20:20

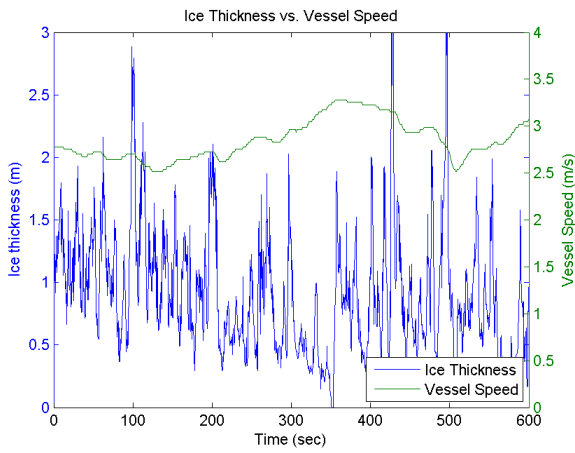


(e) 20:20-20:30

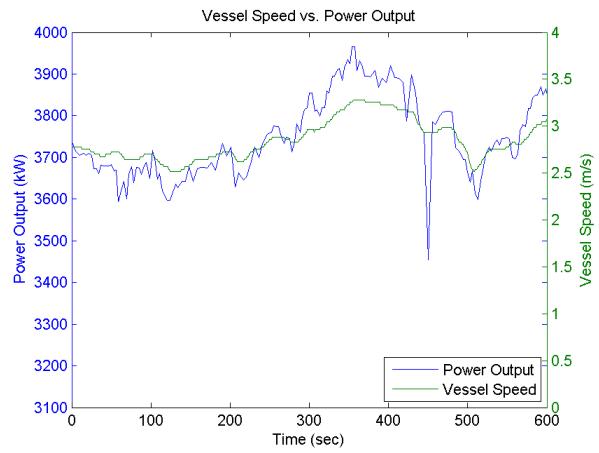


(f) 20:20-20:30

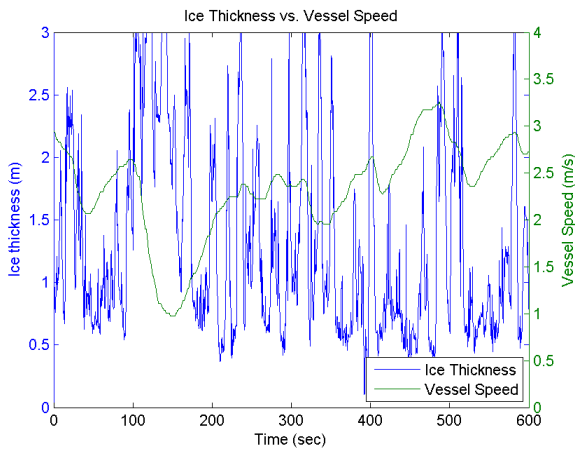
Figure B.9: March 26th



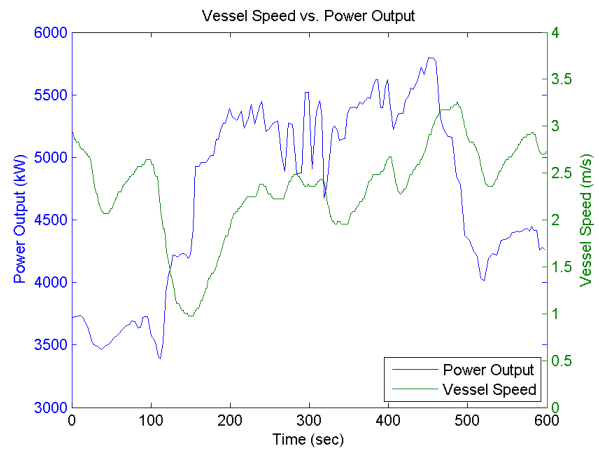
(a) 20:30-20:40



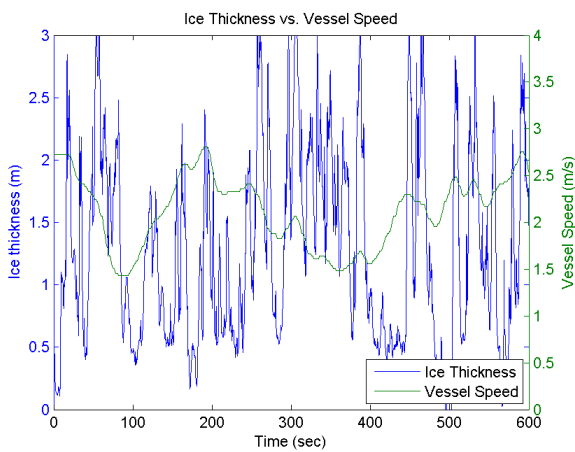
(b) 20:30-20:40



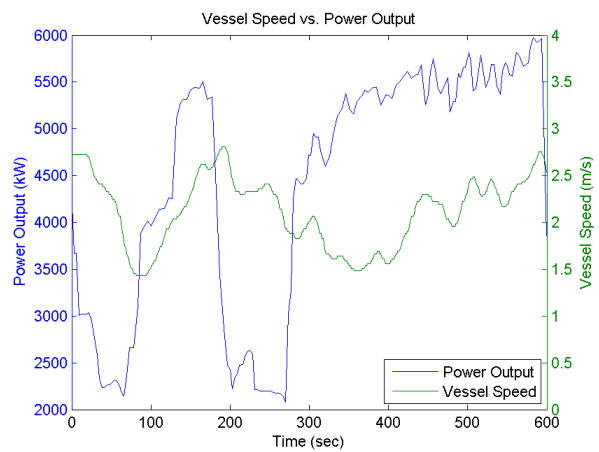
(c) 20:45-20:55



(d) 20:45-20:55

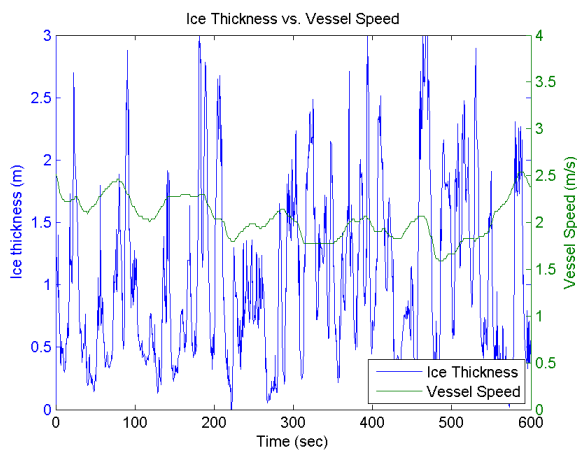


(e) 20:55-21:05

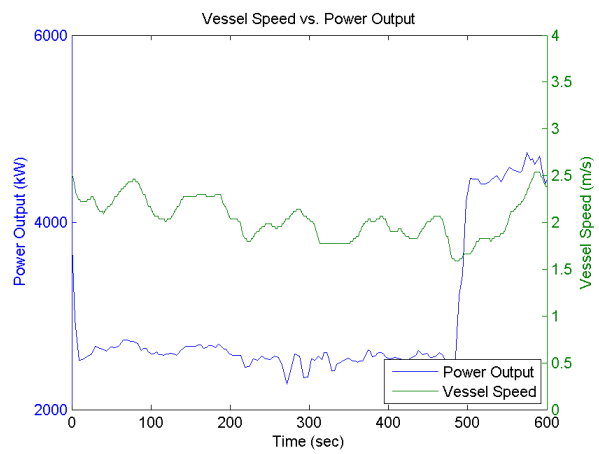


(f) 20:55-21:05

Figure B.10: March 26th



(a) 21:05-21:15



(b) 21:05-21:15

Figure B.11: March 26th

Appendix C

Processed Data

This chapter contains the results from using the proposed formula in this thesis. For all sequences of interest all calculated values are given.

March 24th	Int.		Mean		Std		Work Res	Force Res
	power	peed	power	speed	power	speed		
05:08-05:18	1171261	1174	1953	1.96	937	0.38	1182236	1006
05:18-05:28	1793054	1372	2997	2.29	710	0.18	1790530	1305
05:28-05:38	2090310	1095	3479	1.82	34	0.24	2078146	1898
14:04-14:14	1950947	1907	3231	3.18	65	0.17	1963020	1029
14:29-14:39	2119431	2031	3556	3.39	47	0.21	2115894	1042
14:40-14:50	2158373	755	3587	1.26	73	0.56	2138845	2838
14:50-15:00	2171287	730	3617	1.22	30	0.41	2171610	2974
15:30-15:40	3995002	424	6656	0.71	121	0.15	3995109	9412
15:55-16:05	5832078	786	9671	1.31	179	0.58	5827962	7418

Table C.1: March 24th - 10 minutes long sequences

March 24th	Int.	Int.	Int.	Mean	Mean	Std	Std	Std	Std	Work	Force
	power	peed	ice	power	speed	ice	power	speed	ice	Res	Res
05:08-05:13	375377	607	77	1256	2.03	0.26	176	0.32	0.33	375981	620
05:13-05:18	795884	568	205	2645	1.89	0.68	879	0.42	0.44	806255	1419
05:18-05:23	746888	664	160	2497	2.21	0.53	698	0.18	0.56	743559	1120
05:23-05:28	1046166	708	217	3497	2.36	0.72	33	0.14	0.34	1046971	1479
05:28-05:33	1054705	561	220	3482	1.87	0.73	40	0.26	0.28	1045669	1866
05:23-05:38	1035605	534	317	3477	1.78	1.06	26	0.21	0.48	1032477	1932
14:04-14:09	969566	909	142	3200	3.03	0.47	61	0.08	0.17	975877	1073
14:09-14:14	981381	998	129	3262	3.32	0.43	58	0.08	0.22	987143	989
14:29-14:34	1069846	1029	116	3556	3.44	0.39	62	0.17	0.22	1081187	1051
14:34-14:39	1049585	1002	200	3556	3.34	0.67	27	0.24	0.37	1034707	1033
14:40-14:45	1081772	527	357	3571	1.75	1.19	78	0.30	0.24	1064795	2024
14:45-14:50	1076601	228	433	3603	0.76	1.44	68	0.18	0.19	1074049	4717
14:50-14:55	1083537	313	382	3622	1.04	1.27	32	0.39	0.35	1088613	3475
14:55-15:00	1087750	417	353	3613	1.39	1.17	27	0.36	0.47	1082996	2598
15:30-15:35	1982365	190	487	6605	0.64	1.62	150	0.17	0.29	1984633	10419
15:35-15:40	2012637	234	519	6706	0.78	1.73	34	0.10	0.37	2010476	8593
15:55-16:00	2891465	452	455	9667	1.51	1.52	172	0.74	0.27	2886469	6386
16:00-16:05	2940613	334	463	9675	1.11	1.54	186	0.25	0.22	2941493	8815

Table C.2: March 24th - 5 minutes long sequences

March 25th	Int. power	Int. speed	Int. ice	Mean power	Mean speed	Mean ice	Std power	Std speed	Std ice	Work Res	Force Res
16:00-16:10	1529801	1882	244	2546	3.13	0.41	24	0.07	0.19	1531359	814
16:10-16:20	1643760	1869	236	2743	3.12	0.39	178	0.10	0.21	1648678	882
16:20-16:30	1717683	1899	272	2854	3.17	0.45	39	0.11	0.22	1712241	902
16:45-16:55	2158239	1399	728	3597	2.33	1.21	100	0.25	0.58	2152971	1539
16:55-17:05	2145159	1339	788	3557	2.23	1.31	115	0.30	0.64	2152329	1608
17:05-17:15	2218672	1809	524	3716	3.02	0.87	20	0.10	0.37	2224818	1230
17:32-17:42	1185000	1993	32	1976	3.32	0.05	31	0.11	0.22	1190396	597

Table C.3: March 25th - 10 minutes long sequences

March 25th	Int.	Int.	Int.	Mean	Mean	Mean	Std	Std	Std	Std	Work	Force
	power	peed	ice	power	speed	ice	power	speed	ice	Res	Res	Res
16:00-16:05	774381	933	112	2540	3.11	0.37	25	0.08	0.17	778078	834	
16:05-16:10	755420	949	132	2553	3.16	0.44	20	0.05	0.20	753280	794	
16:10-16:15	787170	913	98	2614	3.05	0.33	167	0.07	0.17	789857	865	
16:15-16:20	856589	956	139	2873	3.18	0.46	25	0.07	0.23	858821	899	
16:20-16:25	864271	974	125	2881	3.24	0.42	19	0.02	0.20	863706	887	
16:25-16:30	853412	925	147	2827	3.09	0.49	33	0.11	0.23	848535	917	
16:45-16:50	1079873	714	350	3613	2.38	1.17	111	0.28	0.61	1070718	1500	
16:50-16:55	1078366	685	378	3581	2.28	1.26	85	0.20	0.55	1082253	1580	
16:55-17:00	1061986	642	384	3527	2.14	1.28	99	0.22	0.58	1065875	1660	
17:00-17:05	1083173	697	404	3587	2.32	1.35	128	0.34	0.70	1086454	1559	
17:05-17:10	1114800	899	261	3717	3.00	0.87	21	0.12	0.37	1121488	1247	
17:10-17:15	1103871	910	263	3716	3.04	0.88	19	0.07	0.38	1103329	1213	
17:32-17:37	588848	978	3	1963	3.26	0.01	37	0.13	0.15	597113	610	
17:37-17:42	596152	1014	30	1988	3.38	0.10	15	0.03	0.27	593283	585	

Table C.4: March 25th - 5 minutes long sequences

March 26th	Int. power	Int. peed	Int. ice	Mean power	Mean speed	Mean ice	Std power	Std speed	Std ice	Work Res	Force Res
19:00-19:10	3213180	1401	843	5330	2.33	1.41	761	0.60	0.82	3240106	2312
19:10-19:20	1397084	1559	550	2331	2.60	0.92	73	0.25	0.43	1380039	885
19:20-19:30	1354272	1406	562	2250	2.35	0.94	56	0.12	0.42	1356796	965
19:30-19:40	1439772	1714	392	2407	2.85	0.65	59	0.18	0.36	1447308	844
19:40-19:50	1486657	1829	305	2470	3.05	0.51	29	0.09	0.26	1489785	815
19:50-20:00	1475592	1839	265	2466	3.07	0.44	47	0.11	0.29	1476671	803
20:00-20:10	1486920	1904	244	2488	3.17	0.41	64	0.19	0.49	1477866	776
20:10-20:20	1378007	1494	572	2292	2.49	0.95	39	0.13	0.37	1372794	919
20:20-20:30	1885733	1445	682	3144	2.41	1.14	679	0.26	0.39	1892830	1309
20:30-20:45	3362123	2512	839	3727	2.79	0.93	136	0.28	0.55	3365596	1340
20:45-20:55	2815702	1401	796	4717	2.33	1.33	714	0.51	0.82	2811278	2006
20:55-21:05	2649091	1272	776	4422	2.12	1.29	1365	0.38	0.77	2645906	2081
21:05-21:15	1763384	1227	621	2934	2.05	1.04	752	0.22	0.69	1760833	1435

Table C.5: March 26th - 10 minutes long sequences

March 26th	Int.	Int.	Int.	Mean	Std	Std	Std	Work	Force		
	power	peed	ice	power	speed	ice	power	Res	Res		
19:00-19:05	1642363	631	490	5474	2.10	1.63	776	0.46	0.80	1647688	2610
19:05-19:10	1570817	770	354	5187	2.56	1.18	706	0.62	0.78	1592417	2067
19:10-19:15	712626	837	255	2382	2.80	0.85	63	0.20	0.38	696822	833
19:15-19:20	684459	722	295	2280	2.40	0.98	34	0.11	0.46	683217	946
19:20-19:25	688023	727	298	2279	2.42	0.99	22	0.07	0.39	686046	944
19:25-19:30	666249	680	263	2222	2.27	0.88	66	0.12	0.45	670751	987
19:30-19:35	704588	829	194	2379	2.76	0.65	67	0.20	0.42	715789	863
19:35-19:40	735184	884	199	2434	2.94	0.66	28	0.09	0.28	731519	827
19:40-19:45	730151	890	162	2450	2.97	0.54	23	0.05	0.28	733279	824
19:45-19:50	756506	938	143	2490	3.13	0.48	16	0.04	0.24	756506	806
19:50-19:55	728783	905	151	2444	3.01	0.50	39	0.05	0.29	725656	802
19:55-20:00	746809	934	114	2488	3.12	0.38	45	0.13	0.28	751016	804
20:00-20:05	760250	969	73	2510	3.23	0.24	24	0.08	0.39	761903	786
20:05-20:10	726671	935	172	2465	3.11	0.57	83	0.25	0.52	715963	766
20:10-20:15	700230	774	263	2317	2.59	0.88	26	0.04	0.36	698865	903
20:15-20:20	677777	720	309	2266	2.40	1.03	33	0.12	0.37	673929	936
20:20-20:25	795838	663	341	2644	2.21	1.14	645	0.21	0.41	800137	1207
20:25-20:30	1089894	783	341	3647	2.61	1.14	43	0.07	0.37	1092693	1396
20:30-20:35	1107184	813	307	3689	2.71	1.02	54	0.10	0.44	1110657	1366
20:35-20:40	1134732	898	238	3806	2.99	0.79	97	0.20	0.52	1136818	1265
20:40-20:45	1120206	801	295	3686	2.67	0.98	183	0.35	0.65	1118121	1397
20:45-20:50	1327835	625	451	4443	2.08	1.50	751	0.52	0.82	1317265	2108
20:50-20:55	1487867	776	345	4992	2.59	1.15	538	0.34	0.77	1494013	1924
20:55-21:00	1023384	658	363	3421	2.20	1.21	1113	0.39	0.69	1012334	1539
21:00-21:05	1625707	613	413	5420	2.04	1.38	351	0.36	0.83	1633572	2662
21:05-21:10	790379	647	259	2610	2.15	0.86	174	0.16	0.62	782864	1211
21:10-21:15	973005	580	362	3264	1.94	1.21	942	0.22	0.72	977969	1685

Table C.6: March 26th - 5 minutes long sequences

Appendix D

Contents on Attached CD

/thesis/

Electronic version of this thesis in .pdf format.

/matlab/

RawHMADB_MatTime.mat Rawdata from Azipod sensor

RawICE_MatTime.mat Rawdata from ice thickness measurements

RawNAV_MatTime.mat Raw data from navigation sensor

/resistance/

RiskaLindqvist.xls Calculation of resistance based on the formulations presented from Riska and Lindqvist

march24to26.xls Resistance results from proposed formulation and comparison with Riska and Lindqvist.

/curve_fitting/

march24.xls Regression lines from March 24th

march25.xls Regression lines from March 25th

march26.xls Regression lines from March 26th

